



# Research and Development

EVALUATION OF THE EFFICIENCY  
OF INDUSTRIAL FLARES: FLARE HEAD  
DESIGN AND GAS COMPOSITION

## Prepared for

Office of Air Quality Planning and Standards

## Prepared by

Air and Energy Engineering Research  
Laboratory  
Research Triangle Park NC 27711

## **RESEARCH REPORTING SERIES**

Research reports of the Office of Research and Development, U.S. Environmental Protection Agency, have been grouped into nine series. These nine broad categories were established to facilitate further development and application of environmental technology. Elimination of traditional grouping was consciously planned to foster technology transfer and a maximum interface in related fields. The nine series are:

1. Environmental Health Effects Research
2. Environmental Protection Technology
3. Ecological Research
4. Environmental Monitoring
5. Socioeconomic Environmental Studies
6. Scientific and Technical Assessment Reports (STAR)
7. Interagency Energy-Environment Research and Development
8. "Special" Reports
9. Miscellaneous Reports

This report has been assigned to the ENVIRONMENTAL PROTECTION TECHNOLOGY series. This series describes research performed to develop and demonstrate instrumentation, equipment, and methodology to repair or prevent environmental degradation from point and non-point sources of pollution. This work provides the new or improved technology required for the control and treatment of pollution sources to meet environmental quality standards.

## **EPA REVIEW NOTICE**

This report has been reviewed by the U.S. Environmental Protection Agency, and approved for publication. Approval does not signify that the contents necessarily reflect the views and policy of the Agency, nor does mention of trade names or commercial products constitute endorsement or recommendation for use.

This document is available to the public through the National Technical Information Service, Springfield, Virginia 22161.

EPA-600/2-85-106  
September 1985

EVALUATION OF THE EFFICIENCY  
OF INDUSTRIAL FLARES: FLARE HEAD DESIGN  
AND GAS COMPOSITION

by

J. H. Pohl and N. R. Soelberg

ENERGY AND ENVIRONMENTAL RESEARCH CORPORATION  
18 MASON  
IRVINE, CALIFORNIA 92718

EPA Contract No. 68-02-3661

EPA Project Officer: Bruce A. Tichenor

Air and Energy Engineering Research Laboratory  
Hazardous Air Technology Branch  
Research Triangle Park, North Carolina 27711

Prepared for:

U.S. ENVIRONMENTAL PROTECTION AGENCY  
Office of Research and Development  
Washington, D.C. 20460

## ABSTRACT

The U.S. Environmental Protection Agency has contracted with Energy and Environmental Research Corporation to conduct a research program which will result in quantification of emissions from, and efficiencies of, industrial flares. The program is divided into four phases. Phase I - Experimental Design and Phase II - Design of Test Facilities have been reported in EPA Report No. 600/2-83-070. Phase III - Development of Test Facilities and the initial work in Phase IV - Data Collection has been reported in EPA Report No. 600/2-84-095. Further data collection during Phase IV is reported herein.

Initial results were limited to tests conducted burning propane-nitrogen mixtures on pipe flames without pilot light stabilization. The work reported here extends the previous results to other gases and flare head designs, and includes a limited investigation of the influence of pilot flames on flare performance. The following results were obtained:

- o Flames from nozzles less than 1-1/2 inches\* in diameter generally are not similar to flames from large nozzles.
- o Flare head design can influence the flame stability curve.
- o Combustion efficiency can be correlated with flame stability based upon gas heating value for the pressure heads and the coanda steam-injected head.
- o For the limited conditions tested, the flame stability and combustion efficiency of the air-assisted head correlated with the momentum

---

\*English units are generally used throughout this report. Appendix E provides conversion factors for English to Metric units.



ratio of air to fuel; the heating value of the gas had only a minor influence.

- o Limited data on an air-assisted flare shows that use of a pilot light improves flame stability.
- o The destruction efficiency of different compounds can be correlated with the flame stability curve for each compound, for the compounds tested in this program.
- o Stable flare flames and high (>98-99 percent) combustion and destruction efficiencies are attained when the flares are operated within operating envelopes specific to each flare head and gas mixture tested. Operation beyond the edge of the operating envelope results in rapid flame de-stabilization and a decrease in combustion and destruction efficiencies.

## TABLE OF CONTENTS

<u>Section</u>	<u>Page</u>
LIST OF FIGURES . . . . .	v
LIST OF TABLES . . . . .	viii
1.0 INTRODUCTION . . . . .	1-1
1.1 Review of Previous Work . . . . .	1-1
1.2 Current EER Flare Program . . . . .	1-6
1.3 References . . . . .	1-11
2.0 SUMMARY AND CONCLUSIONS . . . . .	2-1
3.0 FLARE AERODYNAMICS . . . . .	3-1
3.1 Reynolds Number and Richardson Number . . . . .	3-1
3.2 Flame Length . . . . .	3-4
3.3 Flame Stability . . . . .	3-16
3.4 Pseudo Adiabatic Flame Temperatures and Stability . . . . .	3-16
3.5 References . . . . .	3-23
4.0 COMMERCIAL FLARE HEAD TEST RESULTS . . . . .	4-1
4.1 Coanda Steam-Injected Head D . . . . .	4-3
4.2 Pressure-Assisted Head E . . . . .	4-3
4.3 Pressure-Assisted Head F . . . . .	4-8
4.4 Air-Assisted Head G . . . . .	4-8
4.5 Commercial Head Summary . . . . .	4-19
5.0 GAS COMPOSITION TEST RESULTS . . . . .	5-1
5.1 Compound Selection . . . . .	5-1
5.2 Compound Screening Tests . . . . .	5-1
5.3 Gas Mixture Flare Tests . . . . .	5-3
5.4 Flame Stability Correlations . . . . .	5-11
5.5 References . . . . .	5-17
6.0 FLARE NO <sub>x</sub> AND HYDROCARBON EMISSIONS . . . . .	6-1
APPENDIX A. EPA FLARE TEST FACILITY AND TEST PROCEDURES . . . . .	A-1
APPENDIX B. FLARE SCREENING FACILITY AND TEST PROCEDURES . . . . .	B-1
APPENDIX C. DATA ANALYSIS . . . . .	C-1
APPENDIX D. QUALITY ASSURANCE . . . . .	D-1
APPENDIX E. CONVERSION FACTORS . . . . .	E-1

## LIST OF FIGURES

<u>Figure</u>		<u>Page</u>
2-1	EPA Flare Test Facility (FTF) at EER . . . . .	2-2
2-2	Flare Screening Facility (FSF) . . . . .	2-3
2-3	Region of flame stability for steam-injected and pressure-assisted heads D, E, and F . . . . .	2-14
2-4	Maximum gas exit velocity for stability versus air- assist to gas momentum ratio for the air-assisted head G, with and without pilot . . . . .	2-15
2-5	Combustion efficiency vs. flame stability for steam-injected and pressure-assisted flare heads . . . . .	2-16
2-6	Combustion efficiency vs. air-assist to gas momentum ratio for commercial air-assisted head G . . . . .	2-17
2-7	Flame stability curves for pipe flare heads, 1/16 inch through 2 1/2 inch flares are without flame retention devices. The 3, 6, and 12 inch heads were tested with and without flame retention devices . . . . .	2-18
2-8	Region of flame stability for the 3 inch open pipe flare head burning selected relief gas mixtures . . . . .	2-20
2-9	Destruction efficiency of different gases . . . . .	2-21
3-1	Aerodynamic conditions of flares tested at EER compared to typical commercial flare conditions . . . . .	3-2
3-2	Comparison of flame lengths predicted by available studies with those observed in this study . . . . .	3-5
3-3	Correlation of flame length with heat release for 1/2 inch to 31 inch flares . . . . .	3-6
3-4	Correlation of flame length to heat release for 1/16 inch through 2 1/2 inch flares . . . . .	3-9
3-5	Empirical correlation of radiant heat loss from propane-nitrogen flames. Richardson number=2.0 . . . . .	3-10
3-6	Predicted flame length from modified Richardson number correlation compared to observed flame length for previously tested 3, 6, and 12 inch flare heads . . . . .	3-12
3-7	Predicted flame length from modified Richardson number correlation compared to observed flame length for 1/2 through 2 1/2 inch flare heads . . . . .	3-13
3-8	Predicted flame length from modified Richardson number correlation compared to observed flame length for 1/16 through 1/4 inch flare heads . . . . .	3-14
3-9	Predicted flame length from modified Richardson number correlation compared to observed flame length for 1 1/2 through 12 inch commercial heads . . . . .	3-15
3-10	Flame stability curves for pipe flare heads . . . . .	3-17
3-11	Maximum relief gas exit velocity vs. flame temperature for previously tested 3 through 12 inch flare heads . . . . .	3-19
3-12	Maximum relief gas exit velocity vs. flame temperature for commercial heads D through G . . . . .	3-20

## LIST OF FIGURES (continued)

<u>Figure</u>		<u>Page</u>
3-13	Relation between flame stability and pseudo adiabatic flame temperature . . . . .	3-21
4-1	Flame stability curve for a commercial 12 inch coanda steam-injected head D. Steam flowrate at 140 lb/hr . . . . .	4-4
4-2	Relation of flame stability to combustion efficiency for the commercial 12 inch coanda steam-injected flare head D. Steam flowrate at 140 lb/hr . . . . .	4-5
4-3	Region of flame stability for 1.5 inch commercial pressure-assisted head E . . . . .	4-6
4-4	Relation of flame stability to combustion efficiency for commercial 1.5 inch pressure-assisted head E . . . . .	4-7
4-5	Region of flame stability for 3.8 inch commercial pressure head F . . . . .	4-9
4-6	Relation of flame stability to combustion efficiency for a commercial 3.8 inch pressure-assisted head F . . . . .	4-10
4-7	Region of flame stability for a 1.5 inch commercial air-assisted flare G without a pilot flame . . . . .	4-11
4-8	Region of flame stability for 1.5 inch commercial air-assisted flare G with pilot flame . . . . .	4-12
4-9	Region of flame stability for 1.5 inch commercial air-assisted head G, with no air-assist . . . . .	4-13
4-10	Maximum gas exit velocity for stability versus air- assist to gas momentum ratio for the air-assisted head G, with and without pilot . . . . .	4-15
4-11	Combustion efficiency vs. air-assist to gas momentum ratio for commercial air-assisted head G . . . . .	4-17
4-12	Destruction efficiency of incompletely combusted products from air-assisted head G . . . . .	4-18
4-13	Region of flame stability for steam and pressure- assisted heads D, E, and F . . . . .	4-20
4-14	Combustion efficiency vs. flame stability for steam- injected and pressure-assisted flare heads . . . . .	4-21
5-1	Region of flame stability for the 3 inch open pipe flare head burning selected relief gas mixtures . . . . .	5-5
5-2	Destruction efficiency of different gases . . . . .	5-8
5-3	Hydrocarbon combustion efficiency of gas mixtures . . . . .	5-9
5-4	Pilot-scale FTF destruction efficiency results compared to lab-scale FSF destruction efficiency results. All results at operating conditions near the stability limit. FTF nozzle size = 3 inches. FSF nozzle size = 0.042 inches . . . . .	5-10
5-5	Calculated adiabatic flame temperature vs. limiting stable gas exit velocity for different gas mixtures . . . . .	5-13

# LIST OF FIGURES (continued)

<u>Figure</u>		<u>Page</u>
5-6(a)	Nozzle velocity vs Experimental Index for data from Noble, et al. . . . .	5-15
5-6(b)	Nozzle exit velocity vs Experimental Index for gas mixture tests.	5-15
6-1	NO <sub>x</sub> concentration (air-free basis) at the plume centerline from pilot-scale flares. . . . .	6-2
6-2	NO <sub>2</sub> emissions from pilot-scale flares . . . . .	6-4

# LIST OF TABLES .

<u>Table</u>		<u>Page</u>
1-1	SUMMARY OF PREVIOUS FLARE COMBUSTION EFFICIENCY STUDIES . . . . .	1-2
2-1	COMMERCIAL 12 INCH DIAMETER COANDA STEAM-INJECTED HEAD D TEST RESULTS. STEAM FLOWRATE = 140 LB/HR. . . . .	2-4
2-2	COMMERCIAL 1.5 INCH DIAMETER PRESSURE-ASSISTED HEAD E TEST RESULTS . . . . .	2-5
2-3	COMMERCIAL 3.8 INCH DIAMETER PRESSURE-ASSISTED HEAD F TEST RESULTS . . . . .	2-6
2-4	COMMERCIAL 1.5 INCH DIAMETER AIR-ASSISTED HEAD G TEST RESULTS. . . . .	2-7
2-5	3 INCH DIAMETER OPEN PIPE FLARE (WITH PILOT) TEST RESULTS . . . . .	2-9
2-6	RESULTS OF SCREENING TESTS ON FLARE SCREENING FACILITY. . . . .	2-10
2-7	GAS MIXTURE COMBUSTION AND DESTRUCTION EFFICIENCY TEST RESULTS: 3 INCH FLARE, NO PILOT. . . . .	2-12
4-1	COMMERCIAL HEADS SELECTED FOR COMBUSTION EFFICIENCY TESTS . . . . .	4-2
5-1	RESULTS OF SCREENING TESTS ON FLARE SCREENING FACILITY. . . . .	5-2
5-2	PHYSICAL PROPERTIES (1 ATM, 60°F) OF THE COMPOUNDS TESTED USING THE FLARE TEST FACILITY. . . . .	5-6
6-1	GC-MS ANALYSIS OF PLUME SAMPLE FROM LABORATORY-SCALE TESTS . . . . .	6-6
6-2	GC-MS ANALYSIS OF PLUME CENTERLINE SAMPLES FROM GAS MIXTURE TESTS, USING A 3 INCH OPEN PIPE FLARE . . . . .	6-7

## 1.0 INTRODUCTION

Industrial flares are commonly used to safely and economically destroy large amounts of industrial waste gases. Since most of the gas flared in the United States is from leaks, purges, and emergency vents, the amounts and compositions of flared gases vary widely and are difficult to measure. Flare emissions are also difficult to measure. Most flares are elevated to decrease noise radiation and combustion products at ground level. Probe collection of plume material in such situations is impractical. Remote sensing of flare emissions is an alternative to direct sampling, but instrumentation and techniques for this purpose are still undeveloped.

Evaluation and control of industrial flare emissions requires pilot-scale research with direct sampling of flare emissions. Flare research has been conducted at Energy and Environmental Research Corporation (EER) since 1980. A pilot-scale flare test facility was constructed for the U.S. Environmental Protection Agency in 1982. This research has been sponsored by the U.S. E.P.A. as part of an effort to provide data upon which to base new regulations for industrial flaring practices (1.1, 1.2).

### 1.1 Review of Previous Work

Several previous studies have evaluated flare emissions by testing combustion efficiency of small-scale or pilot-scale flames (1.3). A primary finding of these studies was that flare flame combustion efficiencies can be very high, exceeding 98 percent, but that under certain operating conditions, such as excessive steam injection, low efficiency can result (1.4). Pohl, et al. (1.3) and Keller and Noble (1.5) have also reported that when a flame is stable (i.e., not near blow-out conditions) efficient combustion is achieved. However, flares operating with unstable flames tend to be inefficient.

Test conditions and measured combustion efficiencies for recent flare studies are summarized in Table 1-1. A range of flare sizes, designs, and operating conditions have been examined. The results show combustion efficiencies ranging between 55 - 100 percent. The measured combustion

Table 1-1.

## SUMMARY OF PREVIOUS FLARE COMBUSTION EFFICIENCY STUDIES

STUDY	DATE	FLARE SIZE (in.)	DESIGN	VELOCITY (ft/sec)	GAS FLARED	MEASURED EFFICIENCY (%)
Palmer (1.6)	1972	0.5	Experimental Nozzle	50 - 250	Ethylene	> 97.8
Lee & Whipple (1.7)	1981	2.0	Holes in 2" Cap	1.8	Propane	96 - 100
Siegel (1.8)	1980	27.	Commercial Flaregas Coanda FS-6	0.7 - 16	Refinery Gas <sup>(a)</sup>	97 - > 99
Howes, et al (1.9)	1981	6 <sup>(c)</sup>	Commercial Air Assist. Zink LH	40 - 60	Propane	92 - 100
Howes, et al (1.9)	1981	3 at 4 <sup>(b)</sup>	Commercial H.P. Zink LRGO	Near Sonic (estimate)	Natural Gas	> 99
McDaniel (1.10) Keller and Noble (1.5)	1983	8	Commercial Zink STF-S-8	0.03 - 62	Propylene/Nitrogen <sup>(d)</sup>	67 - 100
McDaniel (1.10) Keller and Noble (1.5)	1983	6 <sup>(c)</sup>	Commercial Air Assist. Zink STF-LH-457-5	1.4 - 218	Propylene/Nitrogen <sup>(e)</sup>	55 - 100
Pohl, et al (1.3)	1984	3-12	Open pipe and commercial	0.2 - 420	Propane/Nitrogen <sup>(f)</sup>	90 - 99.9

(a) 50% hydrogen plus light hydrocarbons

(b) Three spiders, each with an open area of 1.3 in<sup>2</sup>

(c) Supplied through spiders; high Btu gas through area of 5.30 in<sup>2</sup> and low Btu gas through 11.24 in<sup>2</sup>

(d) Heating value varied from 209 to 2183 Btu/scf

(e) Heating value varied from 83 to 2183 Btu/scf

(f) Heating value varied from 291-2350 Btu/scf



efficiencies show that flare flame stability and combustion efficiency may vary, depending on flare head size, design, gas composition, and operating conditions.

Accurate measurement of flare emissions and combustion efficiency is difficult even on a pilot-scale facility. Problems encountered by previous researchers include:

- Inability to close mass balances
- Inability to measure soot emissions
- Sampling only on the plume centerline
- Flare flame fluctuations due to turbulence and/or wind

The Flare Test Facility at EER has been designed and built in order to minimize such problems. The following procedures have been developed to verify the accuracy of combustion efficiency measurements:

- Material balance closure was verified using a hood to capture the entire flare plume for small flames, and by using  $\text{SO}_2$  as a tracer for large flames.
- Soot concentration was measured for all tests.
- The average concentration of completely and incompletely burned combustion species from the flare flame was determined for the entire plume by (1) using a hood to completely capture small flames, and (2) simultaneous sampling at five radial positions in the plume for large flames. These local values were combined with velocities calculated from jet theory and integrated to calculate overall combustion efficiency.

- The effects of flare flame fluctuations were limited by mixing a sample taken over a 20 minute time period. This time span was experimentally determined to be sufficient to average flame fluctuations.

Using the Flare Test Facility, EER has developed a data base of combustion efficiency for a variety of flare heads and operating conditions. Combustion efficiency and flare scaling parameters were studied using 3, 6, and 12 inch open pipe flares with and without flame stabilization devices. Scaling parameters investigated included exit velocity, residence time, Reynolds number, and Richardson number. Flare flame aerodynamics, including lift-off and flame length, were also studied.

Due to industrial interest in higher flare exit velocities, testing was conducted at exit velocities up to 420 ft/sec. The same parameters of scaling, combustion efficiency, and aerodynamics were evaluated at these high velocities, using a 3 inch open pipe flare both with and without flame retention devices.

The previous trials were largely limited to propane/nitrogen mixtures burned on open and commercial pipe flares without pilot flame stabilization. Results from these trials established:

- Flame length can be estimated using Richardson number and an estimate of the flame temperature.
- Flare burn gases with combustion efficiencies greater than 98 percent unless operated within 30 percent of the blow-off limit.
- Soot contributes less than 0.5 percent to the unburned hydrocarbons.
- A single probe can yield good estimates of overall combustion efficiency.

- o For the range of flares and conditions studied, flame structure and combustion efficiency did not depend on flare size or design.

In order to extend the basic open-pipe flare test results to industrial application, three commercial 12 inch heads were also tested. The purpose of these tests was to determine the dependence of combustion efficiency on flare head type and design. Combustion efficiency can vary, depending on commercial flare head type and design, because flare heads are often tailored to achieve specific results for specific gas mixtures and operating conditions, and may not operate well under other conditions.

The EER flare test program has established a data base for evaluation of future flare test results. In general, it has been demonstrated that when a flare flame is operated under stable conditions, combustion efficiency greater than 98 percent is attained. For propane-nitrogen mixtures flare using pipe flares without pilots, a relationship has been demonstrated between the gas heating value and the stability limit, and between the stability limit and combustion efficiency. A similar relationship between heating value, flame stability, and combustion efficiency was observed for the three commercial 12 inch pipe flares tested.

Throughout the EER flare research program, advice and consultation was provided by a Technical Advisory Committee. Committee members included representatives from EER, EPA, California Air Resources Board, flare manufacturers (Peabody Engineering, McGill, Inc., John Zink, and Flaregas Corporation) and industrial flare users (Exxon Chemical Company, Exxon R&E, Union Carbide, Getty Refining and Marketing Co., Chevron USA, and Dow Chemical Company). The industrial users included representatives of the Chemical Manufacturers Association (CMA) and the American Petroleum Institute (API). This committee met throughout the program to review and critique test plans, ensure relevance of the study, and facilitate efficient information transfer.

## 1.2 Current EER Flare Program

The previous EER studies have established accurate flare combustion efficiency test methodology, developed a pilot-scale test facility, and established a data base of combustion efficiency test results for 3 through 12 inch diameter flare heads burning propane-nitrogen mixtures on pipe flares without pilot light stabilization (1.3, 1.11, and 1.12).

The current flare test program is an extension of the previous work. Objectives were based on recommendations of the Flare Advisory Panel and were designed to extend the data base to cover a wider range of flare operating and design conditions.

### 1.2.1 Objectives

The objectives of the flare test program reported here are to:

- o Evaluate the effects of flare head type on flare combustion efficiency.
- o Evaluate effects of relief gas composition on flare combustion and destruction efficiency.

### 1.2.2 Approach

The overall objective of this program is to assess pollutant emissions from industrial flares. Direct measurements on full-scale operating flares are difficult. Therefore, direct measurements were made on pilot-scale flares in order to measure pollutant emissions, combustion and destruction efficiency, and scaling criteria.

The program was divided into four major tasks:

- Task 1 - Evaluation of combustion efficiency from different flare head types
- Task 2 - Identification of representative, potentially difficult to destroy gas compounds
- Task 3 - Evaluation of combustion and destruction efficiency of selected relief gas mixtures.
- Task 4 - Data analysis and reporting

In Task 1, EER obtained from flare suppliers the following four commercial heads:

- 1 air-assisted flare head
- 2 pressure-assisted flare heads
- 1 coanda steam-injected flare head

Each of these heads was tested on the EER pilot-scale Flare Test Facility (FTF). Flame stability and combustion efficiency were measured as functions of the following operating conditions:

- Relief gas and exit velocity
- Relief gas heating value
- Steam injection flow rate (for the coanda steam-injected flare head)
- Air assist velocity (for the air-assisted flare head)

- Relief gas pressure (for the pressure-assisted flare head)
- With and without pilot flame (for the air-assisted flare head)

The relief gas for these tests was propane, mixed with nitrogen to vary the heating value. Natural gas was used for the pilot flame.

Tasks 2 and 3 were designed to measure the effects of relief gas composition on flare pollutant emissions. A wide variety of industrial compounds are frequently flared in the United States. Most often, they are flared in mixtures containing several compounds. Each mixture may exhibit somewhat different flaring characteristics. Pilot or large-scale testing of every conceivable relief gas mixture would be expensive and unending.

A sensible approach is to test compounds in a laboratory-scale facility which are representatives of classes of compounds industrially flared. The small scale laboratory facility produces flames which are not aerodynamically similar to those produced on the pilot-scale flame or in industrial practice, because a 1/16 inch nozzle was used in the screening studies. For a commercial 12 inch diameter flare head, Reynolds numbers may range from 4,000 to 40,000, Richardson numbers range from 0.1 to 1,000, and buoyant forces often dominate over inertial forces. For a 1/16 inch diameter nozzle, Reynolds numbers are  $10^2$  to  $10^4$ , Richardson numbers are typically  $1 \times 10^{-4}$  or smaller, and inertial forces dominate. Even though lab-scale tests using a 1/16 inch diameter nozzle are aerodynamically dissimilar to large-scale flares, such tests can be used to economically screen compounds to determine comparative potential for successful destruction of these compounds by flaring. Compounds which demonstrate flaring difficulties in the Flare Screening Facility (FSF) are candidates for testing on the FTF.

Upon recommendations of the Flare Advisory Committee, twenty-one of the most commonly flared, potentially hazardous, or difficult to flare compounds were selected for laboratory-scale testing on the (FSF). These compounds are representative of:

- Sulfur compounds
- Nitrogen compounds
- Chlorinated compounds
- Oxygenated compounds
- Aliphatic hydrocarbons
- Aromatic hydrocarbons
- Compounds with low heating value

Of the twenty-one compounds screened, six were selected as candidates for testing on the FTF. Selection criteria included low destruction efficiency, poor ignitability, and high soot production. In addition, hydrogen sulfide, although not tested in the screening facility, was also selected due to its industrial importance and toxicity.

Four of the seven compounds selected during the screening tests were tested on the FTF. Hydrogen sulfide and ammonia were each tested in mixtures with propane and nitrogen. Ethylene oxide and 1,3-butadiene were each tested diluted with nitrogen to vary the heating value. Flame stability, combustion and destruction efficiency, soot production, and by-product formation from incomplete combustion were measured for each compound. All tests were conducted using the 3 inch open pipe flare, without pilot flame stabilization.

Sample procedures used during Tasks 1 through 3 were consistent with the protocols of previous EER studies (1.3, 1.11). In the FTF, flare plume samples were taken at five radial positions above the flame. These local samples were analyzed for O<sub>2</sub>, CO, CO<sub>2</sub>, total hydrocarbons, NO<sub>x</sub>, and soot concentration. Where applicable, the samples were also analyzed for H<sub>2</sub>S, SO<sub>2</sub>, and NH<sub>3</sub> concentration. Limited numbers of samples were also adsorbed

using charcoal-Tenax traps. Gases were desorbed from these traps and analyzed by GC-MS for combustion by-products.

Sampling in the FSF was easier. In this facility, the 1/16 inch nozzle was enclosed within a reaction chamber, which isolated the flame from the external environment. Tests verified that the flames behaved as if discharged into air because the flame was very small relative to the size of the chamber. Sampling of the well-mixed products at the reactor outlet required only one probe and ensured complete mass balance closure.

Sample analysis was conducted during tests on both the FSF and FTF to evaluate air dilution, mass balances, combustion efficiency, and destruction efficiency. Sulfur dioxide was injected during some of the pilot tests and used as a tracer for mass balances. Mass balances on the FTF were more difficult because of product loss, air dilution in the large exposed flame, and plume concentration gradients. Local mass balances were used to accurately evaluate local mass fluxes, local combustion efficiency, and destruction efficiency. Local mass fluxes were radially integrated to calculate overall combustion and destruction efficiencies.

In Task 4, flare combustion and destruction efficiencies were correlated to flame stability. Flame stability was correlated to relief gas heating value and exit velocity for the gas mixture tests and for all the commercial heads except for the air-assisted head. Flame stability for the air-assisted head was related to air-fuel stoichiometry and momentum ratios. Results for the air-assisted head showed that the effects of relief gas heating value and exit velocity on flame stability were minimal, compared to the effect of the air-assist stream to fuel stream momentum ratio.

In order to evaluate the dependence of flare flame combustion efficiency on flame stability and operating conditions, it was necessary to investigate flare operating conditions which result in both efficient and inefficient combustion in order to define the region of efficient operation and to determine parameters which are critical to flare performance. Thus, many of



the test cases represent conditions outside the normal range of commercial flare operations.

### 1.3      References

- 1.1      Davis, B. C., "U.S. EPA's Flare Policy: Update and Review", Chemical Engineering Progress, April 1983.
- 1.2      Davis, B. C., "Flares-An Update of Environmental Regulatory Policy", AIChE National Meeting, Philadelphia, PA, August 19-22, 1984.
- 1.3      Pohl, J. H., R. Payne, and J. Lee, "Evaluation of the Efficiency of Industrial Flares: Test Results", EPA Report No. 600/2-84-095, May 1984.
- 1.4      Dubnowski, J. J. and B. C. Davis, "Flaring Combustion Efficiency: A Review of the State of Current Knowledge, "The 76th Annual Air Pollution Control Association Meeting, Atlanta, GA, 1983.
- 1.5      Keller, N. and R. Noble, "RACT for VOC - A Burning Issue", Pollution Engineering, July 1983.
- 1.6      Palmer, P. A., "A Tracer Technique for Determining Efficiency of an Elevated Flare," E. I. du Pont de Nemours and Co., Wilmington, DE, 1972.
- 1.7      Lee, K. C. and G. M. Whipple, "Waste Gas Hydrocarbon Combustion in a Flare, "Union Carbide Corporation, South Charleston, WV, 1981.
- 1.8      Siegel, K. D., "Degree of Conversion of Flare Gas in Refinery High Flares, "Ph.D. Dissertation, University of Karlsruhe (Federal Republic of Germany), February, 1980.
- 1.9      Howes, J. E., T. E. Hill, R. N. Smith, G. R. Ward, and W. F. Herget, "Development of Flare Emission Measurement Methodology, Draft Report," EPA Contract No. 68-02-2682, U.S. Environmental Protection Agency, 1981 (Draft Report).
- 1.10      McDaniel, M., "Flare Efficiency Study," EPA Report No. 600/2-83-052, July 1983.
- 1.11      Joseph, D., J. Lee, C. McKinnon, R. Payne, and J. Pohl, "Evaluation of the Efficiency of Industrial Flares: Background-Experimental Design-Facility", EPA Report No. 600/2-83-070, August 1983.
- 1.12      Pohl, J. H., J. Lee, R. Payne and B. Tichenor, "The Combustion Efficiency of Flare Flames", 77th Annual Meeting and Exhibition of the Air Pollution Control Association, San Francisco, CA., June 1984.

## 2.0 SUMMARY AND CONCLUSIONS

The objective of this phase of "Evaluation of the Efficiency of Industrial Flares" was to determine the influence of additional flare head designs and gas composition on the stability and structure, destruction efficiency (DE), and combustion efficiency (CE) of flare flames. This phase extended the previous programs which reviewed the literature available on flare performance, designed and built a flare test facility, and determined the combustion efficiency of pipe flares firing mixtures of propane and nitrogen in the absence of a pilot flame.

The current program extends previous work to include different classes of commercial flare heads, and types of relief gas mixtures burned on small pipe flares. The flare head types include:

- Coanda steam-injected flare head
- Two pressure-assisted flare heads
- Air-assisted flare head without flame retention devices

Each of these flare heads was evaluated on the Flare Test Facility shown in Figure 2-1.

Twenty-one different gases were selected and screened for potential combustion problems on the Flare Screening Facility (FSF) shown in Figure 2-2, with a 1/16 inch nozzle (ID = 0.042 inches). The combustion and destruction efficiencies of four of these gases were measured on the Flare Test Facility (FTF).

The data collected on the FTF for the different flare heads is summarized in Tables 2-1 through 2-4. The air-assisted head was tested both with and without a pilot flame, as shown in Table 2-4. Limited tests to evaluate the effects of pilot flames were also conducted on a 3 inch open pipe flare, without flame retention devices. These test results are shown in Table 2-5. The results of the FSF gas mixture screening tests are shown in Table 2-6, and the results from the FTF gas mixture tests are shown in

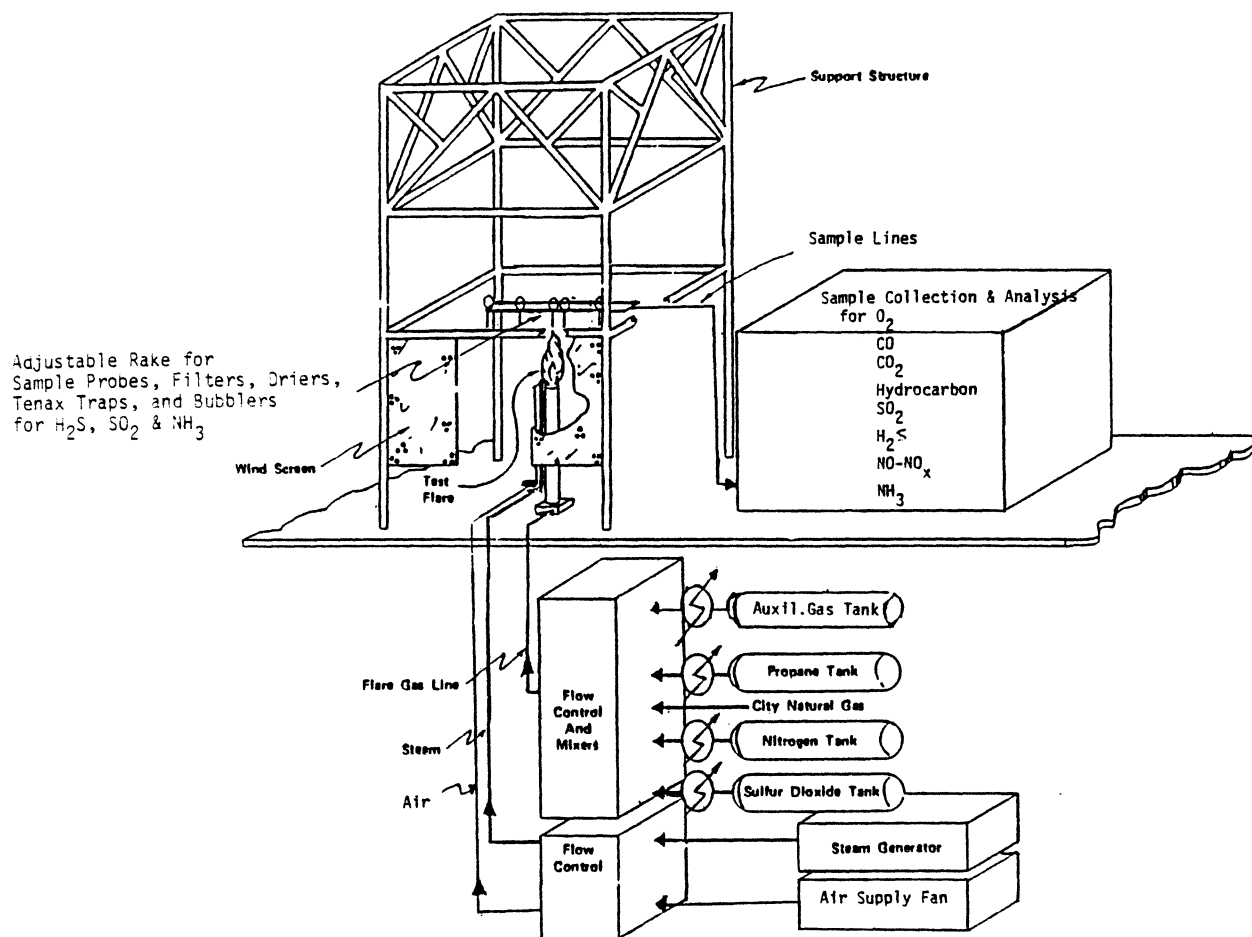


Figure 2-1. EPA flare test facility (FTF) at EER.

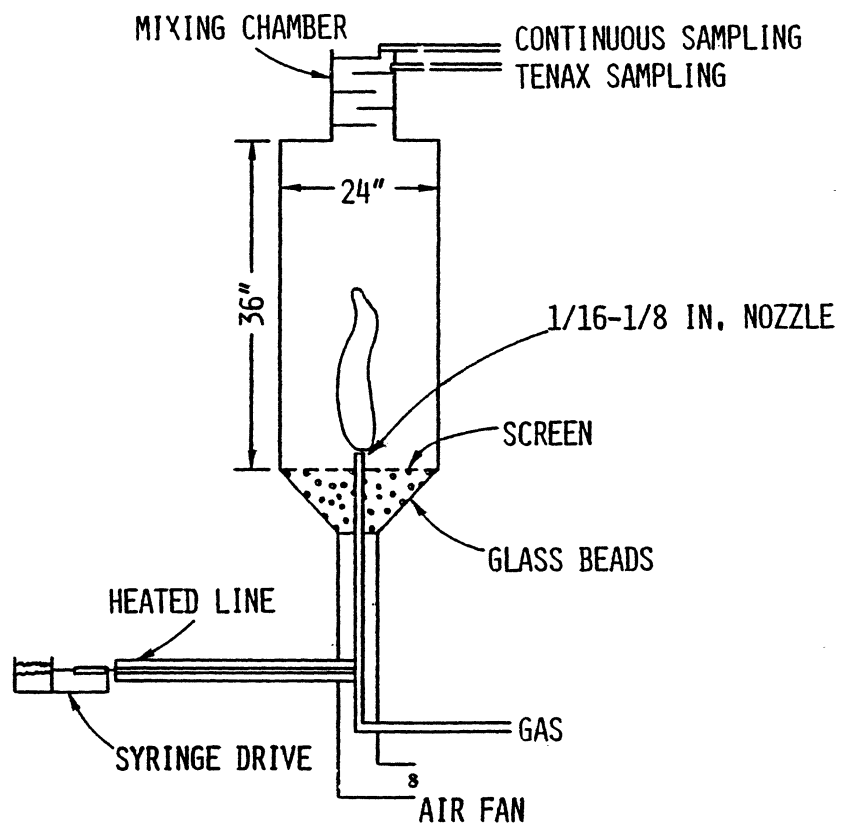


Figure 2-2. Flare screening facility (FSF).

Table 2-1

COMMERCIAL 12 INCH DIAMETER<sup>1</sup> COANDA STEAM-INJECTED HEAD D  
TEST RESULTS. STEAM FLOWRATE = 140 LB./HR

Test No.	Actual Exit Velocity <sup>1</sup> (ft/sec)	%Propane in Nitrogen	Low Htg Val (Btu/ft <sup>3</sup> )	Steam Ratio (lb steam/lb fuel)	Probe Ht <sup>3</sup> (ft)	Observations						Comb Eff (%)	Hydro-Carbon Dest Eff (%)
						Wind Speed (mph)	Flame Length <sup>2</sup> (ft)	Lift Off (in)	Color	Smoke	Sound		
200A	0.17	14.43	338	3.7	} Stability Curve Tests								
200B	0.20	13.0	305	3.3									
200C	4.0	12.1	284	0.64									
200D	4.3	11.1	261	0.15									
200E	9.3	13.1	308	0.068									
200F	9.3	13.0	305	0.068									
201	0.20	13.0	306	3.3	5	8	1.5	0	dim orange	none	none	99.3	99.7
202	4.38	11.7	275	0.15	5	7	6	0	dim orange	none	low roar	99.4	99.8
203	9.19	14.0	329	0.069	15	6	12	0	dim orange	none	jet	97.9	98.6
204	0.20	17.9	421	3.1	4	3	3	0	dim orange	none	none	99.9	100.0
205	3.95	18.1	425	0.16	10	8	7	0	dim orange	none	rumble	99.7	100.0
206	9.90	18.1	425	0.081	22	5	22	0	dim orange	none	roar	99.6	99.9

1 Based on design capacity for a 12 inch flare head. Open area at base of cone = 113 in<sup>2</sup>.

2 Based on light diffraction through flame envelope for invisible flames.

3 Height above flare tip.

Table 2-2

COMMERCIAL 1.5 INCH DIAMETER<sup>1</sup> PRESSURE-ASSISTED HEAD E. TEST RESULTS

Test No.	Actual Exit Velocity <sup>1</sup> (ft/sec)	%Propane in Nitrogen	Low Htg Val (Btu/ft <sup>3</sup> )	$\Delta P$ Across Head (psig)	Probe Ht <sup>3</sup> (ft)	Observations						Comb Eff (%)	Hydro Carbon Dest Eff (%)
						Wind Speed (mph)	Flame Length (ft)	Lift Off (in)	Color	Smoke	Sound		
207	14.3	15.8	371	0	} Stability Curve Tests								
208A	112	20.2	474	0									
208B	94.7	23.9	562	0									
209	472	23.9	562	2									
210	78.5	26.0	612	0									
211	12.4	18.1	426	0	6	6	2	2	dim orange	none	none	97.0	98.4
212	95.9	21.9	514	0	7	7	2.5	2	yellow-purple base	none	dull rumble-roar	94.2	95.1
214	238	48.1	1130	NR <sup>2</sup>	12	3.5	12	1	yellow-blue	none	roar	99.3	99.8
216	384	29.6	696	NR	16	6	12	4	yellow-blue	none	roar	98.3	98.9
217	14.2	23.7	557	0	6	2.5	3	0	yellow	none	none	99.1	99.6
218	470	35.2	828	3	16	5	14	3	blue base	none	jet	96.2	98.0
219	109	28.4	668	0	7	5	5	0	orange-blue	none	low rumble	98.8	99.2
220	761	28.1	661	7	20	5	18	4	yellow-blue	none	loud roar	97.7	98.5
221	907	36.6	870	10	30	6	20	3	yellow-blue	none	load roar	99.4	99.7

1 Based on total open area of exit ports of 1.77 in<sup>2</sup>.

2 NR = Not recorded.

3 Above flare tip.

Table 2-3  
COMMERCIAL 3.8 INCH DIAMETER<sup>1</sup> PRESSURE-ASSISTED HEAD F TEST RESULTS

Test No.	Actual Exit Velocity <sup>1</sup> (ft/sec)	%Propane in Nitrogen	Low Htg Val (Btu/ft <sup>3</sup> )	$\Delta P$ Across Head (psig)	Probe Ht <sup>3</sup> (ft)	Observations						Comb Eff (%)	Hydro Carbon Dest Eff (%)
						Wind Speed (mph)	Flame Length <sup>2</sup> (ft)	Lift Off (in)	Color	Smoke	Sound		
269	33.9	5.93	139	NR	} Stability Curve Tests								
270	119	7.46	175	NR									
271	112	7.49	176	NR									
272	158	7.20	169	NR									
273	11.1	5.18	122	NR									
274	42.3	7.50	176	0	13	4.5	4.5	0	light blue	none	faint hiss	95.8	97.2
275	52.2	9.08	213	0	15	3	4.5	0	dim blue	none	faint hiss	96.5	97.5
276	5.55	9.10	214	0	8	5 <sup>2</sup>	2	0	transparent	none	none	97.6	98.5
277	4.39	9.92	233	0	5	6	2	0	transparent	none	none	85.5	86.4
278	157	13.8	323	4	25	2	17	0	transparent	none	rumble	95.0	95.4
279	139	18.5	453	4	25	7	18	0	yellow-blue	none	rumble	99.5	100.0
280	25.3	10.7	251	1	15	0.5	8.5	0	yellow	none	faint hiss	99.4	99.8

1 Based on total open area of exit ports of 11.3 in<sup>2</sup>.

2 Based on light diffraction through flame envelope for invisible flame.

3 Height above flare tip

4 Not Recorded.

Table 2-4  
COMMERCIAL 1.5 INCH DIAMETER<sup>1</sup> AIR-ASSISTED HEAD G TEST RESULTS

Test No.	Actual Fuel Exit Velocity <sup>1</sup> (ft/sec)	Propane in Nitrogen (%)	Low <sup>2</sup> Htg Val (Btu/ft <sup>3</sup> )	Air-Assist Flowrate (SCFM)	Air-Assist Exit Velocity (ft/sec)	Air-Assist SR <sup>3</sup>	(ρv) <sub>air</sub> <sup>4</sup> ----- (ρv) <sub>fuel</sub>	Observations						Comb. Eff. (%)	Hydro-Carbon Dest. Eff. (%)	Pilot Flow-rate (SCFM)
								Wind Speed (mph)	Flame Length (ft)	Lift Off (in)	Color	Smoke	Sound			
222	0.73	100	2350	1030	112	79.0	99.4	Stability Curve Tests								0
224	28.7	8.03	189	0	0	0	0									0
225	46.8	13.0	305	0	0	0	0									0
226	263	40.3	947	0	0	0	0									0
227	12.2	9.40	221	0	0	0	0									0
227A	13.8	8.57	201	0	0	0	0									0
228	1.15	100	2350	705	76.6	34.3	43.5									0
229	4.21	27.7	650	412	44.8	19.7	9.38									0
230	90.0	21.4	505	0	0	0	0									0
231A	60.1	32.2	756	784	85.1	2.26	1.22									0
232A	64.0	30.0	706	1110	121	3.21	1.65									0
231B	44.0	43.9	1032	780	84.7	2.25	1.57									0
232B	62.7	30.7	722	1100	119	3.18	1.66									0
233	380	38.8	912	0	0	0	0									0
234	03	48.7	1144	780	84.7	0.294	0.224									0
235	368	38.9	913	1110	120	0.434	0.274									0
236	591	29.3	690	0	0	0	0									0
237	469	54.2	1273	1100	120	0.242	0.199									0
238	464	55.8	1311	544	59.1	0.117	0.0987									0
239	301	47.8	1123	542	58.9	0.210	0.157									0
240	4.59	20.1	473	529	57.4	31.9	11.6									0
241	57.7	20.2	475	535	58.1	2.57	0.924									0

<sup>1</sup> Based on total area of fuel exit ports = 1.77 in<sup>2</sup>. Area of co-axial air channel = 22.1 in<sup>2</sup>.

<sup>2</sup> Includes contribution of pilot

<sup>3</sup> S.R. = Stoichiometric ratio

<sup>4</sup> For example, Test No. 228:  $\rho_{air} = 0.0744 \text{ lb/ft}^3$ ,  $v_{air} = 76.6 \text{ ft/sec}$ ,  $\rho_{fuel} = 0.114 \text{ lb/ft}^3$ ,  $v_{fuel} = 1.15 \text{ ft/sec}$ ,  $(\rho v)_{air}/(\rho v)_{fuel} = 43.5$



Table 2-4 (Continued)

COMMERCIAL 1.5 INCH DIAMETER<sup>1</sup> AIR-ASSISTED HEAD G TEST RESULTS

Test No.	Actual Fuel Exit Velocity <sup>1</sup> (ft/sec)	Propane in Nitrogen (%)	Low <sup>2</sup> Htg. Val (Btu/ft <sup>3</sup> )	Air-Assist Flowrate (SCFM)	Air-Assist Exit Velocity (ft/sec)	Air-Assist SR <sup>3</sup>	(ρv) <sub>air</sub> <sup>4</sup> ----- (ρv) <sub>fuel</sub>	Observations						Comb. Eff. (%)	Carbon Dest. Eff. (%)	Pilot Flow-rate (SCFM)
								Wind Speed (mph)	Flame Length (ft)	Lift Off (in)	Color	Smoke	Sound			
242	98.4	30.3	712	515	56.0	0.98	0.494	9	transparent	4	transparent	none	low rumble	88.8	93.5	0
243	8.47	23.1	547	56	56.0	14.7	5.97	4.5	1	1	blue base	none	low rumble	32.1	37.3	0
244	428	65.0	1528	511	55.6	0.10	0.096	6	12.5	10	yellow-blue	none	loud roar	99.7	99.9	0
245	69.1	43.9	1032	1050	114	1.93	1.34	5.5	1	3	blue base	none	roar	62.3	66.6	0
246	425	60.5	1425	1050	114	0.23	0.203	5	10	8	blue base	none	loud roar	99.7	99.9	0
247	10.9	100	2350	1040	113	5.42	6.75	4	transparent	1	blue base	none	drone	54.5	58.4	0
248	504	15.8	376	0	0	0	0	<div style="display: flex; align-items: center; justify-content: center;"> <div style="font-size: 4em; margin-right: 10px;">}</div> <div>Stability Curve Tests</div> </div>								2.1
249	514	17.3	413	515	56.0	0.320	0.101									2.1
250	509	16.5	391	1040	113	0.694	0.208									2.1
251	395	20.1	476	0	0	0	1									2.1
252	327	20.4	474	513	55.7	0.156	1.464									2.1
253	431	14.0	334	1040	113	0.249	0.960									2.1
254	207	9.35	229	0	0	0	0									2.1
255	223	8.48	210	513	55.7	0.244	1.50									2.1
256	126	15.6	380	1030	112	0.836	2.95									2.1
257	87.1	8.69	229	0	0	0	0									2.1
258	67.8	11.1	290	513	55.7	0.788	3.787									2.1
259	41.7	18.0	460	1030	112	2.49	7.64									2.1
260	394	20.9	496	1050	114	0.73	0.265	2.5	1.5	4	blue base	none	loud rumble	57.7	59.1	2.1
261	103	18.2	441	1040	113	3.06	1.01	4	1	2	blue base	none	low roar	34.3	35.8	2.1
262	357	37.3	877	1050	114	0.45	0.267	5	1.5	6	blue base	none	loud roar	99.6	99.9	2.1

<sup>1</sup> Based on total area of fuel exit ports = 1.77 in<sup>2</sup>. Area of co-axial air channel = 22.1 in<sup>2</sup>.

<sup>2</sup> Includes contribution of pilot

<sup>3</sup> S.R. = Stoichiometric ratio

<sup>4</sup> For example, Test No. 228:  $\rho_{air} = 0.0744 \text{ lb/ft}^3$ ,  $v_{air} = 76.6 \text{ ft/sec}$ ,  $\rho_{fuel} = 0.114 \text{ lb/ft}^3$ ,  $v_{fuel} = 1.15 \text{ ft/sec}$ ,  $(\rho v)_{air}/(\rho v)_{fuel} = 43.5$

Table 2-5  
3 INCH DIAMETER OPEN PIPE FLARE (WITH PILOT) TEST RESULTS

Test No.	Actual Exit Velocity <sup>1</sup> (ft/sec)	% Propane in Nitrogen	Low Htg Val <sup>2</sup> (Btu/ft <sup>3</sup> )	Probe Ht. (ft)	Wind Speed (mph)	Flame Length (ft)	Lift Off (in)	Color	Smoke	Sound	Comb Eff. (%)	Hydro-Carbon Dest. Eff (%)	Pilot Flowrate (SCFM)
263	203	9.96	237	}	Flame Stability Tests								2.08
264	68.8	2.89	76.1										2.11
265	9.82	9.07	260										2.10
266	96.7	7.61	184										2.09
267	1.93	7.51	375	11	6	1	2	faint yellow	none	low hiss	98.7	99.2	2.07
268	209	21.0	495	32	5	30	10	blue, yellow	none	med. roar	98.8	99.97	2.09

1 Based upon pipe inside diameter of 3.125 inches.

2 Including pilot contribution.

Table 2-6

## RESULTS OF SCREENING TESTS ON FLARE SCREENING FACILITY

Compound	Gas Composition (%)			Velocity at Stability Limit (ft/sec) <sup>1</sup>	Lower Heating Value (Btu/ft <sup>3</sup> )	DE <sup>2</sup> (%)	CE <sup>3</sup> (%)	Soot (mg/m <sup>3</sup> )
	Compd	Propane	N <sub>2</sub>					
Acetylene	100	0	0	854	1475	99.99	99.97	<1.5
Ethylene	100	0	0	443	1580	99.91	99.92	<1.5
Propylene	100	0	0	184	2300	99.98	99.93	<1.5
1,3-Butadiene	100	0	0	127	2730	99.93	99.93	75 <sup>5</sup>
Butane	100	0	0	58	3321	99.99	99.96	<1.5
Propane	100	0	0	143	2350	99.98	98.18	<1.5
Propane	75	0	25	48	1763	99.97	NA <sup>4</sup>	<1.5
Benzene	1.50	98.5	0	61	2370	99.59	99.95	<1.0
Toluene	1.50	98.5	0	61	2381	99.99	99.90	<1.0
Chlorobenzene	1.15	98.85	0	58	~2350	99.49	99.95	<1.0
Carbon Monoxide	100	0	0		Could Not Ignite <sup>6</sup>			
Carbon Monoxide	20	80	0	108	1943	99.60	99.88	<1.0
Carbon Monoxide	17	37	46	30	923	79.72 <sup>7</sup>	99.42	<1.0
Acetone	1.43	98.57	0	59	2347	99.80	99.96	<1.0
Acetaldehyde	2.07	97.93	0	58	2331	99.99	99.97	<1.5
Ethylene Oxide	1.42	98.58	0	58	2337	96.95	99.95	<1.0
CO <sub>2</sub> Diluent	7.58	92.42	0	93	2171	NA	99.93	<1.0
Methyl Chloride	9.17	90.83	0	65	2212	99.94	99.96	<1.0
Ethylene Dichloride	1.43	98.57	0	58	2335	99.70	99.95	<1.0
Vinyl Chloride	0.11	99.89	0	31	~2350	96.79	NA	<1.0
Methyl Mercaptan	10.7	89.30	0	65	2228	99.39	99.82	<1.0
Acrylonitrile	1.47	98.53	0	58	~2350	99.99	99.96	<1.0
Hydrogen Cyanide	0.013	99.99	0	78	~2350	85.00	NA	<1.0
Ammonia	100	0	0		Could Not Ignite <sup>6</sup>			
Ammonia	20	80	0	74	1967	99.90	NA	<1.0

1 = Nozzle ID = 0.042 inches

2 = Destruction Efficiency

3 = Combustion Efficiency

4 = Not available

5 = Without steam or air assist

6 = On 1/16 inch nozzle without pilot flames

7 = DE calculated assuming no CO originated from propane

Table 2-7. In order to determine the limits of stable operation for these flares and gas mixtures, and the key operating conditions that affect flame stability and efficiency, some conditions with poor stability and low combustion efficiencies were measured. Such results merely indicated flare operation at or beyond the edge of the operating envelope, and are not indicative of normal commercial flare operation.

The results showed that flare head design influenced the flame stability as shown in Figure 2-3 for the coanda steam-injected head and the pressure-assisted heads. The stability of the air-assisted head flame was controlled by the momentum ratio of air-assist to fuel streams as shown in Figure 2-4; heating value of the gas had little influence on flame stability, except under conditions with no air-assist. Combustion efficiency for the pressure and coanda steam-injected heads correlated with the individual flame stability limit for each head as shown in Figure 2-5. Figure 2-6 shows the relationship between combustion efficiency and air to fuel momentum ratio,  $(\rho v)_{\text{air}}/(\rho v)_{\text{fuel}}$ , for the air-assisted head.

The relative flare performance of different gases can be determined on the FSF, although the value determined on the lab-scale FSF for flame structure, flame stability, and combustion and destruction efficiencies will be different than measured on pilot and industrial scale flares. Such differences in stability are shown in Figure 2-7, comparing flame stability for different sized open-pipe nozzles. Comparison of ethylene oxide destruction efficiency on the FSF (1/16 inch nozzle) and the pilot-scale FTF (3 inch open pipe flare) shows the difference in destruction efficiency measured in the two facilities. Ethylene oxide DE on the FSF was 96.95 percent, compared to 98.4 and 99.5 percent on the FTF. Also, industrial flares typically employ pilots and/or flame retention devices to stabilize the flame and enhance combustion which were absent in these tests.

Tests identified six compounds which were difficult to destroy on the FSF, using a 1/16 inch nozzle (ID = 0.042 inches). These were:

Table 2-7

GAS MIXTURE COMBUSTION AND DESTRUCTION EFFICIENCY  
TEST RESULTS: 3 INCH FLARE, NO PILOT

Test	ID	Actual Exit Velocity (ft/sec)	Gas Composition <sup>1</sup> (%)	Gas Htg Val <sup>3</sup> (Btu/ft <sup>3</sup> )	Probe Ht. <sup>3</sup> (ft)	Observations						Hydro-Carbon Comb. Eff (%)	Dest Eff (%)
						Wind Speed (mph)	Flame Length (ft)	Lift-Off (in.)	Color	Smoke	Sound		
281	NH <sub>3</sub>	8.79	NH <sub>3</sub> 1.5	561	12	5	6	3	Blue base, orange	None	None	99.3	92.1
282	NH <sub>3</sub>	9.47	NH <sub>3</sub> 1.7 Propane 36.9	877	12	5	7	0	Bright Orange	Very Little	None	99.6	99.7
283	NH <sub>3</sub>	0.15	NH <sub>3</sub> 4.43 Propane 13.2	336	4	2	0.5	0	Orange	None	None	99.3	95
284	NH <sub>3</sub>	138	NH <sub>3</sub> 4.02 Propane 27.0	658	33	3	20	36	Blue-orange	None	Rumble	99.7	99.5
285	NH <sub>3</sub>	9.56	NH <sub>3</sub> 1.98 Propane 17.2	416	12	1	8	24	Blue base, orange	None	None	92.1	Tenax
286	H <sub>2</sub> S	8.89	H <sub>2</sub> S 1.5 Propane 23.3	556	12	5	7	24	Orange	None	None	93.2	NA <sup>2</sup>
287	H <sub>2</sub> S	139.1	H <sub>2</sub> S 4.14 Propane 26.5	646	36	3	22	24	Blue base, orange	None	Rumble	98.1	NA <sup>2</sup>
288	H <sub>2</sub> S	9.11	H <sub>2</sub> S 4.29 Propane 31.2	757	14	6	9	0	Bright orange	None	None	99.4	NA <sup>2</sup>

<sup>1</sup> Remainder N<sub>2</sub>

<sup>2</sup> Destruction efficiency data for H<sub>2</sub>S is not available due to analytical errors in the measurements.

<sup>3</sup> Height above flare tip

Table 2-7 (Continued)

GAS MIXTURE COMBUSTION AND DESTRUCTION EFFICIENCY  
TEST RESULTS: 3 INCH FLARE, NO PILOT

Test	ID	Actual Exit Velocity (ft/sec)	Gas Composition <sup>1</sup> (%)		Gas Htg Val (Btu/ft <sup>3</sup> )	Probe Ht. <sup>3</sup> (ft)	Observations						Hydro- Carbon Comb. Eff (%)	Dest Eff (%)
							Wind Speed (mph)	Flame Length (ft)	Lift Off (in.)	Color	Smoke	Sound		
289	H <sub>2</sub> S	9.11	H <sub>2</sub> S 7.61 Propane 21.1		539	14	5	8	12	Orange	V.Little	None	99.2	Tenax
290	H <sub>2</sub> S	0.669	H <sub>2</sub> S 4.74		370	4	4	1.5	0	Dim-orange	None	None	97.7	Outside Sample Limits
291	1,3- Butadiene	0.296	1,3- But. 11.2		305	4	3	1	2	Orange	Slight Dark	None	98.2	99.2
292	1,3- Butadiene	6.87	1,3- But. 5.32		145	13	3	6	6	Orange	Slight	None	95.8	96.8
293	1,3- Butadiene	7.03	1,3- But. 7.77		212	15	7	5	0	Orange	Grey- Black	None	97.7	99.9
294	Ethylene Oxide	0.320	Eth. 13.2 Oxide		178	4	2	1	0	Dim-orange	None	None	98.4	99.2
295	Ethylene Oxide	4.63	Eth. 13.0 Oxide		175	7	7	4	NR	Transparent	None	None	99.5	99.7

<sup>1</sup> Remainder N<sub>2</sub>

<sup>2</sup> Destruction efficiency data for H<sub>2</sub>S is not available due to analytical errors in the measurements.

<sup>3</sup> Height above flare tip

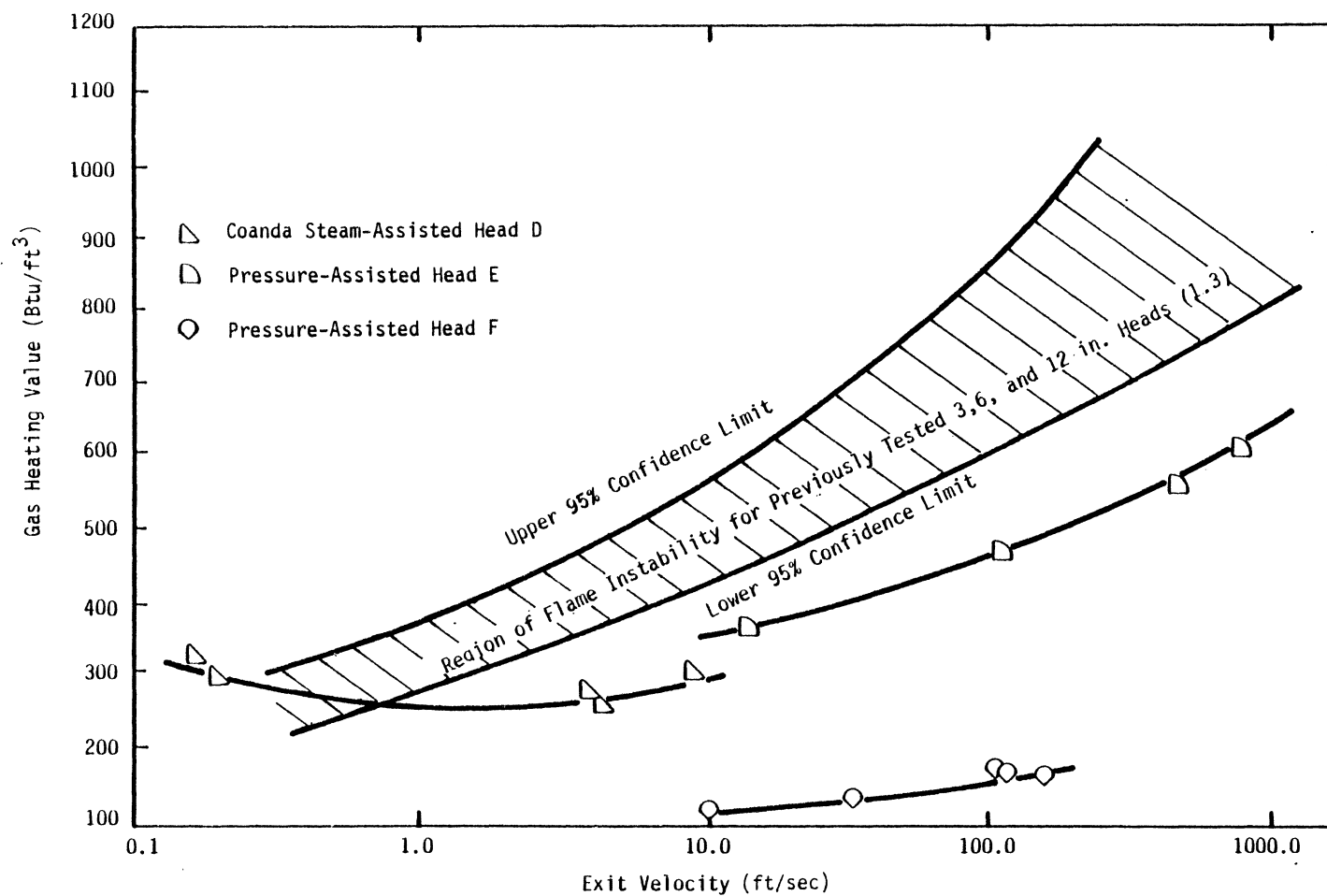


Figure 2-3. Region of flame stability for steam-injected and pressure-assisted heads D, E, and F.

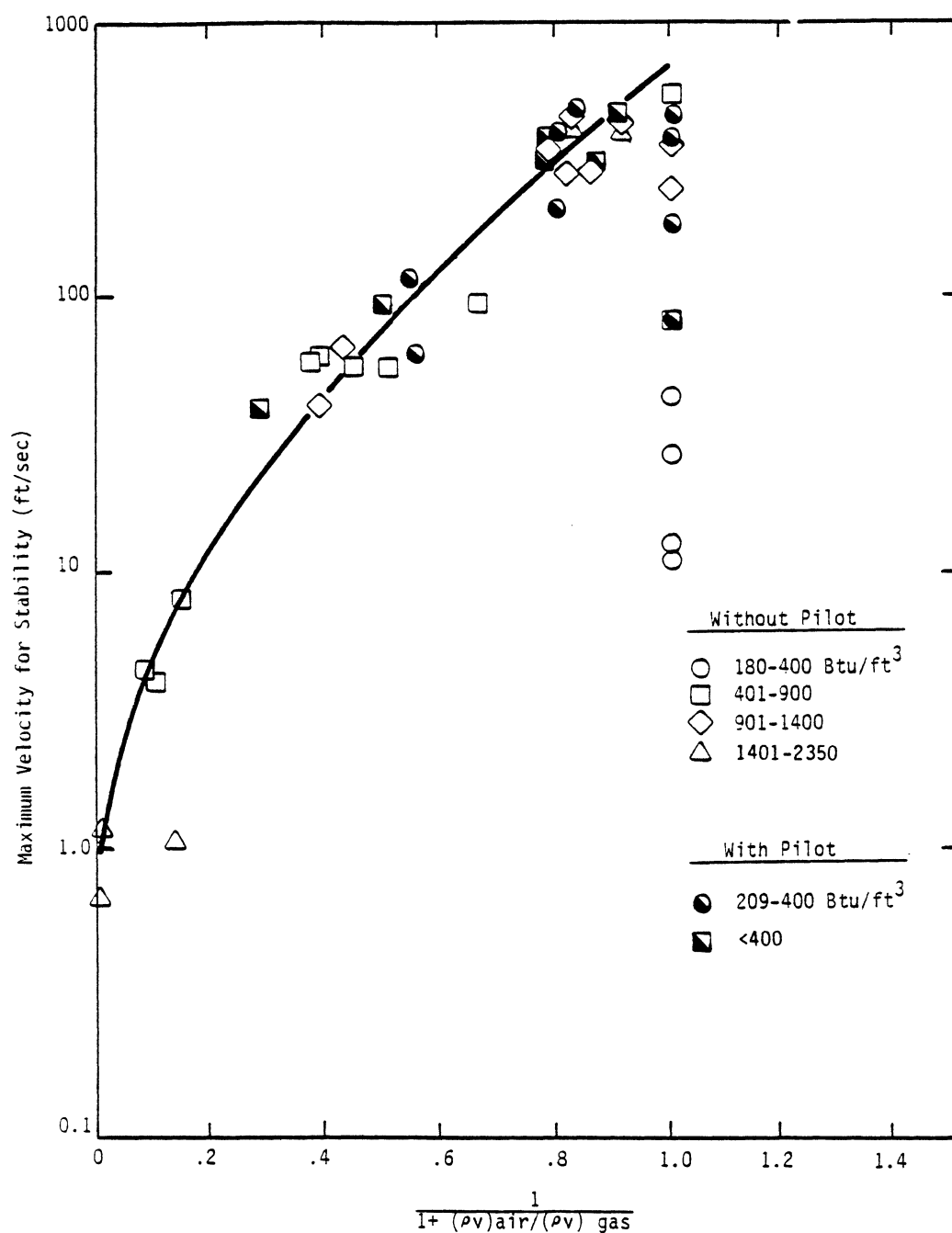


Figure 2-4 . Maximum gas exit velocity for stability versus air-assist to gas momentum ratio for the air-assisted head G, with and without pilot.



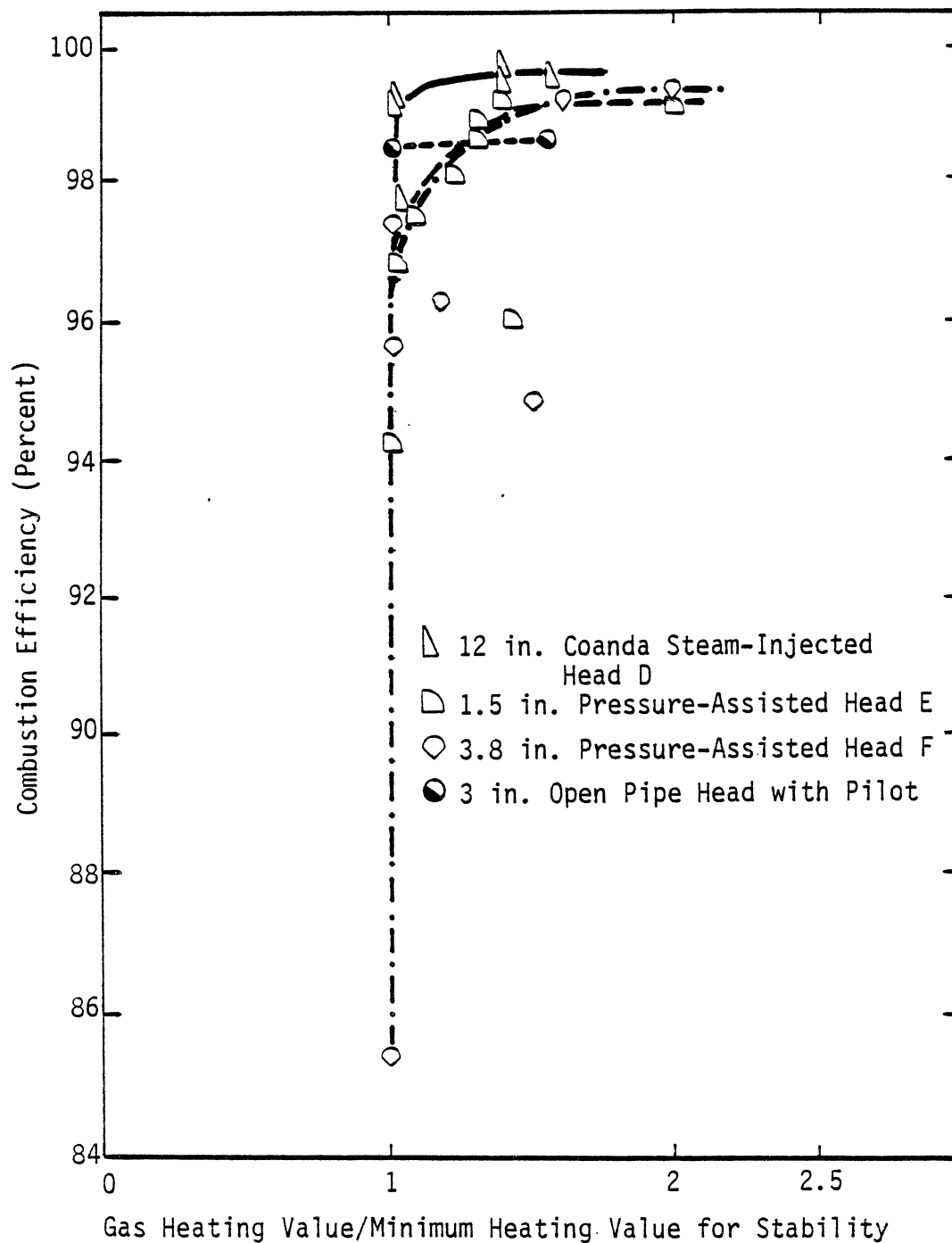


Figure 2-5. Combustion efficiency vs. flame stability for steam-injected and pressure-assisted flare heads.

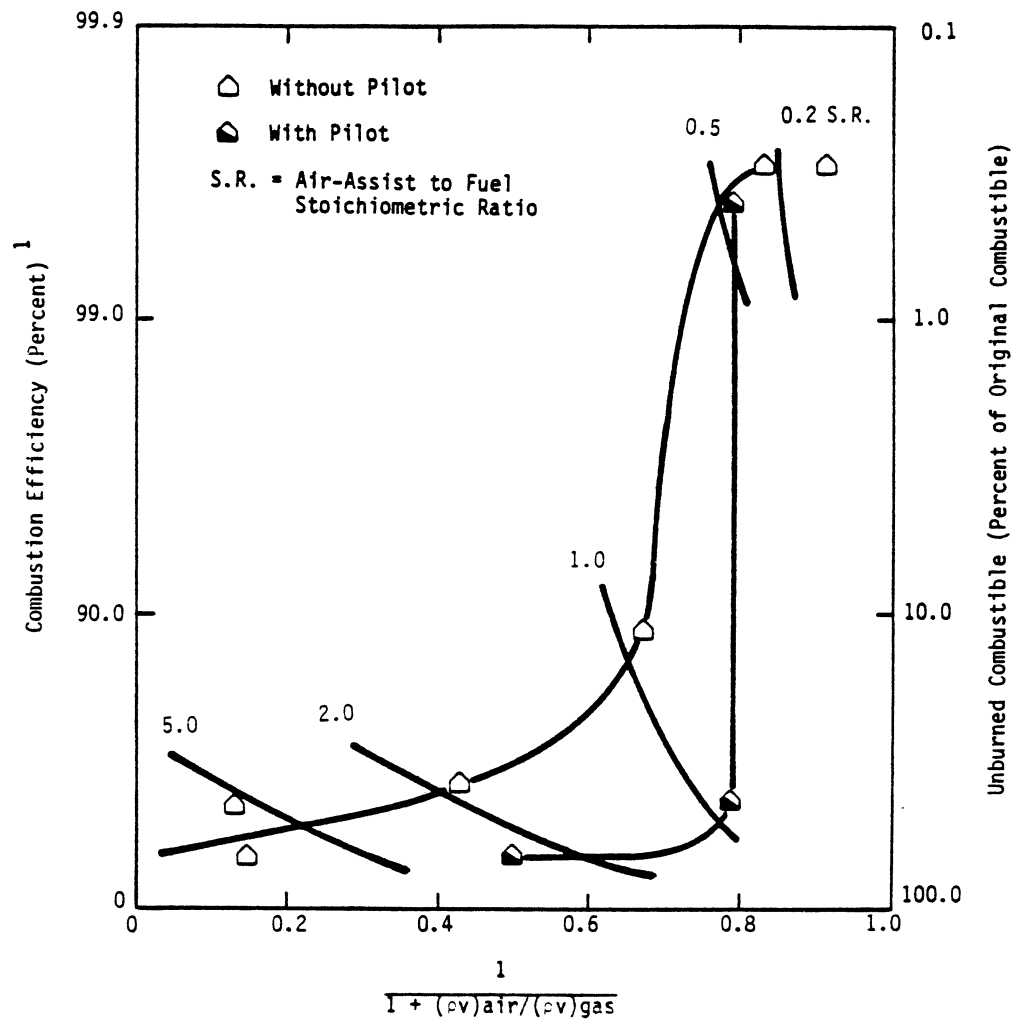


Figure 2-6. Combustion efficiency vs air-assist to gas momentum ratio for commercial air-assisted head G.

<sup>1</sup> Scale is  $\log(100-CE)$

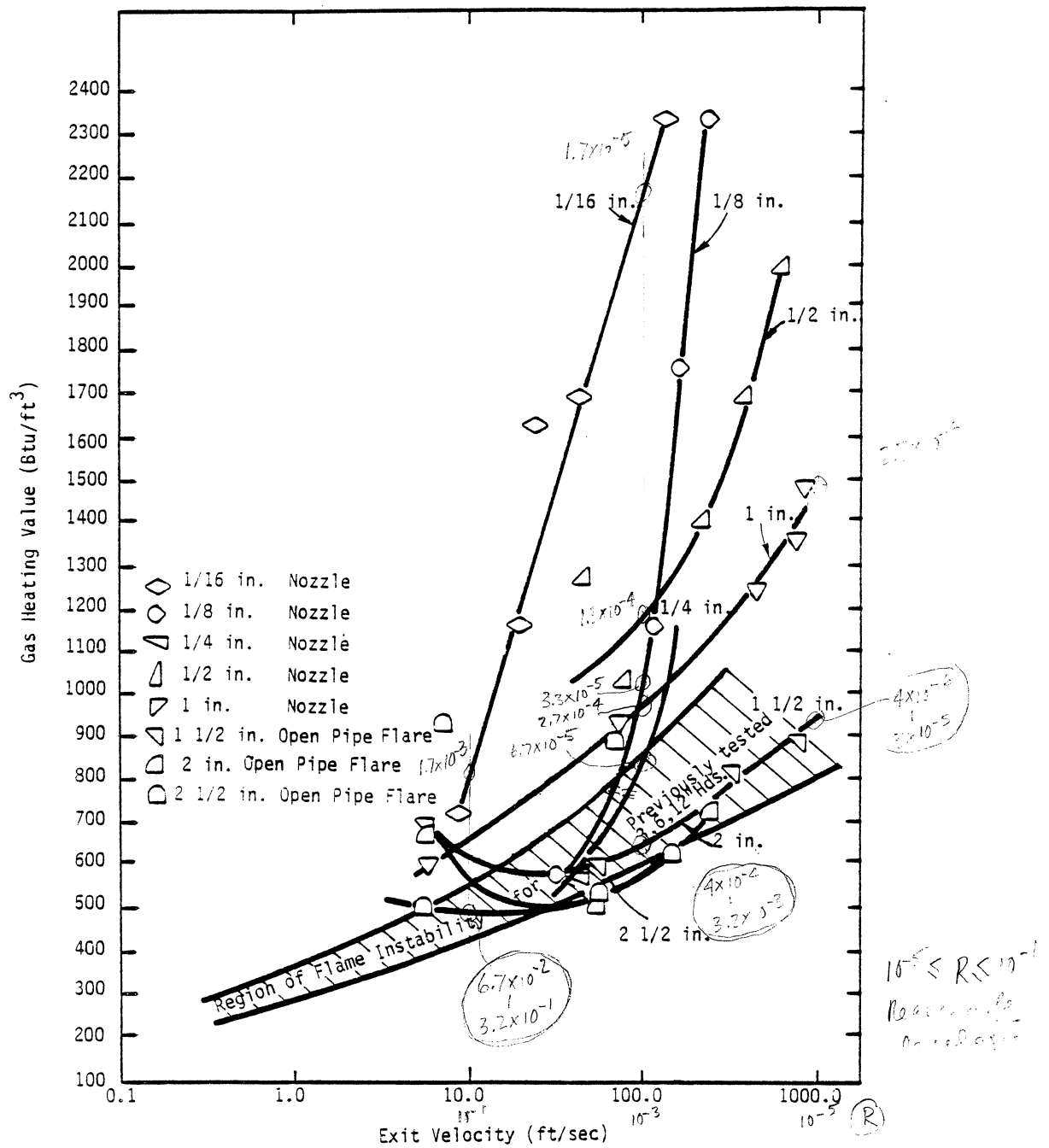


Figure 2-7. Flame stability curves for pipe flare heads, 1/16 in. through 2 1/2 in. flares are without flame retention devices. The 3, 6, and 12 in. heads were tested with and without flame retention devices.

- 1,3-butadiene has the potential without steam or air assist to yield large amounts of soot (75 mg/m<sup>3</sup>)
- CO was difficult to ignite when pure
- Ethylene oxide yielded destruction efficiency of 96.95 percent
- Vinyl chloride yielded destruction efficiency of 96.79 percent
- HCN yielded low destruction efficiency of 85.00 percent
- NH<sub>3</sub> was difficult to ignite when pure without a pilot

Destruction efficiencies (DE's) for NH<sub>3</sub>, 1,3-butadiene, ethylene oxide, propane, and H<sub>2</sub>S were measured on the FTF. The flame stability curve depended on the compound as shown in Figure 2-8. (H<sub>2</sub>S and NH<sub>3</sub> were tested as minor constituents in propane-nitrogen mixtures). The DE of the individual compounds depended on compound type but correlated with the respective stability curve for NH<sub>3</sub>, 1,3-butadiene, ethylene oxide, and propane as shown in Figure 2-9. The primary influence on destruction and combustion efficiency is flame stability, not gas heating value or exit gas velocity. H<sub>2</sub>S destruction efficiency results are unavailable because of analytical problems. The destruction efficiency of propane in mixtures with small amounts of NH<sub>3</sub> or H<sub>2</sub>S are reported in Figure 2-9 as propane in ammonia tests and propane in hydrogen sulfide tests.

The following conclusions were reached based on the results:

- Flames from nozzles less than 1 1/2 inches in diameter generally are not similar to flames from larger nozzles.
- Flare head design can influence the flame stability curve.
- Combustion efficiency can be correlated with flame stability based upon gas heating value for the pressure heads and the coanda steam-injected head.
- For the limited conditions tested, the flame stability and combustion efficiency of the air-assisted head correlated with the

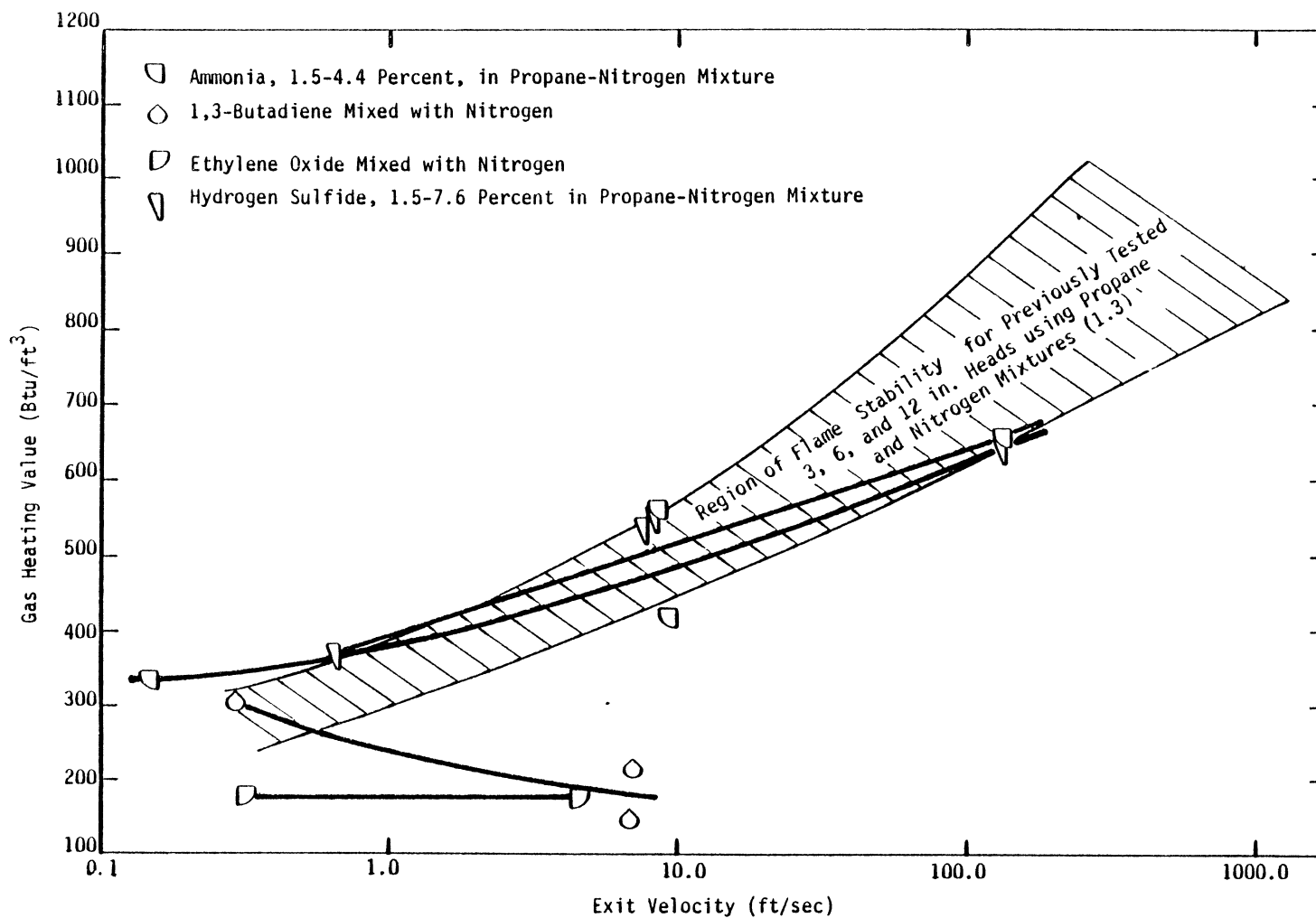


Figure 2-8. Region of flame stability for the 3 inch open pipe flare head burning selected relief gas mixtures.

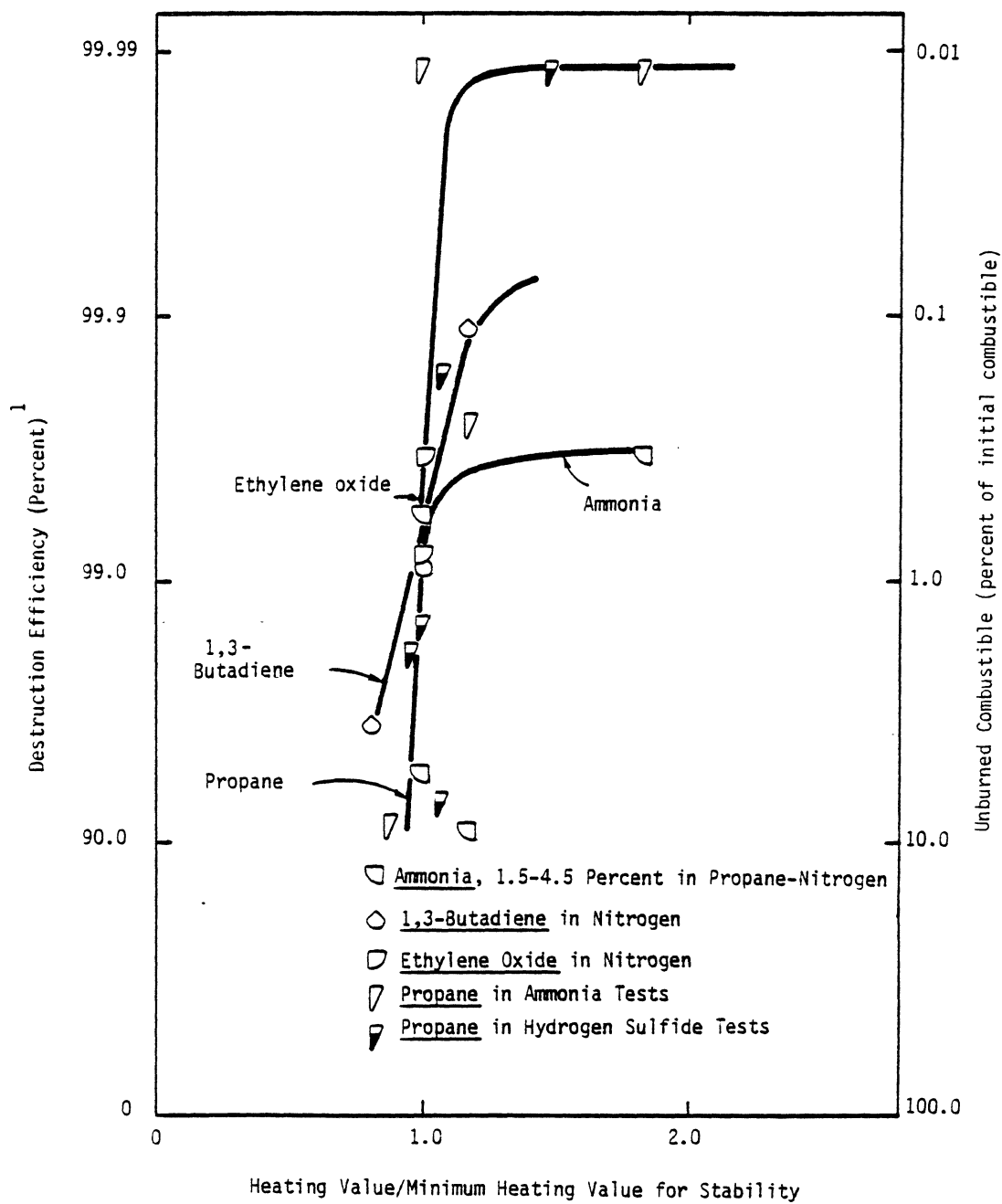


Figure 2-9. Destruction efficiency of different gases.

<sup>1</sup> Scale is  $\log(100-DE)$

momentum ratio of air to fuel; the heating value of the gas had only a minor influence.

- Limited data on an air-assisted flare shows that use of a pilot light improves flame stability.
- The destruction efficiency of compounds depends on the structure of the compounds.
- The destruction efficiency of different compounds can be correlated with the flame stability curve for each compound, for the compounds tested in this program.
- Stable flare flames and high (>98-99 percent) combustion and destruction efficiencies are attained when the flares are operated within operating envelopes specific to each flare head and gas mixture tested. Operation beyond the edge of the operating envelope results in rapid flame de-stabilization and a decrease in combustion and destruction efficiencies.

### 3.0 FLARE AERODYNAMICS

The aerodynamics of different sized flare heads was studied prior to testing the influence of flare head types or gas composition on flare efficiency. The aerodynamic studies were conducted to determine the minimum head size which would yield results similar to full scale commercial flare heads. Flare flame length prediction techniques were also investigated during this study. The results were used to select flare head sizes for the commercial head and gas composition tests.

The aerodynamics study included a review of previous flare studies as well as experimental work testing 1/2 inch to 2 1/2 inch open pipe flare heads, without flame retention devices. The results were used to develop relations between Reynolds number and Richardson number and flame length, flame stability and flame temperature. (3.1)

#### 3.1 Reynolds Number and Richardson Number

The relief gas Reynolds number ( $Re$ ) and Richardson number ( $Ri$ ) at the nozzle exit determine the aerodynamic structure of the flare flames. Reynolds Number ( $Re$ ) is a measure of the inertial to viscous forces of the flame, and  $Ri$  is a measure of buoyant forces to inertial forces of the flame. A flame with  $Ri$  greater than one is dominated by buoyant forces and one with  $Ri$  less than one is dominated by inertial forces. Figure 3-1 compares  $Re$  and  $Ri$  for 1/16 inch through 12 inch flare heads tested at EER, using simulated relief gas mixtures of propane-nitrogen. The shaded area indicates the region of head size and exit velocities for typical industrial sized flares. Since  $Re$  depends on the relief gas composition, the data points are frequently not exactly on the approximate grid line drawn for flares of different sizes. The general trend, however, is evident. As the flare size decreases, the nozzle  $Re$  and  $Ri$  decrease. Flames from smaller nozzles are dominated by inertial and turbulent forces, and are aerodynamically dissimilar to larger, buoyancy dominated flames from industrial flare heads.



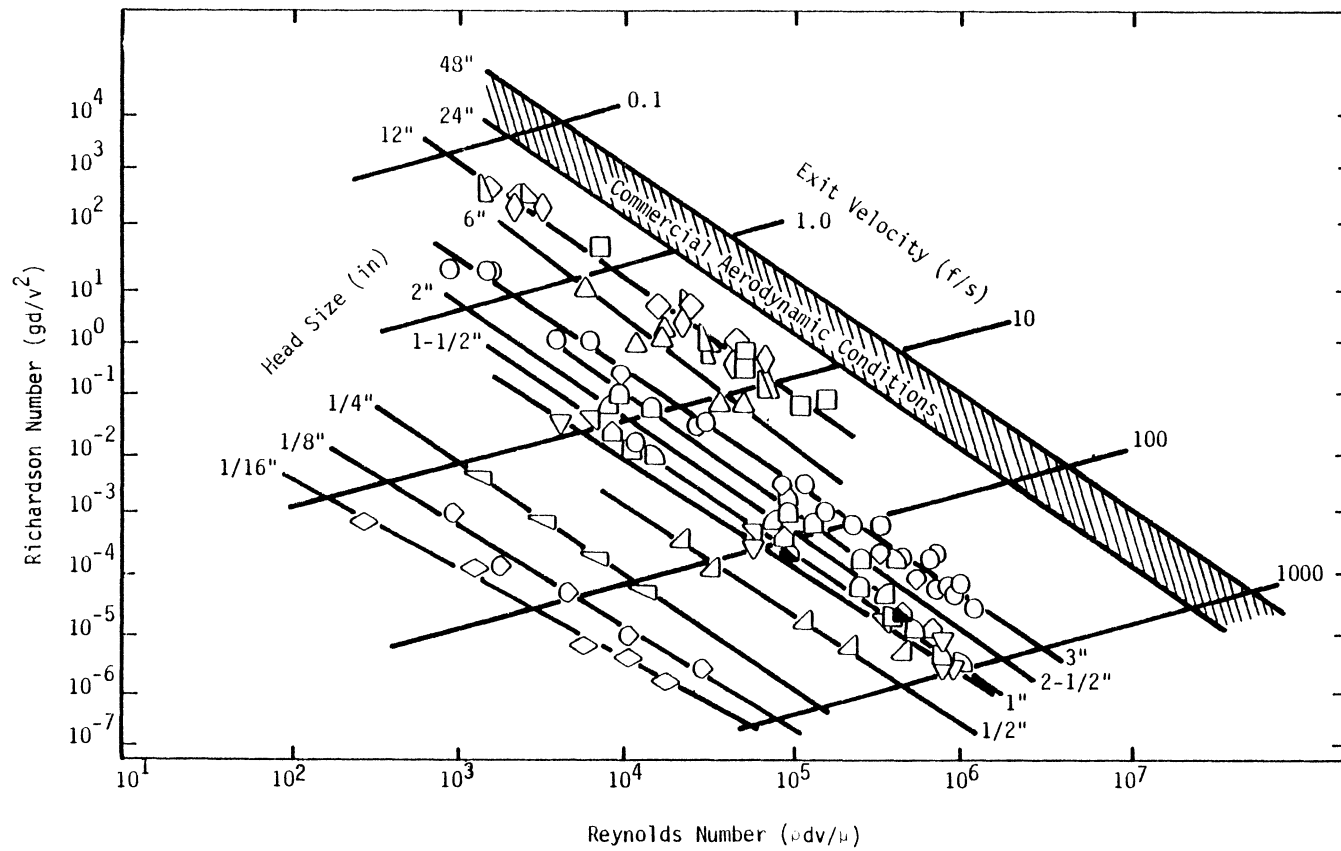


Figure 3-1. Aerodynamic conditions of flares tested at EER compared to typical commercial flare conditions.

# Legend for Figure 3-1

## New EER Data

- ◇ 1/16 in. (0.042 in. ID) Nozzle
- ◇ 1/8 in. (0.085 in. ID) Nozzle
- ▽ 1/4 in. (0.180 in. ID) Nozzle
- △ 1/2 in. Nozzle
- ▽ 1 in. Nozzle
- ▽ 1 1/2 in. Nozzle
- ◻ 1 1/2 in. Commercial Pressure-Assisted Head E
- ◻ 1 1/2 in. Commercial Air-Assisted Head G
- ◼ 1 1/2 in. Commercial Air-Assisted Head G with pilot
- ◻ 2 in. Open Pipe Flare Head
- ◻ 2 1/2 in. Open Pipe Flare Head
- ◇ 3.8 in. Commercial Pressure-Assisted Head F
- △ 12 in. Commercial Coanda Steam-Injected Head D

## Previous EER Data (1.3)

- 3 in. Open Pipe Flare Head
- △ 6 in. Open Pipe Flare Head
- ◇ 12 in. Open Pipe Flare Head
- △ 12 in. Commercial Head A
- ◇ 12 in. Commercial Head B
- 12 in. Commercial Head C

### 3.2 Flame Length

Current and previous test results of measured flame lengths from flares were compared to predicted flame lengths using information and techniques available in the literature (3.2-3.4). Neither empirical (3.5-3.7), complex integral (3.8, 3.9), nor differential (3.10-3.13) techniques could predict the flame lengths or trends in the flame length of this or other studies of large flare flames. Figure 3-2 shows the comparison of flame length measured in a previous EER flare study (1.3) with predictions using techniques suggested in the literature. For example, the technique of Brzustowski, et al. (3.14) predicted a flame length of 18-28 feet, depending upon conditions, and Becker, et al. (3.9, 3.15, 3.16) predicted a flame length of 18 to 35 feet, when the observed flame length was 30 feet.

Much better agreement between observed and predicted flame lengths was achieved by fitting the data with a cruder approach (3.1, 3.2). The approach used by API (3.2) correlates the flame length with the heat release. This correlation, suggested by Hottel and Hawthorne (3.17), is based on data from small flames, where combustion was limited by air diffusion into the flame. Although this prediction has been criticized for its inaccuracy (3.18), Figure 3-3 shows relatively good agreement with the data of this study, data from larger flares, and the original data of the API study. For flame length predictions of large flares, the coefficients in this correlation were adjusted. Using the same API prediction with coefficients adjusted for large flares of this study, poorer agreement was found for the flame lengths produced from some smaller flares. Flame lengths not accurately predicted by the API correlation were from small nozzles ( $\triangle$ -1/2 inch,  $\nabla$ -1 inch,  $\nabla$ -1 1/2 inch,  $\triangleleft$ -2 inch), the coanda steam-injected head ( $\Delta$ ), and the air-assisted head ( $\triangle$  and  $\blacktriangle$ ). The flame length from nozzles smaller than 1/2 inch agree with previous predictions. However, use of the relationship derived from nozzles less than 1 1/2 inch in diameter would severely under-predict the length of the flames from large flare heads.

Figure 3-3 also shows the least-squares fit of flame length vs heat release for 3 through 12 inch heads tested previously at EER. Data from the

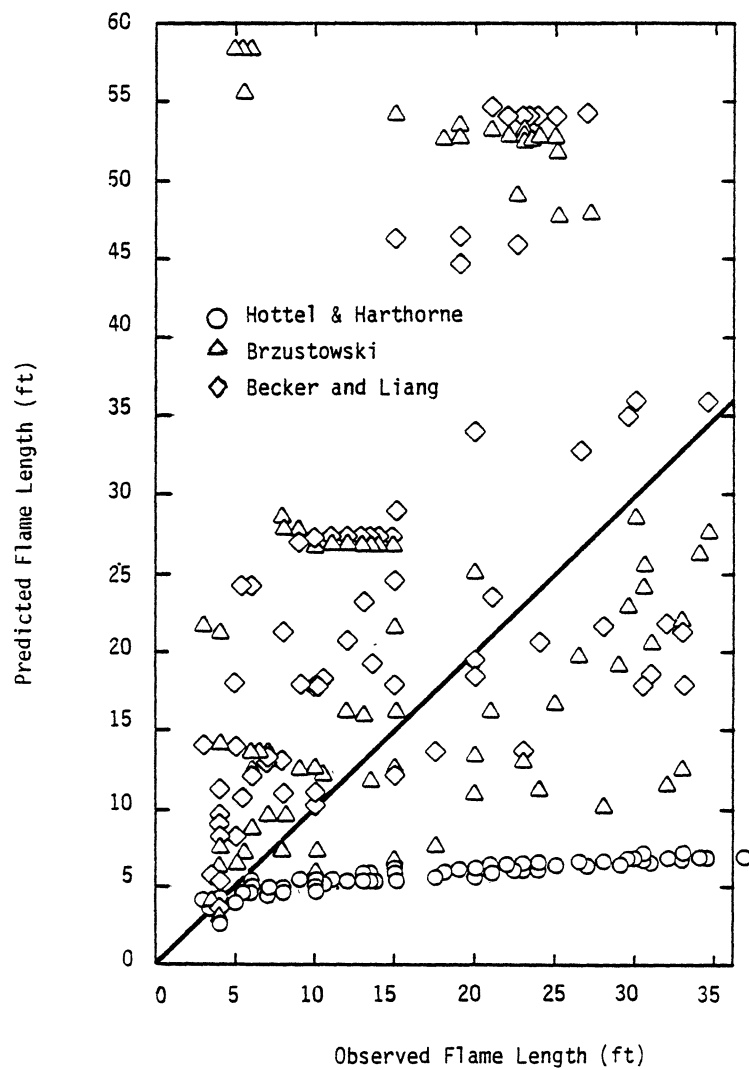


Figure 3-2. Comparison of flame lengths predicted by available studies with those observed in this study.

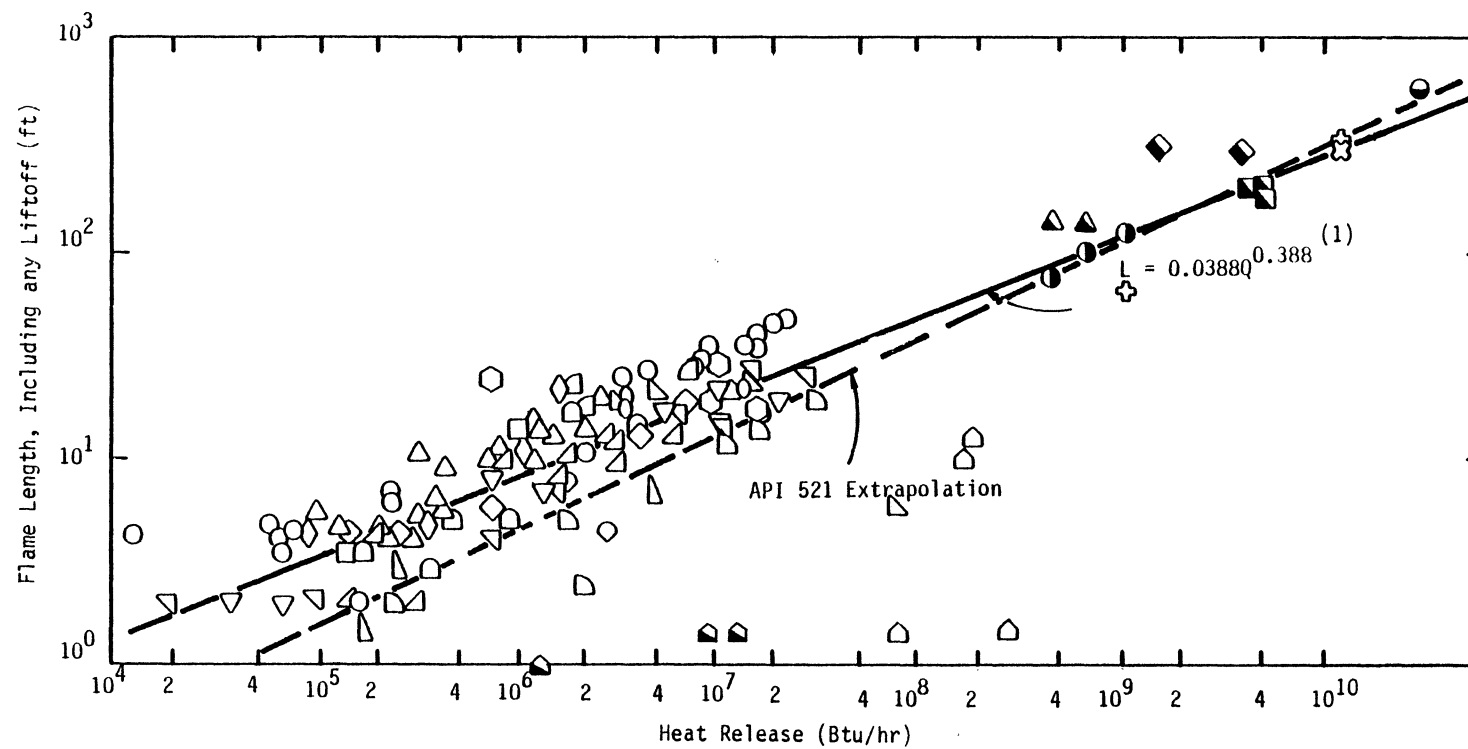


Figure 3-3. Correlation of flame length with heat release for 1/2 inch to 31 inch flares.

(1) Correlation based on 3 through 12 inch flare heads tested previously (1.3).

### Legend for Figure 3-3

API Data (3.2)	<ul style="list-style-type: none"> <li>● Fuel Gas--20 in. Stack (in line)</li> <li>● Algerian Gas Well</li> <li>▲ Catalytic Reformer--Recycle Gas--24 in. Stack</li> <li>■ Catalytic Reformer--Reactor Effluent Gas--24 in. Stack</li> <li>◆ Dehydrogenation Unit--12 in. Stack</li> <li>✱ Hydrogen--31 in. Stack</li> <li>✚ Hydrogen--30 in. Stack</li> </ul>
Straitz Data (3.3, 3.4)	<ul style="list-style-type: none"> <li>○ Natural Gas, 2, 3, 6 in. Head</li> <li>○ Propane, 2, 3 in.</li> </ul>
New EER Data	<ul style="list-style-type: none"> <li>△ 1/2 in. Nozzle</li> <li>▽ 1 in. Nozzle</li> <li>▽ 1 1/2 in. Open Pipe Flare Head</li> <li>◐ 1 1/2 in. Commercial Pressure-Assisted Head E</li> <li>◑ 1 1/2 in. Commercial Air-Assisted Head G without Pilot</li> <li>◒ 1 1/2 in. Commercial Air-Assisted Head G with Pilot</li> <li>◓ 2 in. Open Pipe Flare Head</li> <li>◔ 2 1/2 in. Open Pipe Flare Head</li> <li>◕ 3.8 in. Commercial Pressure-Assisted Head F</li> <li>◖ 12 in. Commercial Coanda Steam-Injected Head D</li> </ul>
Previous EER Data (1.3)	<ul style="list-style-type: none"> <li>○ 3 in. Open Pipe Flare Head</li> <li>△ 6 in. Open Pipe Flare Head</li> <li>◇ 12 in. Open Pipe Flare Head</li> <li>◐ 12 in. Commercial Head A</li> <li>◑ 12 in. Commercial Head B</li> <li>◒ 12 in. Commercial Head C</li> </ul>

present test program shows surprisingly good correlation with this least squares fit for flame lengths from 1/16 through 1/4 inch nozzles (Figure 3-4), but somewhat poorer correlation for some of the larger, commercial heads as discussed above.

A correlation was developed in previous work (1.3) relating flame length to the Richardson number, corrected for the volume change caused by increase in the gas temperature from ambient to the flame temperature:

$$L/d = 7.41 \frac{q \times F}{C_{p\infty} T_{\infty} (1+26x)}^{0.60} Ri^{-0.216} \quad 3-1$$

where L = flame length, ft

d = flare head diameter, ft

q = 2,350 Btu/ft<sup>3</sup>, propane gas lower heating value

x = mole fraction of propane in the fuel

F = fraction of heat lost by radiation from the flame

C<sub>p∞</sub> = constant pressure heat capacity of the air, Btu/ft<sup>3</sup>R

T<sub>∞</sub> = ambient temperature, R

26 = factor to account for the change in moles as a result of stoichiometric combustion of propane.

Ri = Richardson Number based on conditions at flare head (gd/v<sup>2</sup>)

The factor F was not measured in this study, but its relative value was obtained from a single set of data with different mole fraction of propane and a constant Richardson number of 2.0 as shown in Figure 3-5. This relation was then applied to all other flames. The absolute value of F does not matter for a correlation with a single fuel. However, F factors are available in the literature and will be required for correlations of flames burning different gases.

Equation 3-1 was empirically derived, but is based upon results of several previous studies. Workers in combustion research (3.19-3.25) have

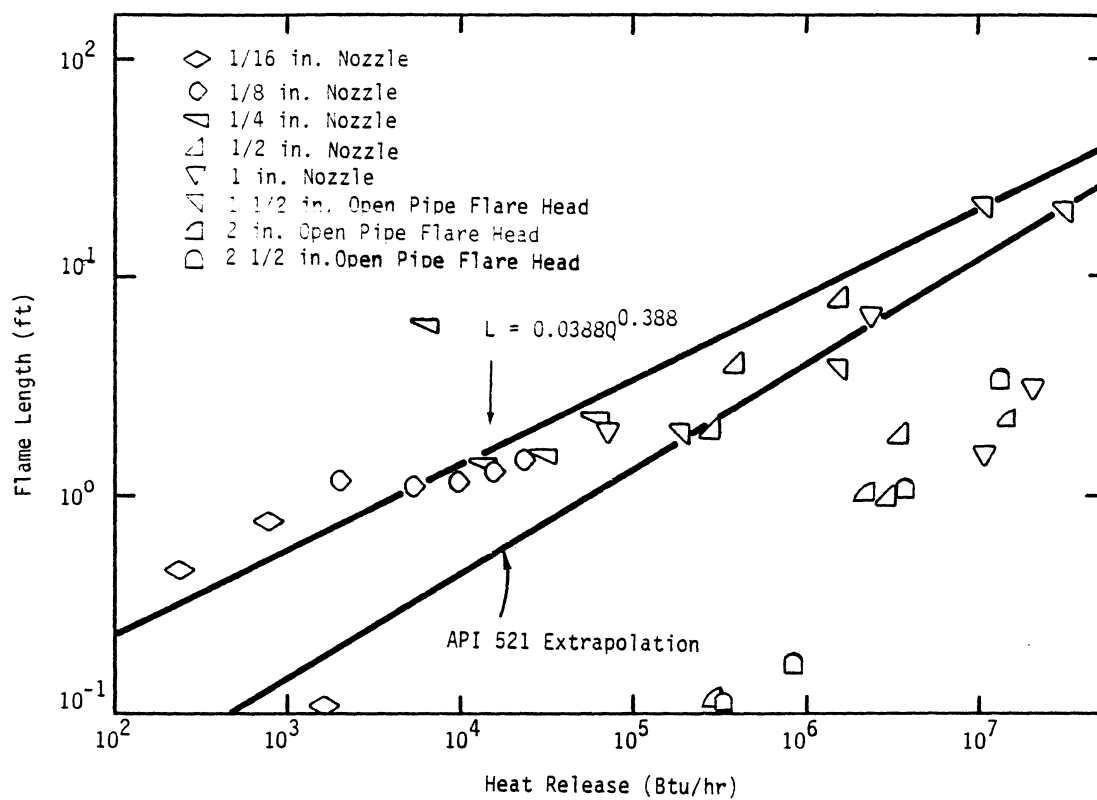


Figure 3-4. Correlation of flame length to heat release for 1/16 inch through 2 1/2 inch flares.



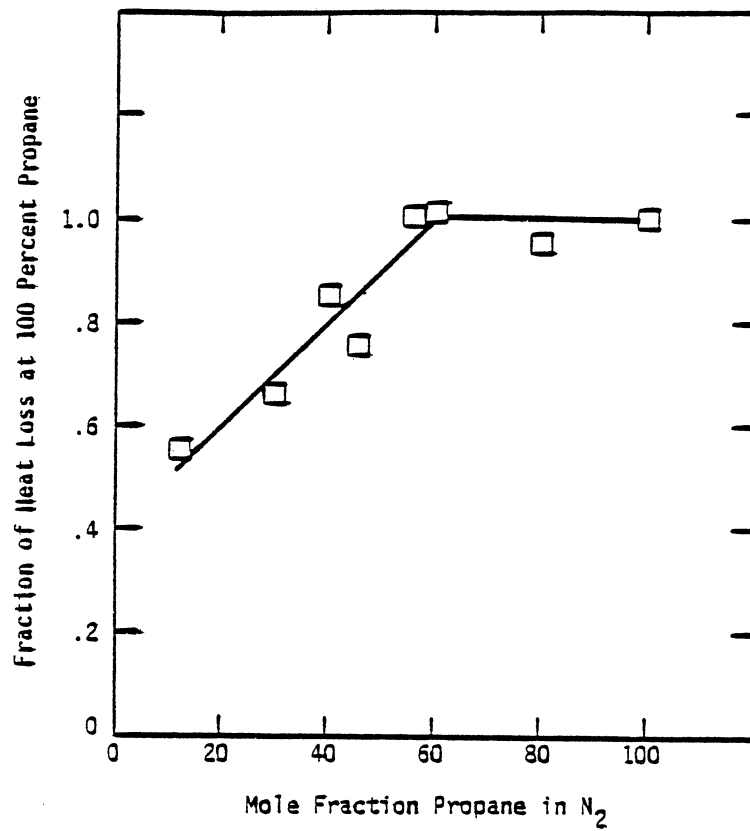


Figure 3-5. Empirical correlation of radiant heat loss from propane-nitrogen flames. Richardson number = 2.0.

correlated flame length to heat release to the 0.4 power. This is close to the exponent of 0.388 determined by a least squares fit of 3, 6 and 12 inch head data as shown in Figure 3-3. Such good agreement also verified the success in correlating large flames using Hottel and Hawthorne's calculations. In addition, conversion of Stewart's (3.25) formula for combustion number, predicts flame length based upon density to the 0.4 power and Richardson number to the -0.2 power. Flame lengths correlated with equivalent expressions by Thomas (3.19) predicted that the flame length should be proportional to the density change to the 0.61 power and the Richardson Number to the -0.3 power.

Using Equation 3-1, good correlation is seen in Figure 3-6 for previously tested 3, 6 and 12 inch flare heads (3.1). Good agreement is also seen for 2 and 2 1/2 inch flare heads shown in Figure 3-7, but the correlation overestimates the length for 1/2, 1, and 1 1/2 inch flames. Flames burned on small nozzles have low Richardson numbers (see Figure 3-1). In operation, the length of these flames is not completely controlled by the Richardson number and hence equation 3-1 tends to overestimate the flame length. In addition the fraction of heat lost by radiation may be different for small flames than large ones. Inspection of Figure 3-7 shows that correlations for each individual small nozzle could be developed by altering the constants in Equation 3-1. However, the correlation would not be universal, as it apparently is for open pipe flares greater than 2 inches in diameter. Similar discrepancies between the correlation and even smaller nozzles are shown in Figure 3-8.

The observed flame lengths of the air-assisted heads shown in Figure 3-9 are considerably shorter than predicted. This may be the result of the smaller individual ports in the fuel spider and/or the increased mixing caused by the co-flowing air stream.

Flame length predictions shown in Figure 3-9 for commercial flare heads D, E, F, and G also deviate from measured lengths. Poor agreement between predicted and measured flame lengths for these heads is due to the effect of

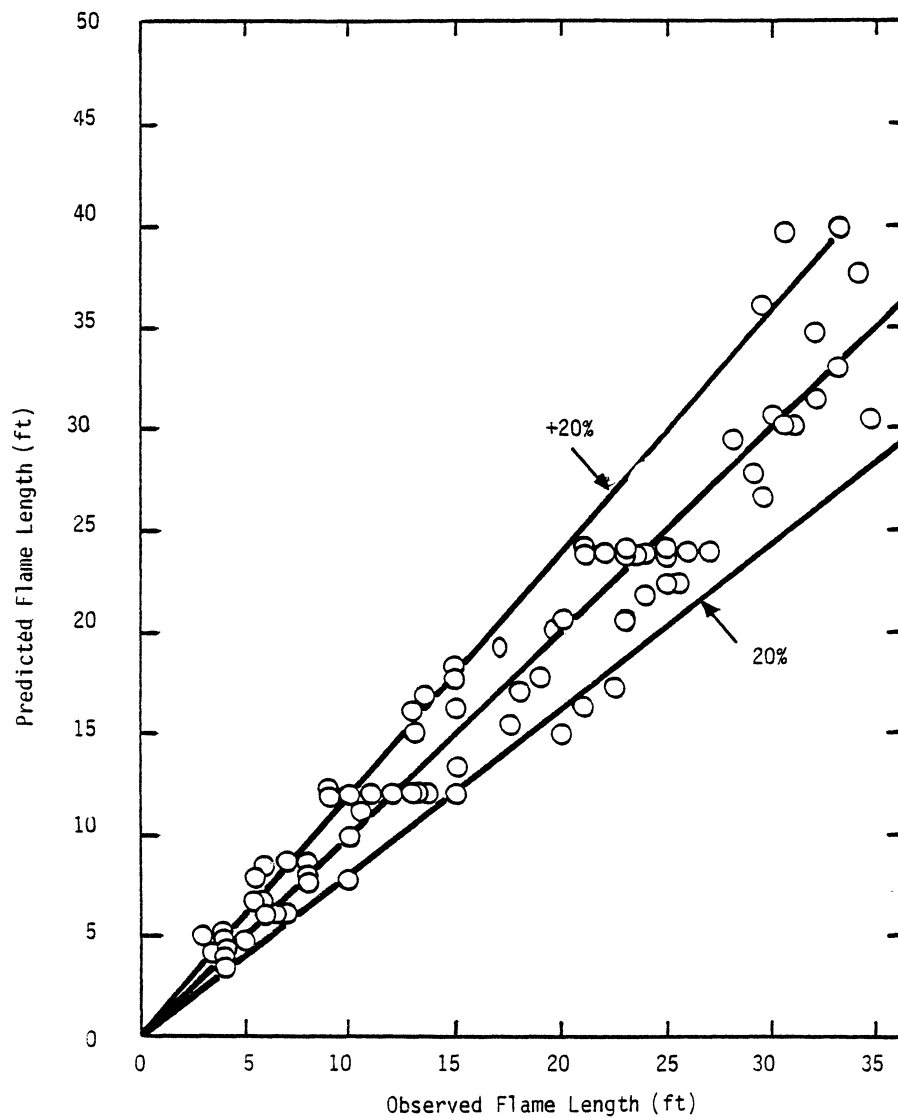


Figure 3-6. Predicted flame length from modified Richardson number correlation compared to observed flame length for previously tested 3,6 and 12 inch flare heads. (From 3.1)

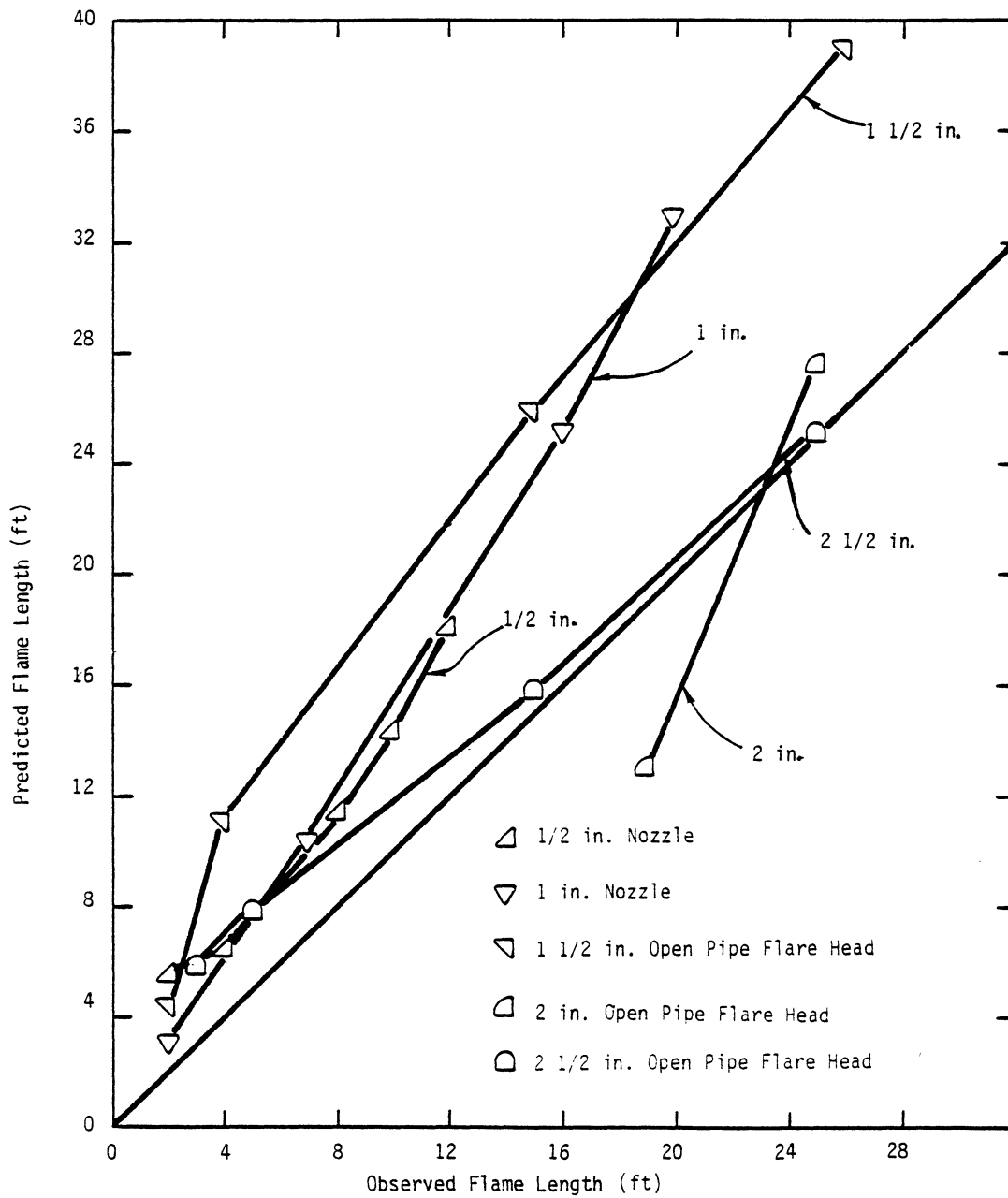


Figure 3-7. Predicted flame length from modified Richardson number correlation compared to observed flame length for 1/2 through 2 1/2 inch flare heads.

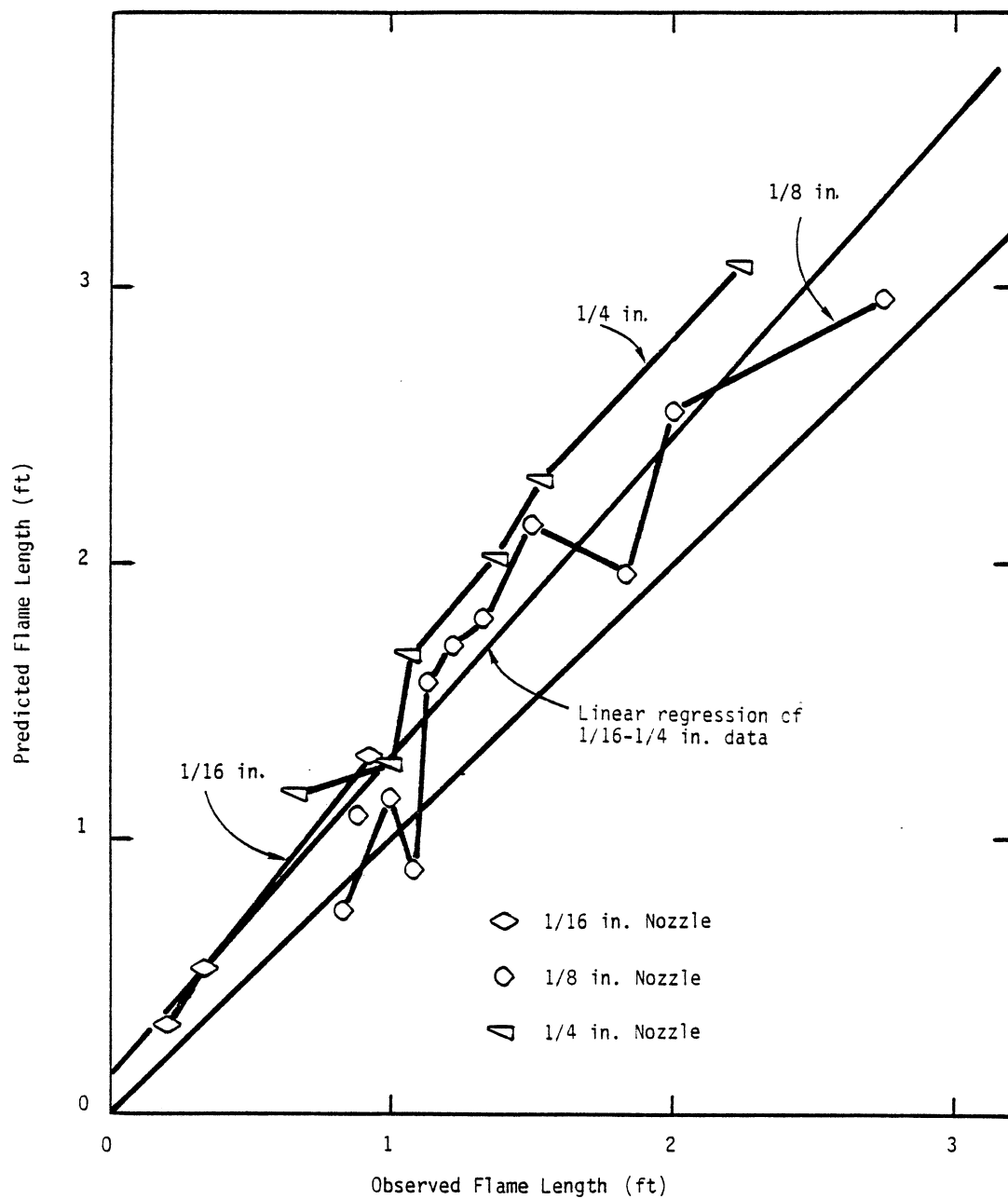


Figure 3-8. Predicted flame length from modified Richardson number correlation compared to observed flame length for 1/16 through 1/4 inch flare heads.

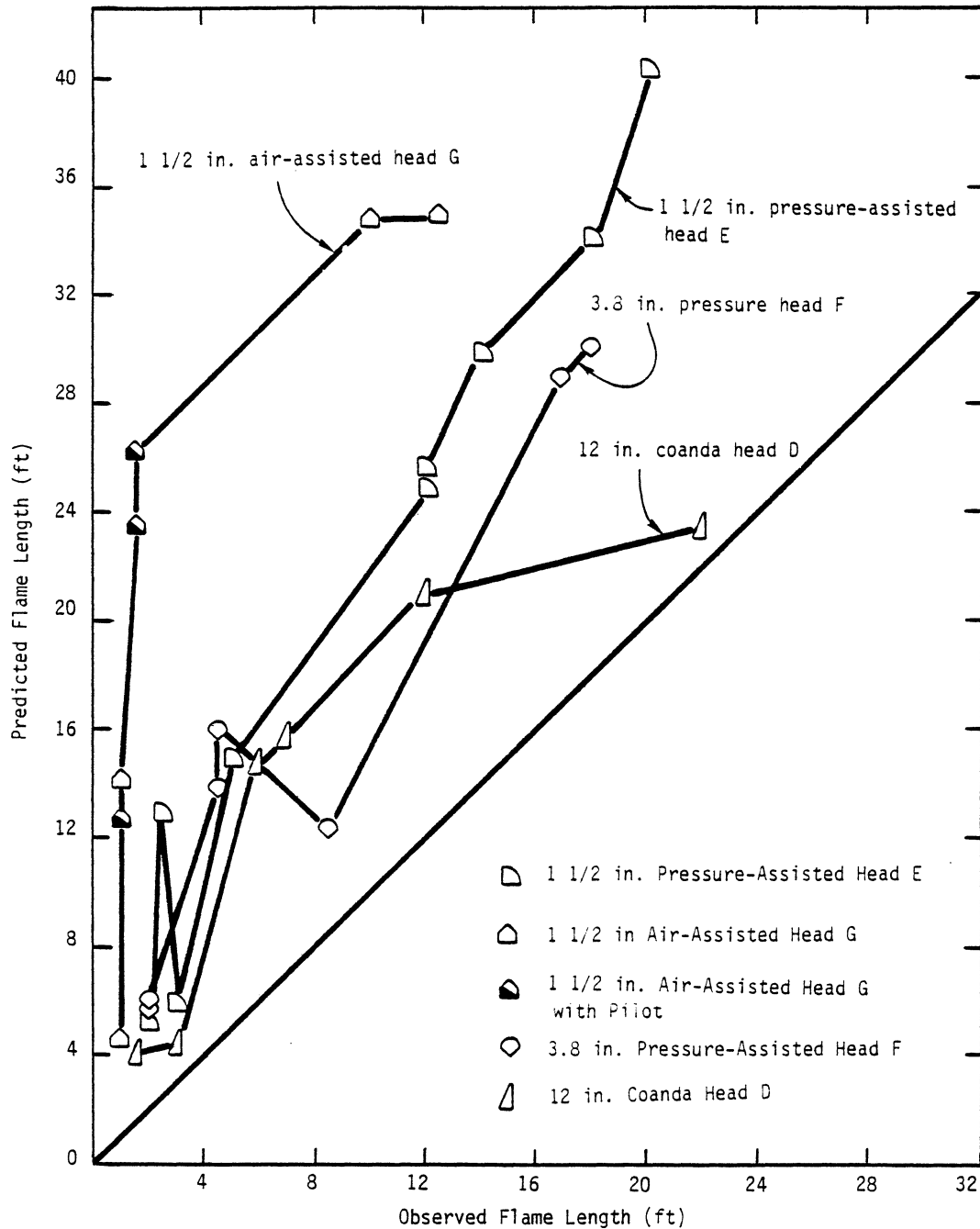


Figure 3-9. Predicted flame length from modified Richardson number correlation compared to observed flame length for 1 1/2 through 12 inch commercial heads.

steam, pressure, and design on flare flames, combined with the previously mentioned aerodynamic differences between small and large flares.

### 3.3 Flame Stability

The flame stability limit for a given propane-nitrogen gas exit velocity is the minimum gas heating value that maintains a flare flame. For each flare head, the minimum heating value to maintain a stable flame was evaluated at several velocities. Limiting heating values for 1/16 through 2 1/2 inch heads are compared with previous values for 3 through 12 inch flare heads in Figure 3-10. At heating values on or above the stability curve for a given flare heads, a flame is maintained. The flame is extinguished when the gas heating value drops below the minimum value defined by the stability curve.

The broad stability band on Figure 3-10 is for stability curves of previously tested 3, 6, and 12 inch diameter flare heads (1.3). The 1 1/2, 2, and 2 1/2 inch flare heads exhibit stability curves within this region. This indicates that flare stability is similar for 1 1/2 inch through 12 inch flare heads. The stability of 1 inch and 1/2 inch nozzles, however, is quite different. As shown by comparison of the Reynolds number and Richardson number and by the incompatibility of large and small flame length predictions, the characteristics of flames burned on large flare heads are different from characteristics of flames burned on small nozzles. This conclusion is verified by the flame stability results, which show that flare heads less than 1 1/2 inches in diameter have different stability characteristics than flare heads 1 1/2 - 12 inches in diameter.

### 3.4 Pseudo Adiabatic Flame Temperatures and Stability

A flame will be stable when the flame velocity is equal to or greater than the relief gas velocity in all directions. The flame will be unstable when the gas velocity remains greater than the flame velocity until the gas is diluted beyond its lower flammability limit. The flame velocity, however, is controlled by the Arrhenius kinetic parameters of the flame reactions.

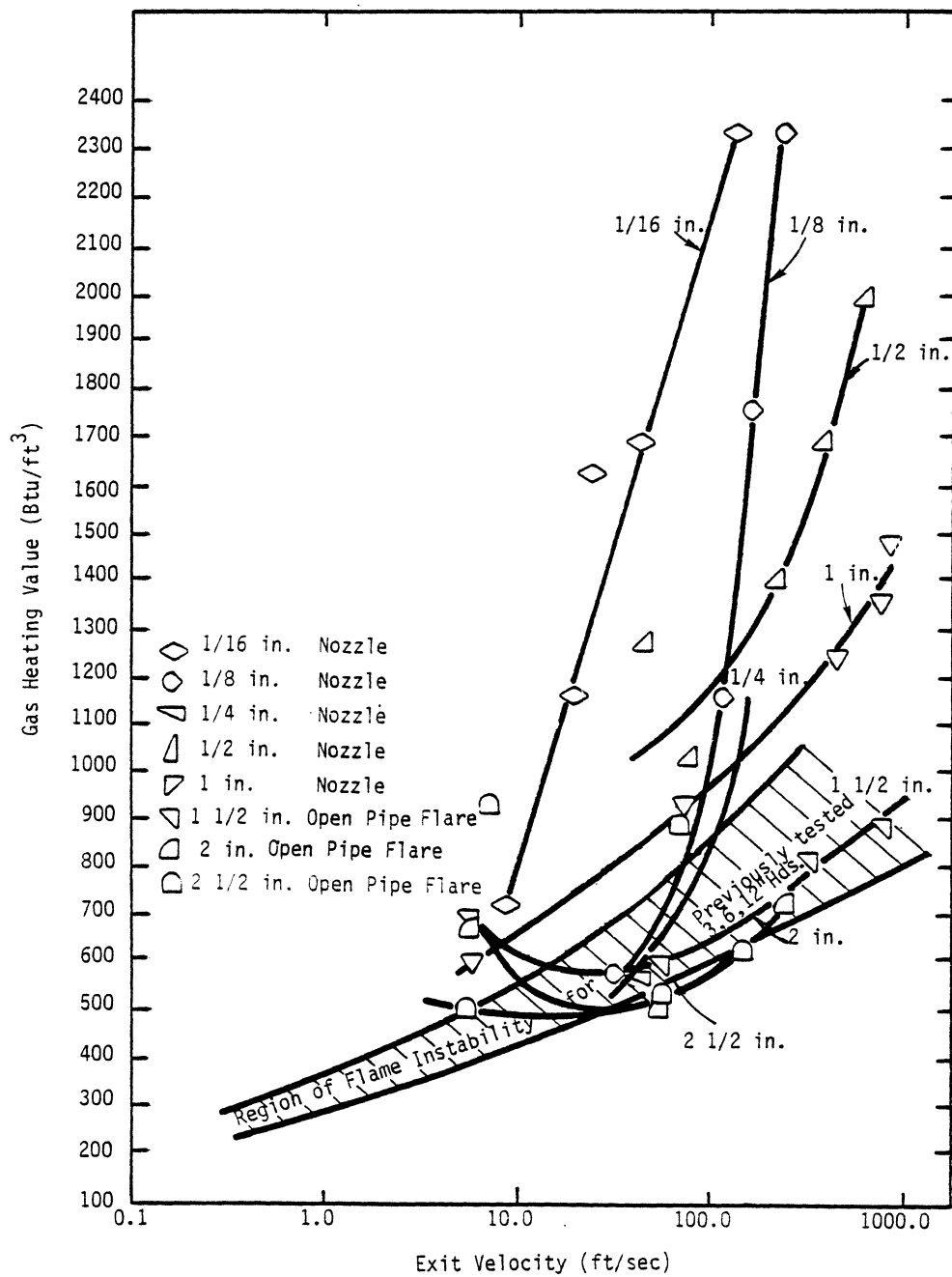


Figure 3-10. Flame stability curves for pipe flare heads.



Higher relief gas exit velocities can be attained when the adiabatic flame temperature is high, because the flame speed increases with temperature. Figure 3-11 shows the maximum gas exit velocity versus pseudo adiabatic flame temperature for previously tested 3 through 12 inch flare heads. A relatively good correlation is obtained, and there is little difference between the performance of different head sizes.

Different flame temperature and stability results are shown in Figure 3-12 for the coanda steam-injected, pressure-assisted, and air-assisted commercial heads tested in the current study. Correlations of the limiting velocity with pseudo adiabatic flame temperature are good for each head, but head size and design have a large influence on the correlation. The design criteria for these commercial pressure and air-assisted flare heads were:

- Relief gas flow capacity of 3,440 lb/hr (36,000 SCFH) for gas with 1,200 Btu/ft<sup>3</sup> heating value.
- Approximately 0.01 ft<sup>2</sup> open area, for an equivalent diameter of 1.5 inches.
- For the pressure-assisted heads, a maximum pressure drop across the flare head of 15 psig.
- For the air-assisted head, two air delivery rates, with a maximum rate of 200,000 ft<sup>3</sup>/hr at 20 inches water pressure.

Pressure-assisted head E and air-assisted head G met these criteria, but pressure-assisted head F had an open area of 0.0785 ft<sup>2</sup>, and an equivalent diameter of 3.8 inches. For the same calculated flame temperature, each of the commercial heads can be operated at a higher stable velocity than the open pipe flares. Pressure-assisted head E produces stable flames at much higher velocities than other flare heads tested.

The size of smaller flare heads adversely affects flame stability. Figure 3-13 shows that for 1/16 through 2 1/2 inch heads, the maximum stable

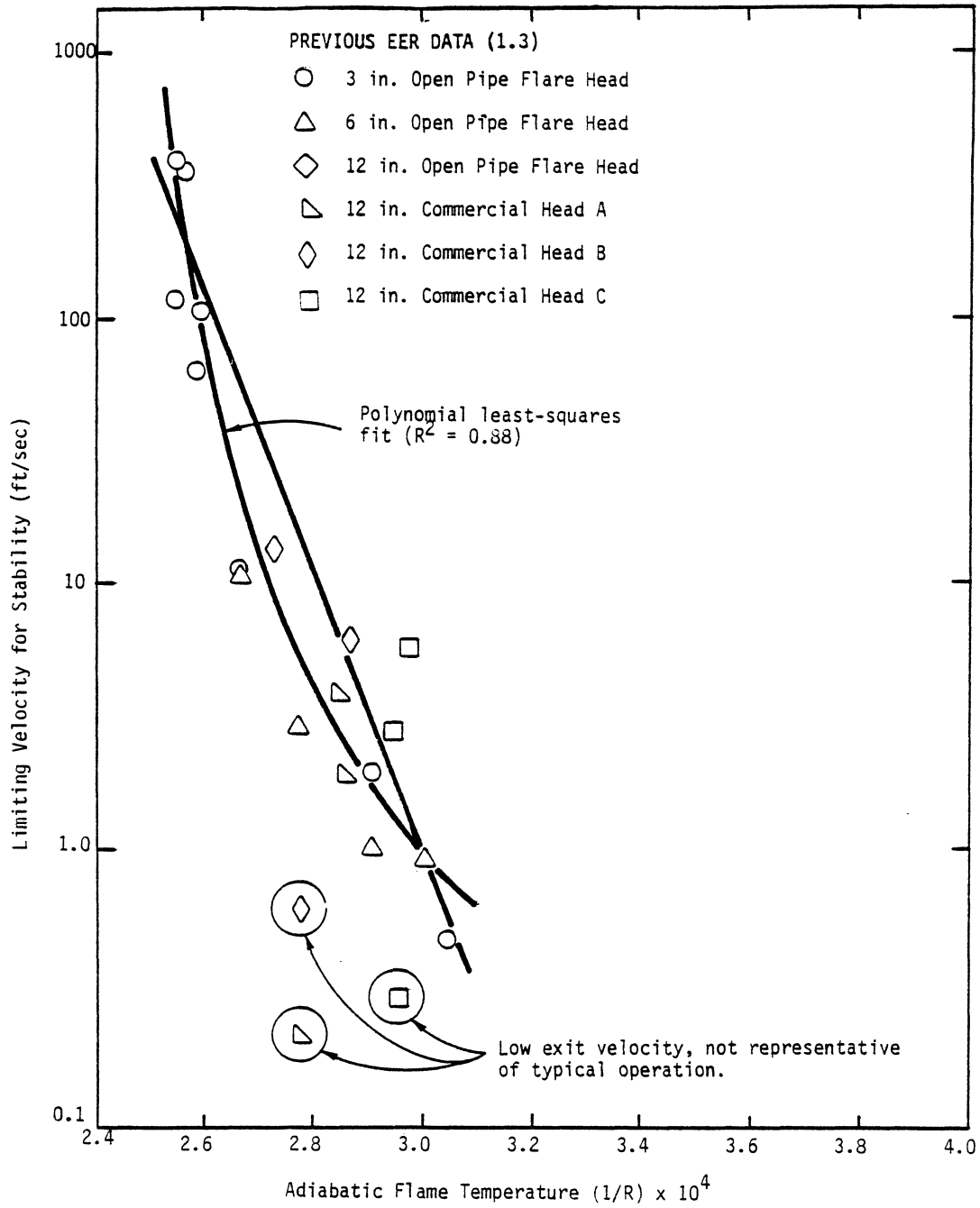


Figure 3-11. Maximum relief gas exit velocity vs flame temperature for previously tested 3 through 12 inch flare heads.

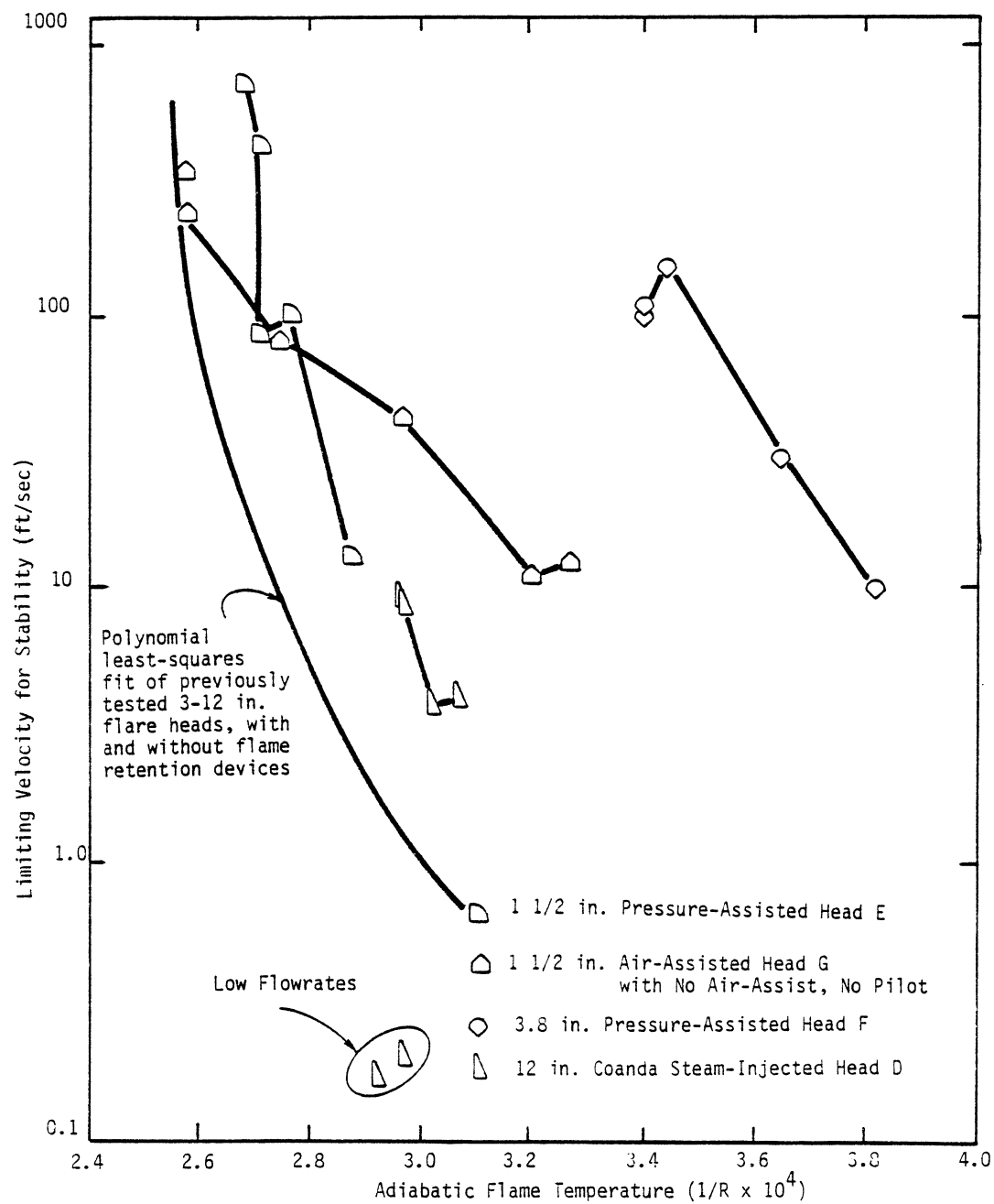


Figure 3-12. Maximum relief gas exit velocity vs flame temperature for commercial heads D through G.

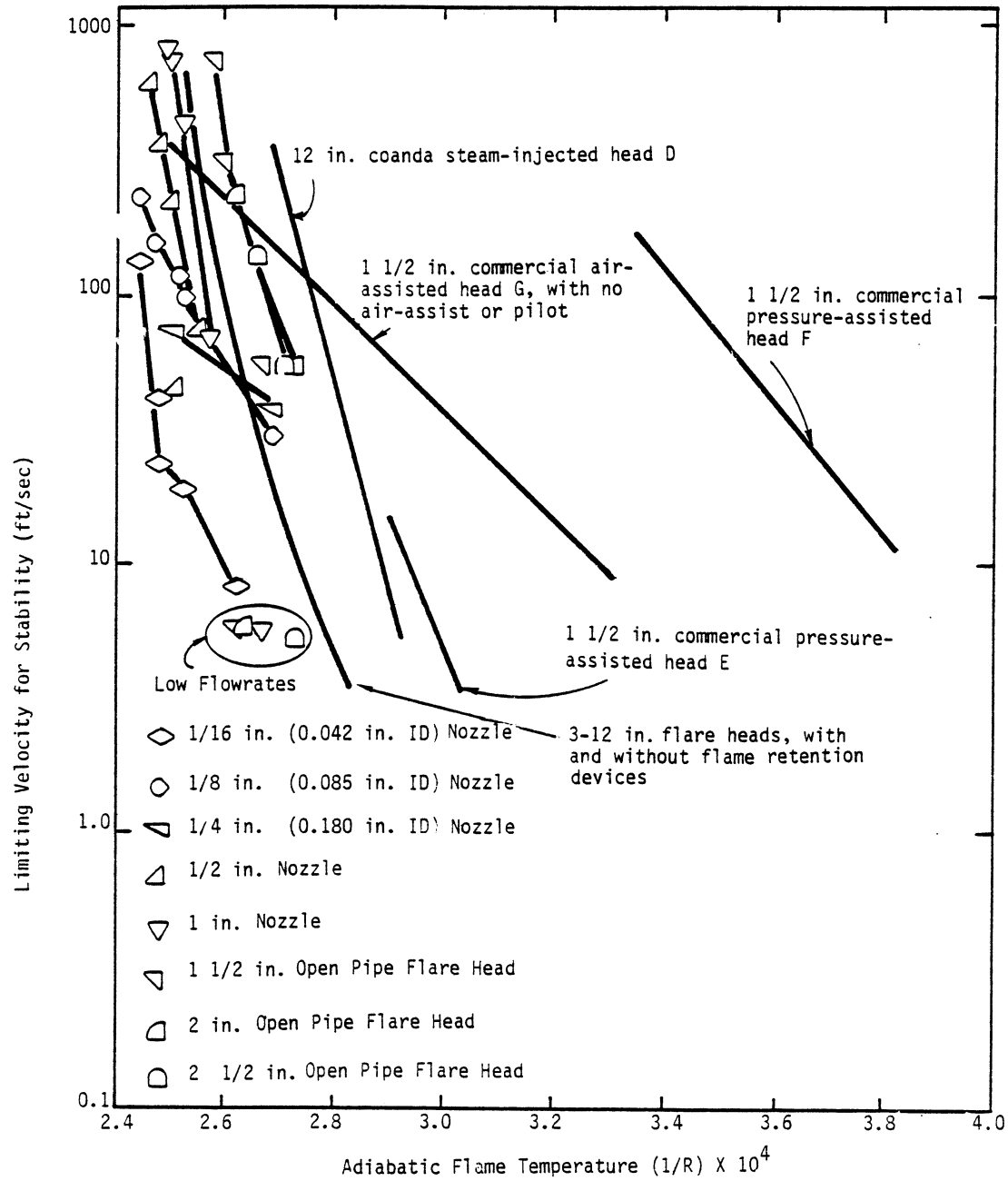


Figure 3-13. Relation between flame stability and pseudo adiabatic flame temperature.

exit velocity decreases with decreasing diameter. The limiting velocity for flares 1 through 2 1/2 inches in diameter is similar to the limiting velocity obtained for flare heads 3 through 12 inches in diameter, but lower than for the commercial heads D through G. Figures 3-11 through 3-13 show that for many of the flare heads there is a minimum gas flowrate and corresponding exit velocity, below which the flame becomes less stable. This may be due to flame operation below the velocity where the flame will become unstable from minor fluctuations in flow or wind conditions, and/or where there is too little heat input to overcome heat losses.

In conclusion, small flares and commercial flares tested were found to yield flame length and stability curves which are different from previously reported 3 to 12 inch flares heads. The characteristics of flames produced on nozzles less than 1 1/2 inches in diameter depend on the nozzle diameter and are less stable than flames produced by larger diameter pipe flares. Flames produced on commercial pressure-assisted and coanda steam-injected heads are more stable than flames produced on previously tested 3 to 12 inch pipe flares.

### 3.5 References

- 3.1 Pohl, J. H., N. R. Soelberg, E. Poncelet, and B. A. Tichenor, "The Structure of Large Buoyant Flames", American Flame Research Committee Fall Meeting, Livermore, CA, 16-18 October 1985. (Abstract submitted)
- 3.2 "Guide for Pressure - Relieving Despresuring Systems", API RP 521, Washington, DC, 1982.
- 3.3 Straitz, III, J. F. and J. A. O'Leary, "Flare Radiation", presented at the 2nd International Symposium on Loss Prevention and Safety Promotion in the Process Industries, Heidelberg, Germany, September 1977.
- 3.4 Straitz, III, J. F., "Flaring for Gaseous Control in the Petroleum Industry", presented at 1978 Annual Meeting of the Air Pollution Control Association, Paper 78-58.8, Austin, Texas, 1978.
- 3.5 Kent, G. R., Hydrocarbon Processing 43(8), 121, 1964.
- 3.6 Reed, R. D., Chemical Engineering Progress 64(6), 53, 1968.
- 3.7 Kalghatgi, G. T., Combustion and Flame 52, 91, 1983.
- 3.8 Escudier, M. P., Combustion Science and Technology 4, 293, 1972.
- 3.9 Becker, H. A., D. Kiang, and C. I. Downey, Eighteenth Symposium (International) on Combustion, p. 1061, The Combustion Institute, 1981.
- 3.10 Tamanini, F., Combustion and Flame 30, 85, 1977.
- 3.11 Botros, P. E. and T. A. Brzustowski, Seventeenth Symposium (International) on Combustion, p. 389, The Combustion Institute, 1979.
- 3.12 Galant, S., "Un Modele Simplifie de Rayonnement Emis par les Flames de Diffusion Libres," Societe Bertin and Cie, Report Number N. 52.81.15, Plaisir, France, 1981.
- 3.13 You, H. Z. and G. M. Faeth, Combustion and Flame 44, p. 261, 1982.
- 3.14 Brzustowski, T. A., S. R. Gollahalli and H. F. Sullivan, Combustion Science and Technology 11, 29, 1975.
- 3.15 Becker, H. A. and D. Diang, Combustion and Flame 32, 115, 1978.
- 3.16 Becker, H. A. and S. Yamazaki, Combustion and Flame 33, 123, 1978.
- 3.17 Hottel, H. C. and W. R. Hawthorne. Third Symposium (International) on Combustion, The Williams and Wilkins Company, p. 254, 1949.

- 3.18 Heitner, I., Hydrocarbon Processing, 209, 1970.
- 3.19 Thomas, P. H., Ninth Symposium (International) on Combustion, p. 844, The Combustion Institute, 1977.
- 3.20 Morton, B. R., Tenth Symposium (International) on Combustion, p. 973, Academic Press, 1965.
- 3.21 Putnam, A. A. and C. F. Speich, Ninth Symposium (International) on Combustion, p. 867, Academic Press, 1963.
- 3.22 Cox, C. and R. Chitty, Combustion Flame 39, 191, 1980.
- 3.23 Zukoski, E. E., T. Kubota and B. Cetegen, Fire Safety Journal 3, 107, 1980/1981.
- 3.24 Orloff, L. and J. Deris, Nineteenth Symposium (International) on Combustion, p. 905, The Combustion Institute, 1982.
- 3.25 Stewart, F. B., Combustion Science and Technology 2, 203, 1970.

#### 4.0 COMMERCIAL FLARE HEAD TEST RESULTS

The primary objective of these tests was to determine the influence of flare head design on flare combustion efficiency. The flare combustion efficiency was measured for propane-nitrogen mixtures flared using different commercial heads. Results show that the combustion efficiency is greater than 98 percent for flare heads, except for the air-assisted flare head, when operated within their stable flame regimes. The air-assisted head test results were less conclusive.

The Flare Advisory Committee recommended in January 1984 that additional combustion efficiency tests be conducted on other types of commercially available flare heads. Table 4-1 lists the four different head types that were tested. The design of the commercial flare heads is proprietary, and limited design information can be disclosed. Due to the proprietary nature of the flare heads, each is identified only by type and the letters D, E, F, and G. The coanda steam-injected flare head was tested at gas exit velocities ranging from 0.2 to 9.9 ft/sec based on the 12 inch design opening. The actual imposed velocities vary in this head because of induction of steam and air and the variable cross section. Pressure-assisted head E had an equivalent diameter of 1.5 inches, and was tested at 14.2 - 907 ft/sec. Pressure-assisted head F had an equivalent diameter of 3.8 inches. This head was tested at 4.4-157 ft/sec. The air-assisted head G had an equivalent diameter of 1.5 inches, and was tested between 8.5 and 428 ft/sec.

Due to the difference in size and design of the heads, combustion efficiencies measured on the heads could not be directly compared. Flare heads are designed for specific conditions, such as relief gas composition, heating value and exit velocity. The operating regime was defined experimentally for each flare head by determining the minimum heating value required to maintain the flame at a given gas exit velocity. A minimum stability curve was generated in this manner for each flare head. Combustion efficiency of each head was measured at conditions on this curve of minimum stability and at heating values 50 percent greater than required to maintain a stable flame. Therefore, combustion efficiency was measured at flare



Table 4-1.

## COMMERCIAL HEADS SELECTED FOR COMBUSTION EFFICIENCY TESTS

EER Designation	Flare Head	Geometry	Open Area (in. <sup>2</sup> )	Equivalent Diameter (in.)	Equipped With Flame Retention Device
D	Coanda Steam-Injected Head	Upward opening cone with steam-injection ports	113	12	no
E	Pressure-Assisted Head	Horizontal bar	1.77	1.5	yes
F	Pressure-Assisted Head	Open	11.3	3.8	yes
G	Air-Assisted Head	Cross spider	1.77	1.5	no

operating conditions both within and at the limits of the operating envelope for the flare. Low combustion efficiency results for tests at the limits of the operating envelope are expected, and are not indicative of normal commercial operation.

#### 4.1 Coanda Steam-Injected Head D

Flame stability and combustion efficiency were measured on the coanda steam-injected flare head. This head was designed to have the capacity of a 12 inch open pipe flare. Figure 4-1 shows the limits of flame stability for this head. For a given exit velocity indicated by each data point, reduction of the heating value resulted in blow-out of the flame. All measurements on this head were made with the minimum steam flow (140 lb/hr) to prevent the relief gas from exiting the injection ports. The shaded area on Figure 4-1 represents the region of flame stability previously reported for 3, 6, and 12 inch diameter flare heads, both with and without flame retention devices.

Combustion efficiency was measured at relief gas exit velocities between 0.2 and 9.9 ft/sec, and at gas heating values near and above the minimum heating value required for flame stability. In Figure 4-2, combustion efficiency is correlated to flame stability using the ratio of gas heating value to that minimum heating value required to maintain flame stability. High combustion efficiency (>99 percent) is obtained where the gas heating value is greater than 10 percent above the heating value required for a stable flame. Combustion efficiency decreases as the heating value for a stable flame limit is approached.

#### 4.2 Pressure-Assisted Head E

Similar measurements were made for pressure-assisted head E. Figure 4-3 shows the flame stability curve for pressure-assisted head E. Combustion efficiency was measured at gas exit velocities between 12.4 and 907 ft/sec, for gas heating values at and above the stability curve. Figure 4-4 shows the correlation between combustion efficiency and flame stability. The correlation is the same as for other heads tested. Combustion efficiencies

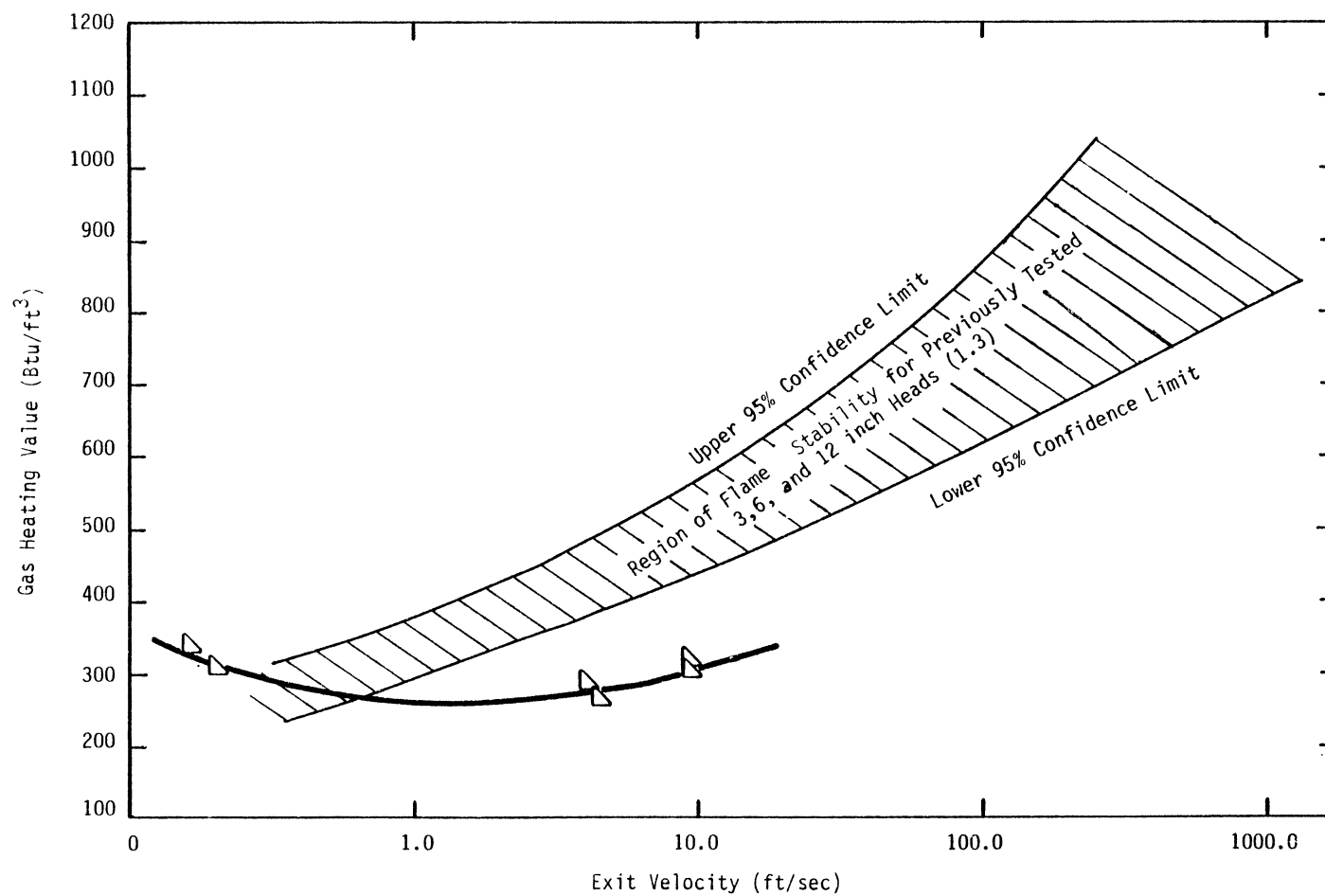


Figure 4-1. Flame stability curve for commercial 12 inch coanda steam injected head D. Steam flowrate at 140 lb /hr.

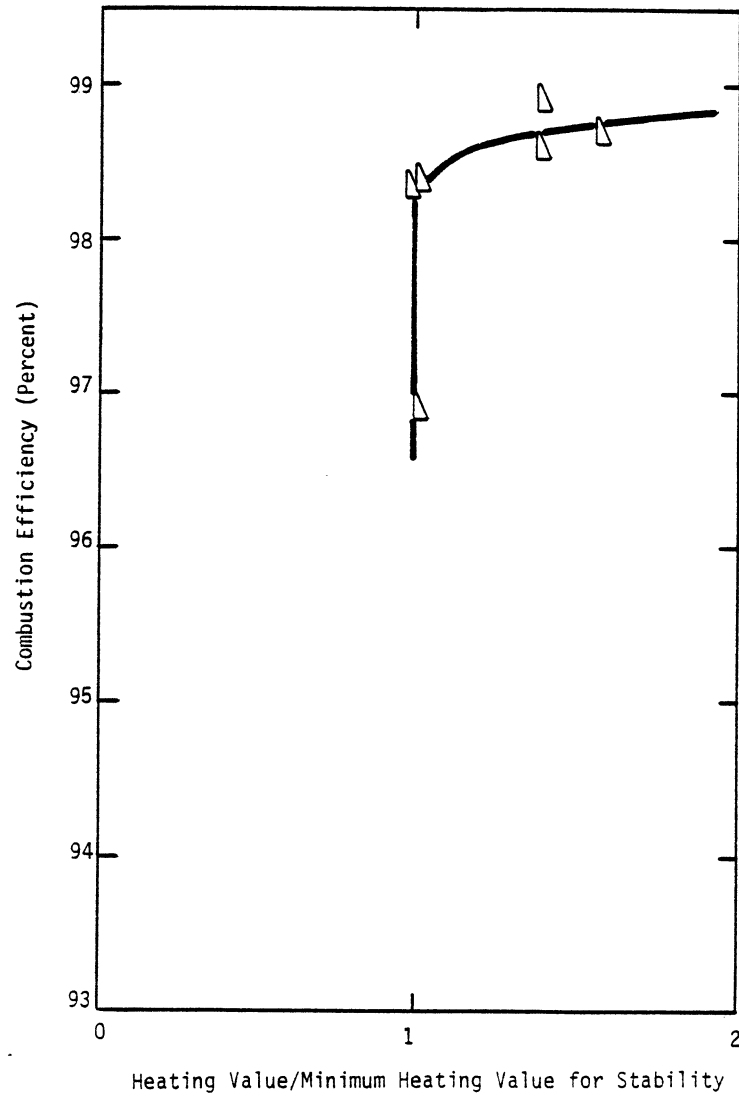


Figure 4-2. Relation of flame stability to combustion efficiency for commercial 12 inch coanda steam-injected flare head D. Steam flowrate at 140 lb /hr.

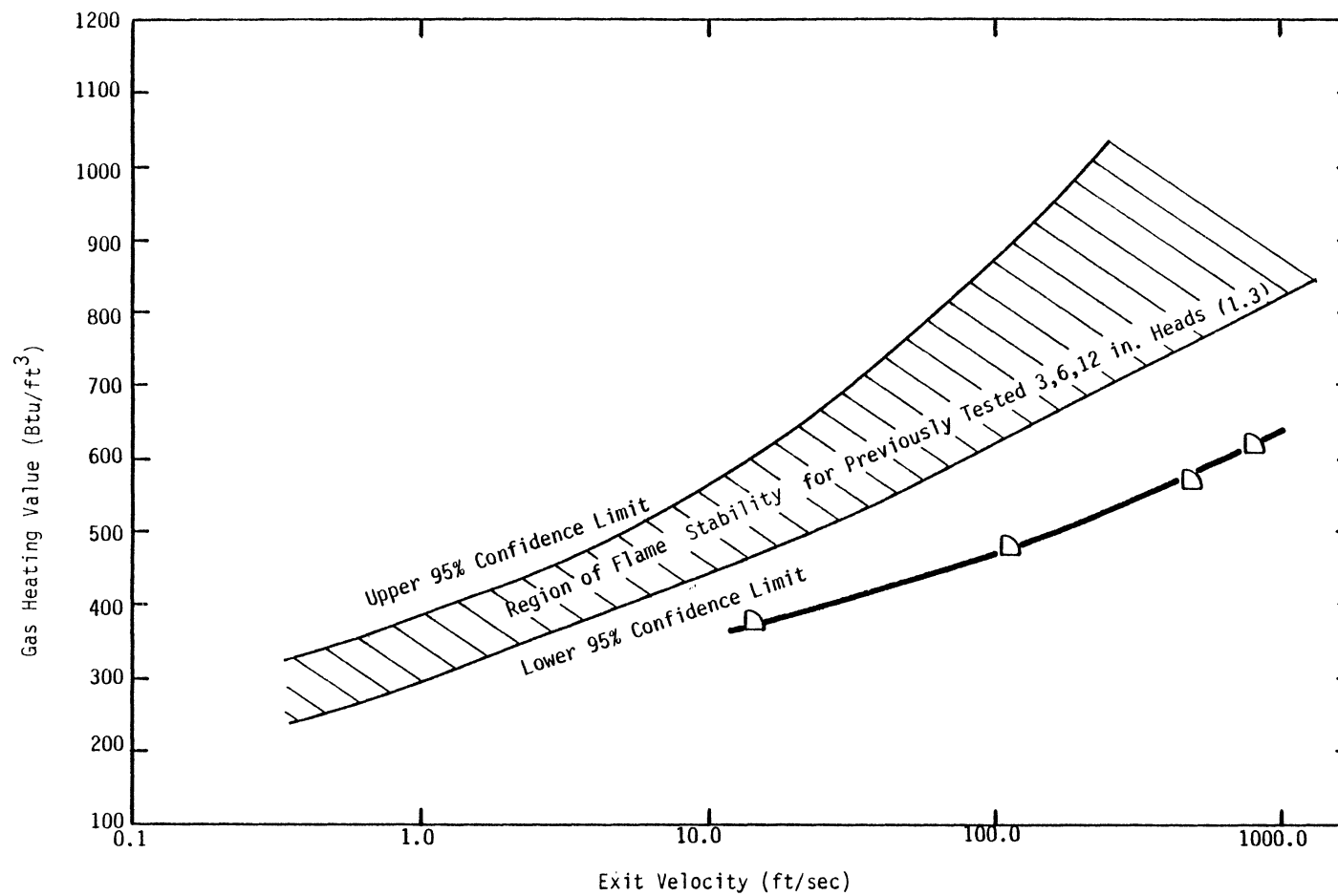


Figure 4-3. Region of flame stability for 1.5 inch commercial pressure-assisted head E.

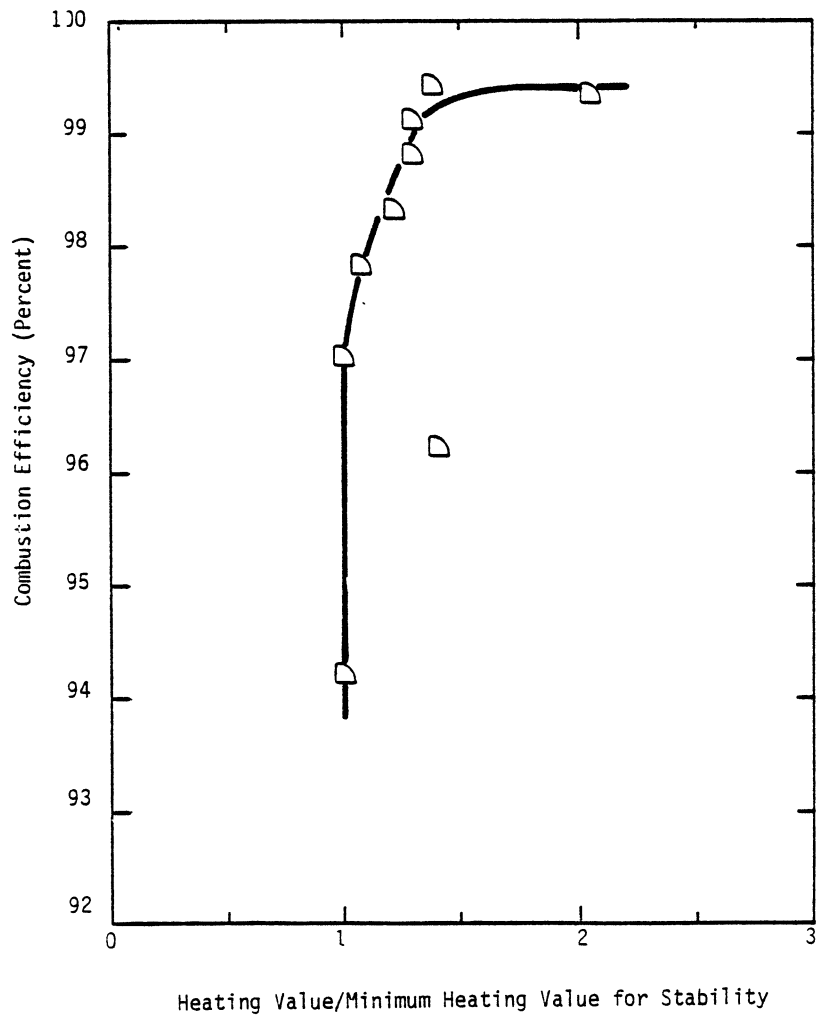


Figure 4-4. Relation of flame stability to combustion efficiency for commercial 1.5 inch pressure-assisted head E.

greater than 98 percent are achieved under stable operating conditions. Stable operating conditions are those for which the ratio of heating value of the gas to the minimum heating value required for stability is greater than 1.3. Combustion efficiency rapidly decreases as the limit of stability is approached.

#### 4.3 Pressure-Assisted Head F

Figure 4-5 shows the stability curve for pressure head F. The stability limit curve is significantly lower than those curves for previously tested heads. Figure 4-6 shows that combustion efficiency can be correlated to flame stability. Combustion efficiency is greater than 98 percent when the gas heating value ratio is greater than 1.3, but decreases rapidly as the heating value ratio approaches 1.0.

#### 4.4 Air-Assisted Head G

The air-assisted head G performed differently from the steam-injected and pressure-assisted heads. Figure 4-7 shows a poor correlation of flame stability with gas heating value and exit velocity when the flare is air-assisted. The air-assist flowrate influences flame stability. The minimum gas heating value required to produce a stable flame increased as the flow rate of assist air increased relative to the propane flowrate. A reasonable correlation of limiting gas heating value to exit velocity is obtained only when there is no air-assist flow.

Results of stability tests with one pilot flame (natural gas at 2.1 SCFM) also show a poor correlation of flame stability with gas heating value and exit velocity (Figure 4-8). Also, use of the pilot flame allows a stable flame to be maintained at a lower gas heating value (including the pilot gas contribution) than without the pilot, at the same gas exit velocity and air-assist rate (Figure 4-9). As in the tests conducted without the pilot flame, the air-assist flowrate influences flame stability.

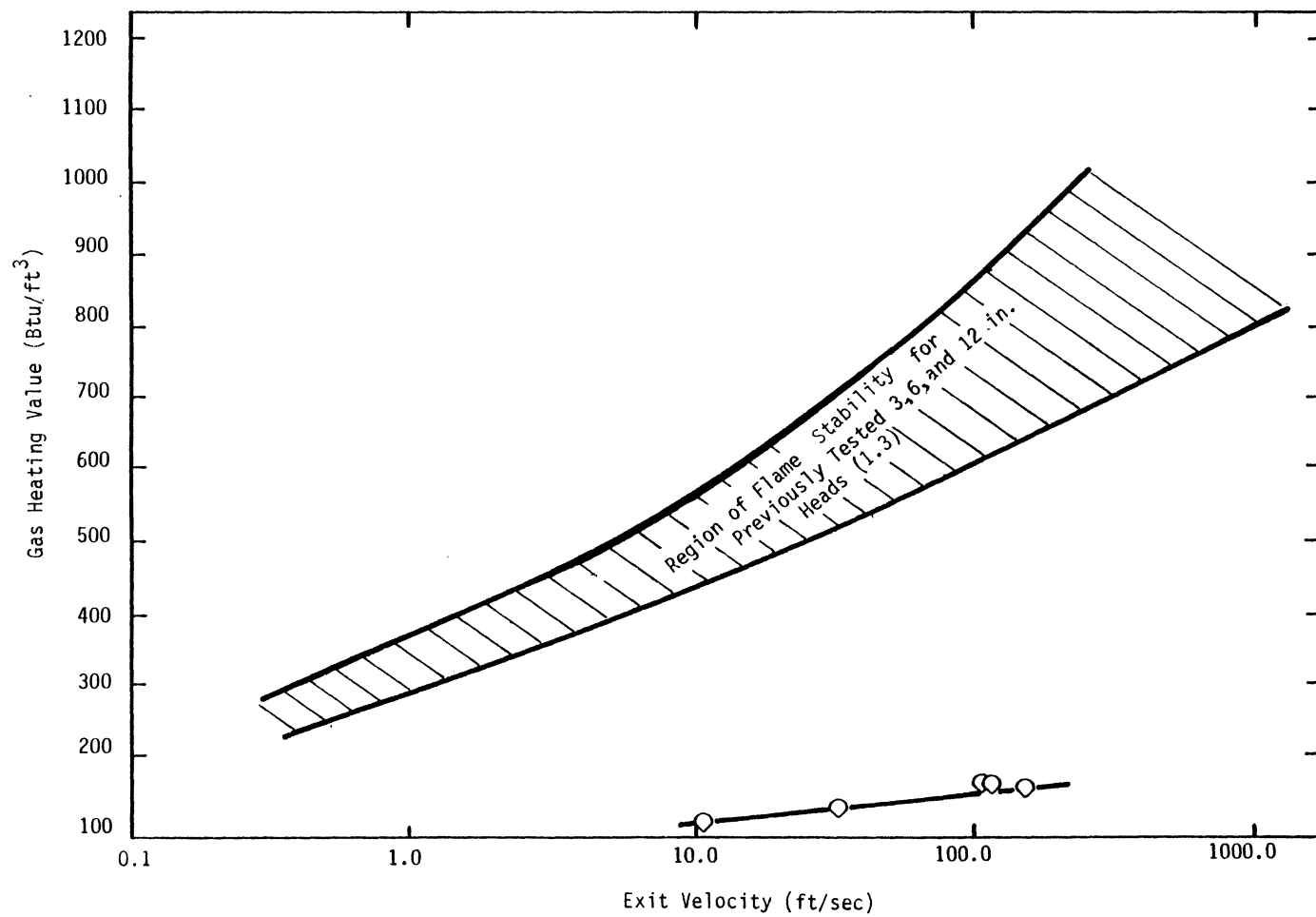


Figure 4-5. Region of flame stability for 3.8 inch commercial pressure head F.



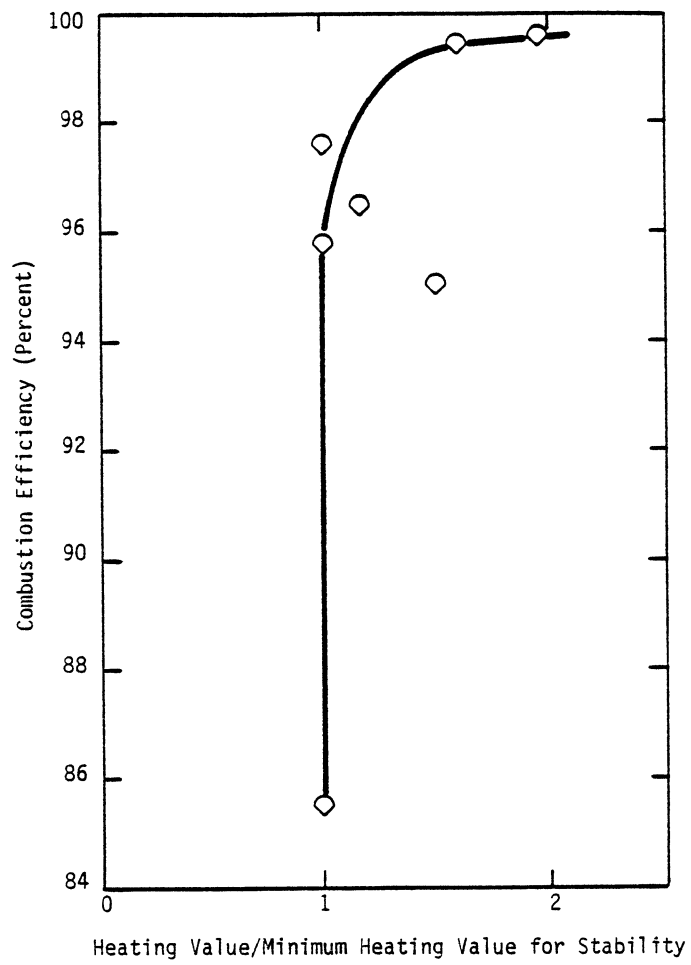


Figure 4-6. Relation of flame stability to combustion efficiency for commercial 3.8 inch pressure-assisted head F.



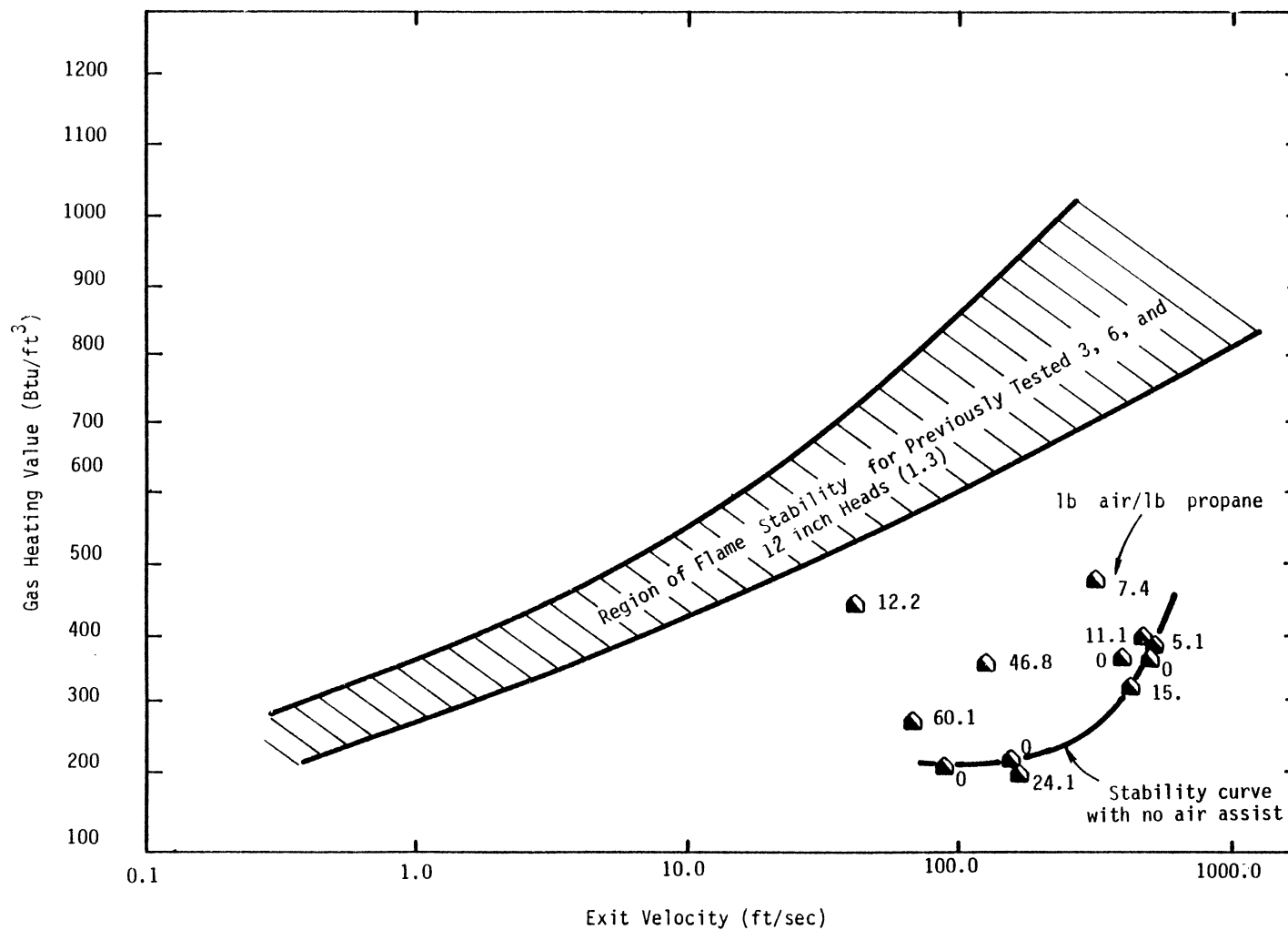


Figure 4-8. Region of flame stability for 1.5 inch commercial air-assisted flare G with pilot flame.

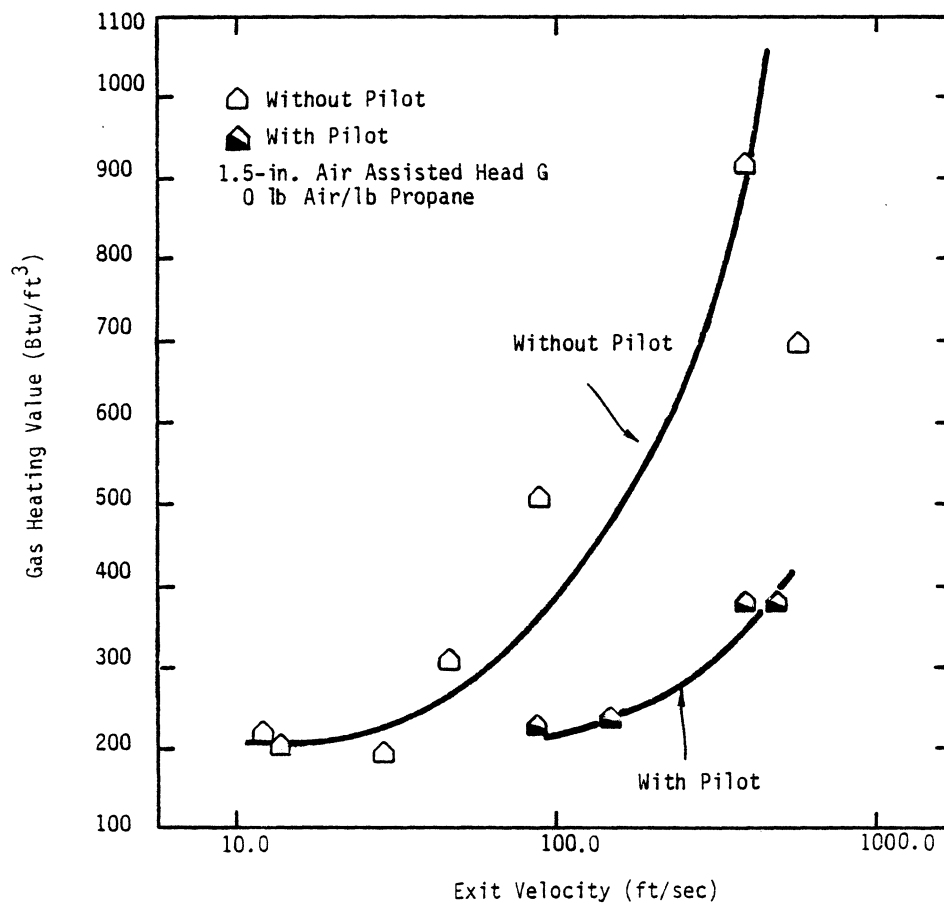


Figure 4-9. Region of flame stability for 1.5 inch commercial air-assisted head G, with no air-assist.

A considerable amount of data was collected on the air-assisted flare. However, the available data does not allow a systematic evaluation of the performance of air-assisted flares because factors controlling this flare were not recognized prior to the test program and the experimental and data analysis procedures were not properly designed to establish definite conclusions concerning air-assisted flare performance. The hypothesis on the performance of the air-assisted head that is presented below is based upon this test data and requires further data collection for verification.

The results show that the degree of air-assist affects the flare flame stability. The flame will become unstable when the gas velocity is not reduced to the flame velocity before the gas is diluted below its lower flammability limit. The gas velocity is reduced by entrainment with the surrounding assist and ambient air. Large differences between the co-axial air-assist and relief gas stream will increase mixing (entrainment) of air with the relief gas, but will inhibit the reduction of the gas velocity to the flame velocity when the air-assist velocity is higher than the relief gas velocity. This causes rapid relief gas dilution and narrows the region of flammability. With no air-assist, flame stability at a given velocity is a function of the gas heating value as shown in Figure 4-9. When air-assist is applied, the dominate factor affecting flame stability is the relative amount of air assist to relief gas.

The momentum ratio of the air-assist stream to the fuel gas stream,  $(\rho v)_{\text{air}}/(\rho v)_{\text{gas}}$ , is a measure of the amount of shear between the air and fuel and controls the entrainment rate. Figure 4-10 compares the maximum relief gas velocity allowable for stability to the momentum ratio. The correlating parameter is chosen so that it equals 1 when the air momentum is zero. For tests using no air-assist, the maximum velocity generally increases with increasing gas heating value, as indicated by the vertical line at 1.0 on the x-axis. When air-assist is applied in flame operation the dominate factor affecting the flame stability is the momentum ratio of air-assist to relief gas streams. In fact, the two tests (No. 222 and No. 228) with the highest momentum ratios (99.4 and 43.5) exhibited the lowest maximum exit velocity, even though the gas heating value was high (2,350 Btu/ft<sup>3</sup>).

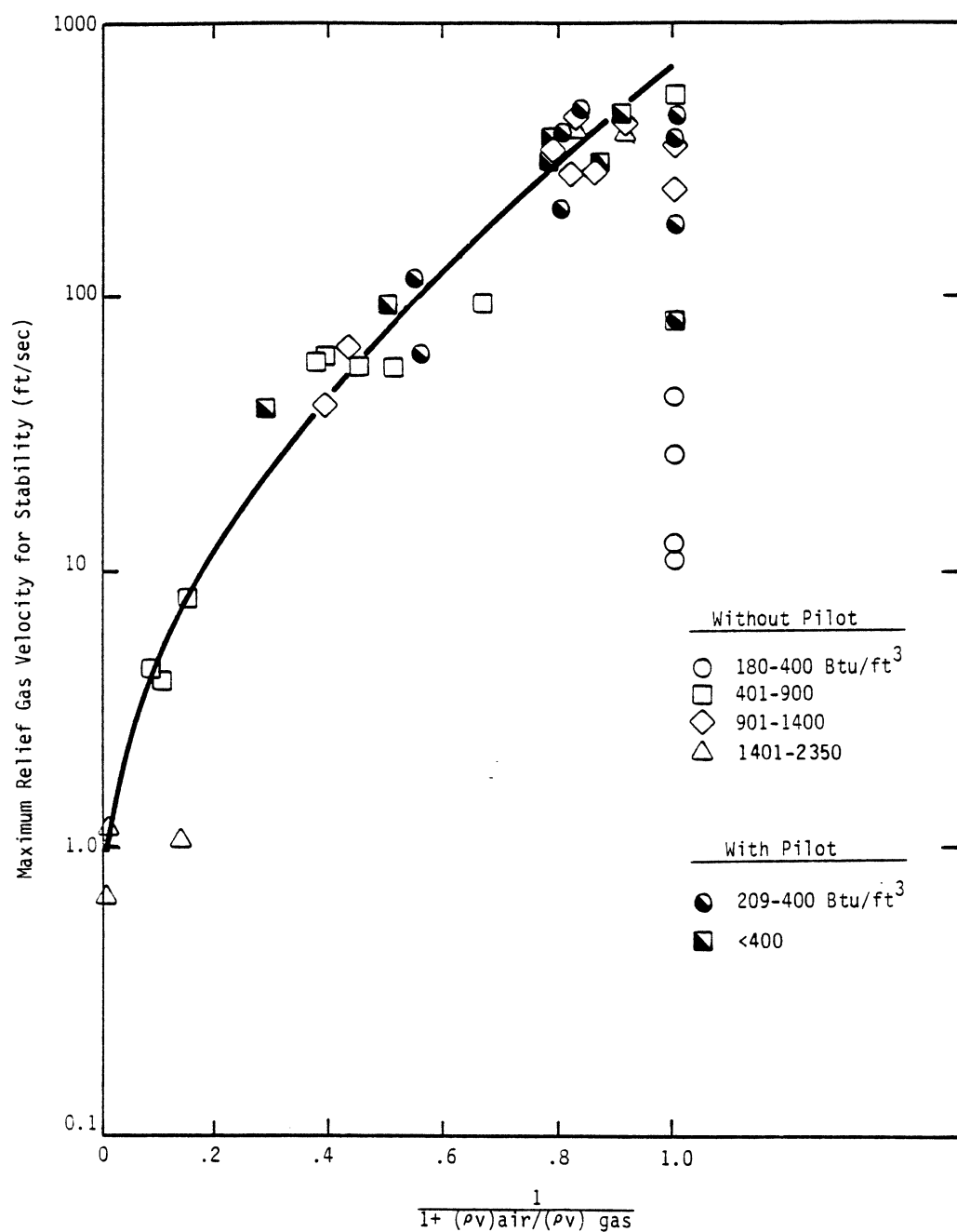


Figure 4-10. Maximum gas exit velocity for stability versus air-assist to gas momentum ratio for air-assisted head G, with and without pilot.

The combustion efficiency of the air-assisted head may be correlated directly to the air-to-gas momentum ratio as shown in Figure 4-11. Combustion efficiency is 99 percent or greater when the momentum ratio is less than about 0.39 for tests conducted without the pilot. For tests with the pilot, >99 percent combustion efficiency is attained when the momentum ratio is less than 0.25. Figure 4-11 also shows curves indicating air-assist to fuel stoichiometric ratio (S.R.) for the air-assisted head tests. Combustion efficiency is greater than 99 percent when S.R. is less than 0.7, but drops rapidly to less than 90 percent (without pilot) when S.R. increases to 1.0. Limited data for the pilot tests indicates a decrease in combustion efficiency to less than 55 percent when S.R. exceeds 1.0. Combustion efficiency with the pilot flame is lower than without, probably due to the wide stability range achieved with the pilot flame. Much of this data was taken outside the normal operating range of commercial air-assisted flares (S.R.  $\leq$  0.3) to establish the limits of efficient operation for air-assisted flare flames.

Figure 4-11 is presented as a mechanism for discussing the relationship between combustion efficiency and the air/relief gas momentum ratios for air-assisted flares. Only the data obtained during this study were used to develop this figure. A full and more accurate description of this relationship must await additional data.

Industrial air-assisted flare heads are typically employed to reduce soot production in flare flames. Since several of the air-assisted head tests exhibited low combustion efficiency, analysis was conducted to evaluate the emission levels of the incompletely combusted products--soot, hydrocarbons, and CO. Figure 4-12 shows the combustion inefficiency caused by incomplete combustion of soot, hydrocarbons, CO, versus stoichiometric ratio. Soot combustion efficiency was very high, greater than 99.9 percent, even when total combustion efficiency was low (30-40 percent). Unburned hydrocarbons were the major incomplete burned products at high and low values of combustions efficiency. Carbon monoxide was the second major contributor

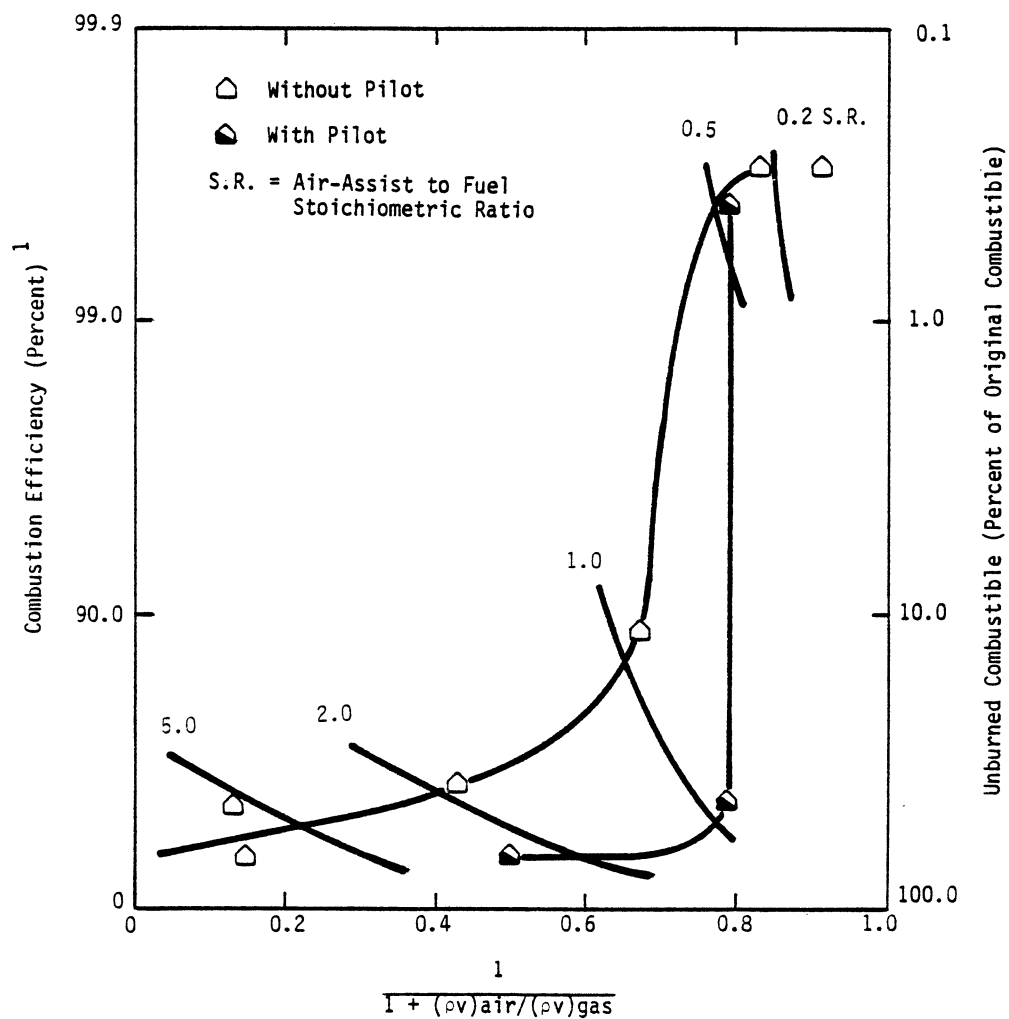


Figure 4-11. Combustion efficiency vs air-assist to gas momentum ratio for commercial air-assisted head G.

<sup>1</sup> Scale is  $\log(100-CE)$



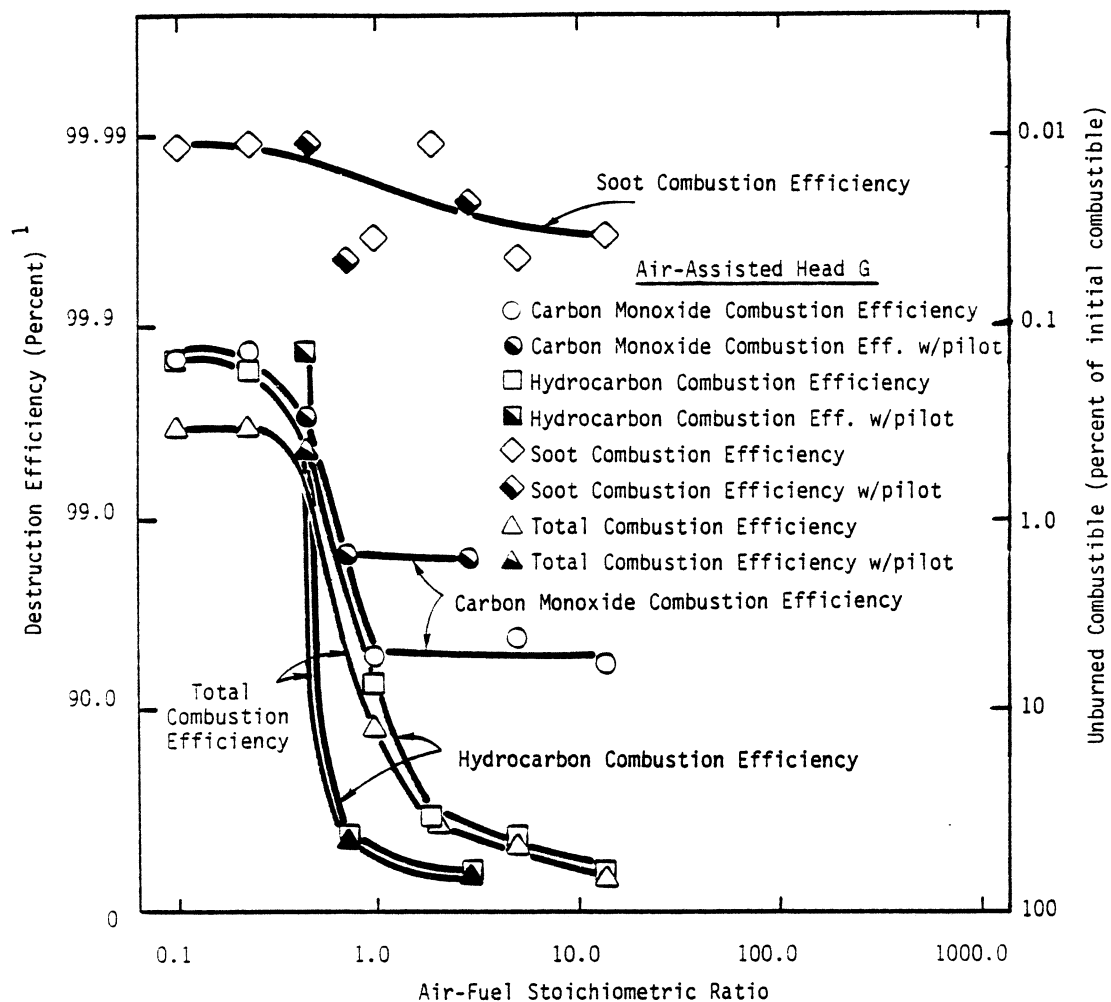


Figure 4-12. Destruction efficiency of incompletely combusted products from air-assisted head G.

<sup>1</sup> Scale is  $\log(100-CE)$

to incomplete combustion, but CO combustion efficiency was still relatively high, ranging from 95-99.8 percent.

#### 4.5 Commercial Head Summary

Flame stability and combustion efficiency were measured for four commercial flare heads. For the coanda steam-injected head and the two pressure heads, flame stability was related to relief gas heating value and exit velocity, according to Figure 4-13. The pressure assisted head F is capable of stable flaring of propane-nitrogen gas mixtures with lower heating values than the other heads.

Combustion efficiency was measured for the steam-injected and pressure-assisted heads at operating conditions near and above the stability limit as defined for each head in Figure 4-13. As Figure 4-14 shows, high combustion efficiency, 98 percent or greater, was obtained for each flare head when the heating value ratio was greater than about 1.3. Combustion efficiency was high when the flames were operated within the limits defined by their respective stability curve. Operations at conditions on the edge or outside the stability envelope resulted in a rapid decrease in combustion efficiency.

Flame stability and combustion efficiency measurements for the air-assisted head required a different treatment. The momentum ratio of air-assist to fuel streams was found to be the major factor affecting flame stability; the relief gas heating value appeared to be less important for the limited tests of this series. Therefore, flame stability and combustion efficiency was correlated with the air-assist to fuel momentum ratio (Figures 4-10 and 4-11), for tests with and without pilot flame. Limited tests of the air-assisted head were conducted using pilot flame to increase stability. Tests without pilot flames indicated high combustion efficiency (>99 percent) when the momentum ratio is less than 0.39 (stoichiometric ratio (S.R.) less than about 0.7). For tests with the pilot flames, combustion efficiencies greater than 99 percent were obtained at momentum ratios less than 0.25 (S.R. less than about 0.6).

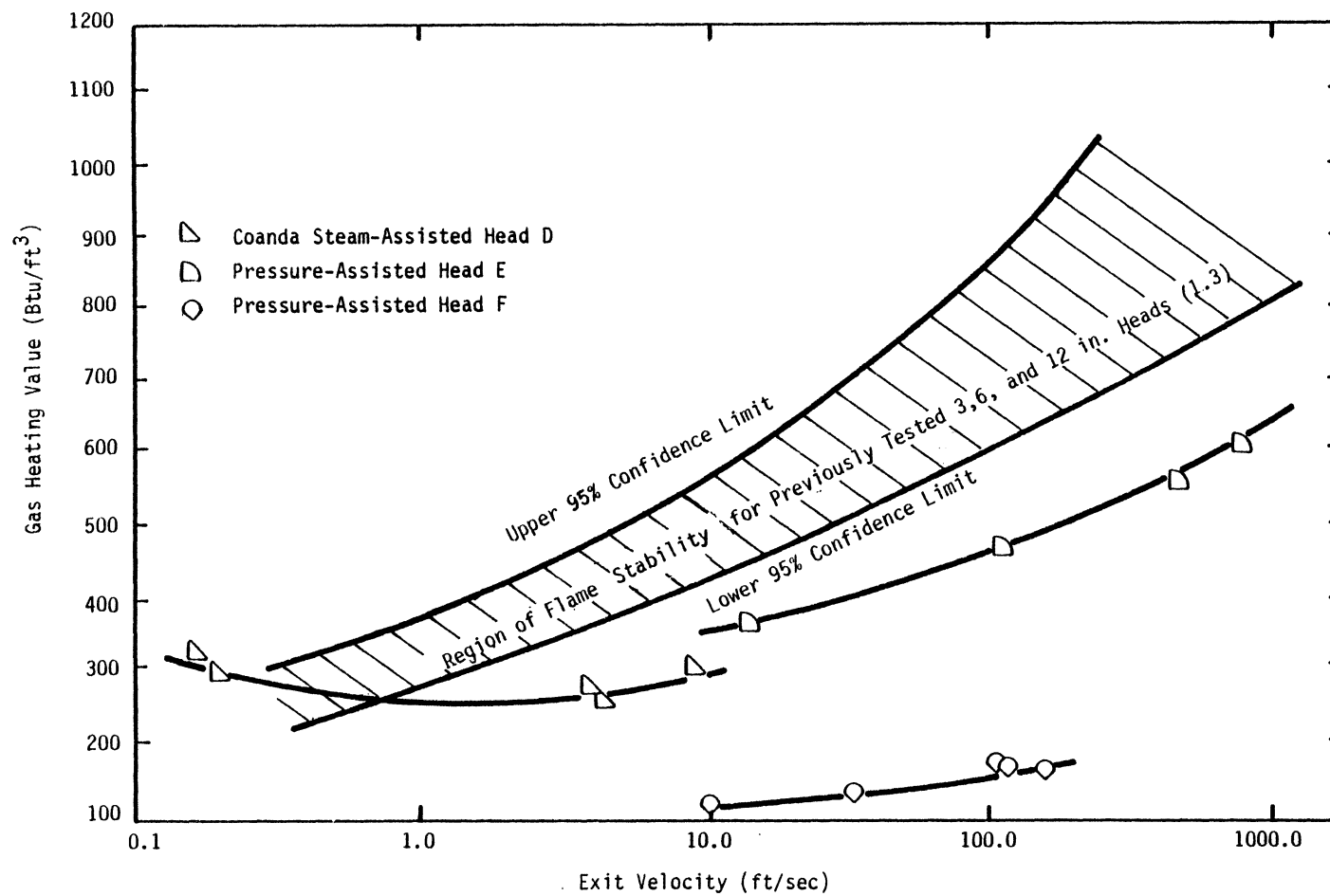


Figure 4-13. Region of flame stability for steam and pressure-assisted heads D, E, and F.

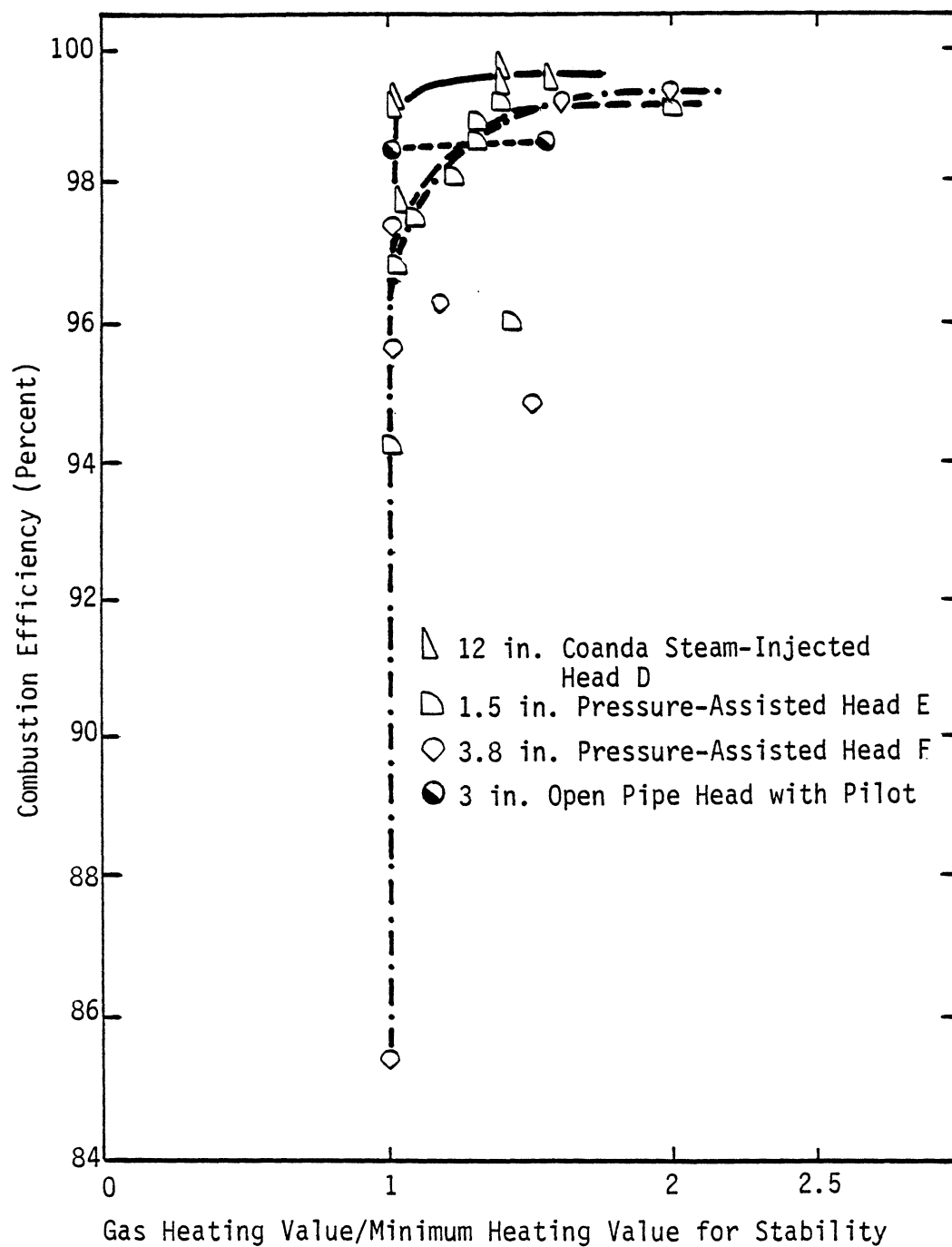


Figure 4-14. Combustion efficiency vs. flame stability for steam-injected and pressure-assisted flare heads.

## 5.0 GAS COMPOSITION TEST RESULTS

The second major objective of this program was to evaluate the effects of relief gas composition on flare combustion and destruction efficiency. This portion of the program included Tasks 2 and 3 of the test program. In Task 2, destruction efficiency, soot production, and ignitability were measured in screening tests conducted on the lab-scale Flare Screening Facility (FSF) for 21 different compounds. Of these 21 compounds, only six exhibited any suggestion of flaring difficulty. In Task 3, combustion and destruction efficiencies of three of the six compounds identified in Task 2 as potentially having combustion problems were tested on the pilot-scale Flare Test Facility (FTF). Hydrogen sulfide, although not screened, was also selected for testing on the FTF. Unique sampling procedure problems prevented completion of the H<sub>2</sub>S tests. Reliable sample techniques have since been developed, and H<sub>2</sub>S destruction efficiency tests are planned for the next series of tests.

### 5.1 Compound Selection

Compounds screened were selected based on the potential flaring problems of the compound and the extent to which the compound is industrially flared. Information was collected from literature, industrial sources, and the EPA. Final compound selection was accomplished with the advice of the Technology Advisory Committee and the EPA Project Officer.

### 5.2 Compound Screening Tests

Potential flaring difficulties of 21 different compounds were evaluated on the FSF. The compounds tested were representative of aliphatic, aromatic, sulfur, nitrogen, chlorinated, oxygenated, and low heating value compounds industrially flared. Each compound was either mixed with propane and/or nitrogen gas, or tested as a pure compound.

Table 5-1 presents the results of the screening tests. The nozzle used for these tests was a 1/16 inch O.D. (0.042 inch I.D.) stainless steel tube.

Table 5-1

## RESULTS OF SCREENING TESTS ON FLARE SCREENING FACILITY

Compound	Gas Composition (%)			Velocity at Stability Limit (ft/sec) <sup>1</sup>	Lower Heating Value (Btu/ft <sup>3</sup> )	DE <sup>2</sup> (%)	CE <sup>3</sup> (%)	Soot (mg/m <sup>3</sup> )
	Compd	Propane	N <sub>2</sub>					
Acetylene	100	0	0	854	1475	99.99	99.97	<1.5
Ethylene	100	0	0	443	1580	99.91	99.92	<1.5
Propylene	100	0	0	184	2300	99.98	99.93	<1.5
1,3-Butadiene	100	0	0	127	2730	99.93	99.93	75 <sup>5</sup>
Butane	100	0	0	58	3321	99.99	99.96	<1.5
Propane	100	0	0	143	2350	99.98	98.18	<1.5
Propane	75	0	25	48	1763	99.97	NA <sup>4</sup>	<1.5
Benzene	1.50	98.5	0	61	2370	99.59	99.95	<1.0
Toluene	1.50	98.5	0	61	2381	99.99	99.90	<1.0
Chlorobenzene	1.15	98.85	0	58	~2350	99.49	99.95	<1.0
Carbon Monoxide	100	0	0		Could Not Ignite <sup>6</sup>			
Carbon Monoxide	20	80	0	108	1943	99.60	99.88	<1.0
Carbon Monoxide	17	37	46	30	923	79.72 <sup>7</sup>	99.42	<1.0
Acetone	1.43	98.57	0	59	2347	99.80	99.96	<1.0
Acetaldehyde	2.07	97.93	0	58	2331	99.99	99.97	<1.5
Ethylene Oxide	1.42	98.58	0	58	2337	96.95	99.95	<1.0
CO <sub>2</sub> Diluent	7.58	92.42	0	93	2171	NA	99.93	<1.0
Methyl Chloride	9.17	90.83	0	65	2212	99.94	99.96	<1.0
Ethylene Dichloride	1.43	98.57	0	58	2335	99.70	99.95	<1.0
Vinyl Chloride	0.11	99.89	0	31	~2350	96.79	NA	<1.0
Methyl Mercaptan	10.7	89.30	0	65	2228	99.39	99.82	<1.0
Acrylonitrile	1.47	98.53	0	58	~2350	99.99	99.96	<1.0
Hydrogen Cyanide	0.013	99.99	0	78	~2350	85.00	NA	<1.0
Ammonia	100	0	0		Could Not Ignite <sup>6</sup>			
Ammonia	20	80	0	74	1967	99.90	NA	<1.0

1 = Nozzle ID = 0.042 inches

2 = Destruction Efficiency

3 = Combustion Efficiency

4 = Not available

5 = Without steam or air assist

6 = On 1/16 inch nozzle without pilot flames

7 = DE calculated assuming no CO originated from propane

Combustion efficiency (CE), destruction efficiency (DE), and soot production were measured at the stability limit conditions for each gas or gas mixture on the 1/16 inch nozzle. Most compounds demonstrated high CE and DE and low soot production. Six compounds did not. Two compounds, pure carbon monoxide and pure ammonia, could not be ignited when flared on the 1/16 inch nozzle. Carbon monoxide is known to be difficult to ignite in the absence of hydrogen. Also, ignition, but not combustion, of ammonia is known to be difficult. One compound, 1,3-butadiene, resulted in high soot production. Four compounds or mixtures of compounds resulted in low DE. These gases were CO-N<sub>2</sub> mixture (79.72 percent DE), ethylene oxide (96.92 percent), vinyl chloride (96.79 percent), and hydrogen cyanide (85.00 percent).

Based upon poor ignitability, high soot production, or low DE, carbon monoxide, ammonia, 1,3-butadiene, ethylene oxide, vinyl chloride, and hydrogen cyanide were selected as candidates for pilot-scale testing on the Flare Test Facility. Hydrogen sulfide, although not screened, was also selected for FTF testing because of its toxicity and industrial importance in flaring.

### 5.3 Gas Mixture Flare Tests

Pilot-scale destruction efficiency tests were conducted on four of the seven candidate compounds identified in the FSF Tests. These four compounds were ammonia, 1,3-butadiene, ethylene oxide, and hydrogen sulfide. The other three, carbon monoxide, hydrogen cyanide, and vinyl chloride, were not tested in this program due to cost and restricted availability. The four compounds were tested on the Flare Test Facility (FTF) using a 3 inch open pipe flare head, without flame retention devices, steam, or pilot assist. Two of the gases, ammonia and hydrogen sulfide, were tested in mixtures with propane and nitrogen. This was done to increase operational safety and reduce cost while matching low concentration levels of these gases (~5 percent) sometimes found in industrial relief gases. Ammonia can also be flared as a pure compound. The propane-nitrogen proportion was varied to maintain the gas heating value near the limit of flame stability. Ethylene oxide and 1,3-butadiene were each tested diluted with nitrogen only. Propane was not mixed with these

gases, since the products of propane combustion would have interfered with interpretation of DE for these compounds. The heating value was varied for these tests by varying the amount of nitrogen in the relief gas.

Results from testing these gases were similar to the previous results on commercial flare heads. By varying the gas exit velocity and heating value, the stability curve was defined for each mixture (Figure 5-1). The velocity for these stability tests ranged from 0.15 to 139 ft/sec, although most of the tests were conducted at velocities between 0.5 and 10 ft/sec. The gas heating value was varied between 145-877 Btu/ft<sup>3</sup>. The stability curves for the ammonia and hydrogen sulfide mixtures were within the region of stability for propane-nitrogen mixtures. This is not surprising, since the majority of combustible gas in those tests was propane. Stability curves for 1,3-butadiene and ethylene oxide are lower than for the ammonia-propane and hydrogen sulfide-propane mixtures.

Physical properties of these compounds are shown in Table 5-2, and can be used to help explain differences in the stability curves. A lower stability curve is indicative of increased flame stability for that compound, due to flammability in a wider concentration range and/or higher flame speed. The flammability range for ethylene oxide is very wide, from 3 percent to 100 percent, and the calculated adiabatic flame temperature (4,038 R) is slightly higher than that of propane (3,838 R). Typically, the higher the flame temperature, the higher the flame speed. Although the flammability limits for 1,3-butadiene differ only slightly from propane flammability limits, the adiabatic flame temperature (4,105 R) and flame speed are higher. In addition, the high lower flammability limits and lower adiabatic flame temperature of ammonia can be used to explain why pure ammonia could not be ignited in the screening tests.

Destruction efficiency tests were conducted for each gas mixture at operating conditions near the stability limit. Measurements were thus made under conditions of potentially low combustion and destruction efficiency. Tests were also conducted under more optimum conditions within the operating envelope to measure efficiencies more representative of normal flare



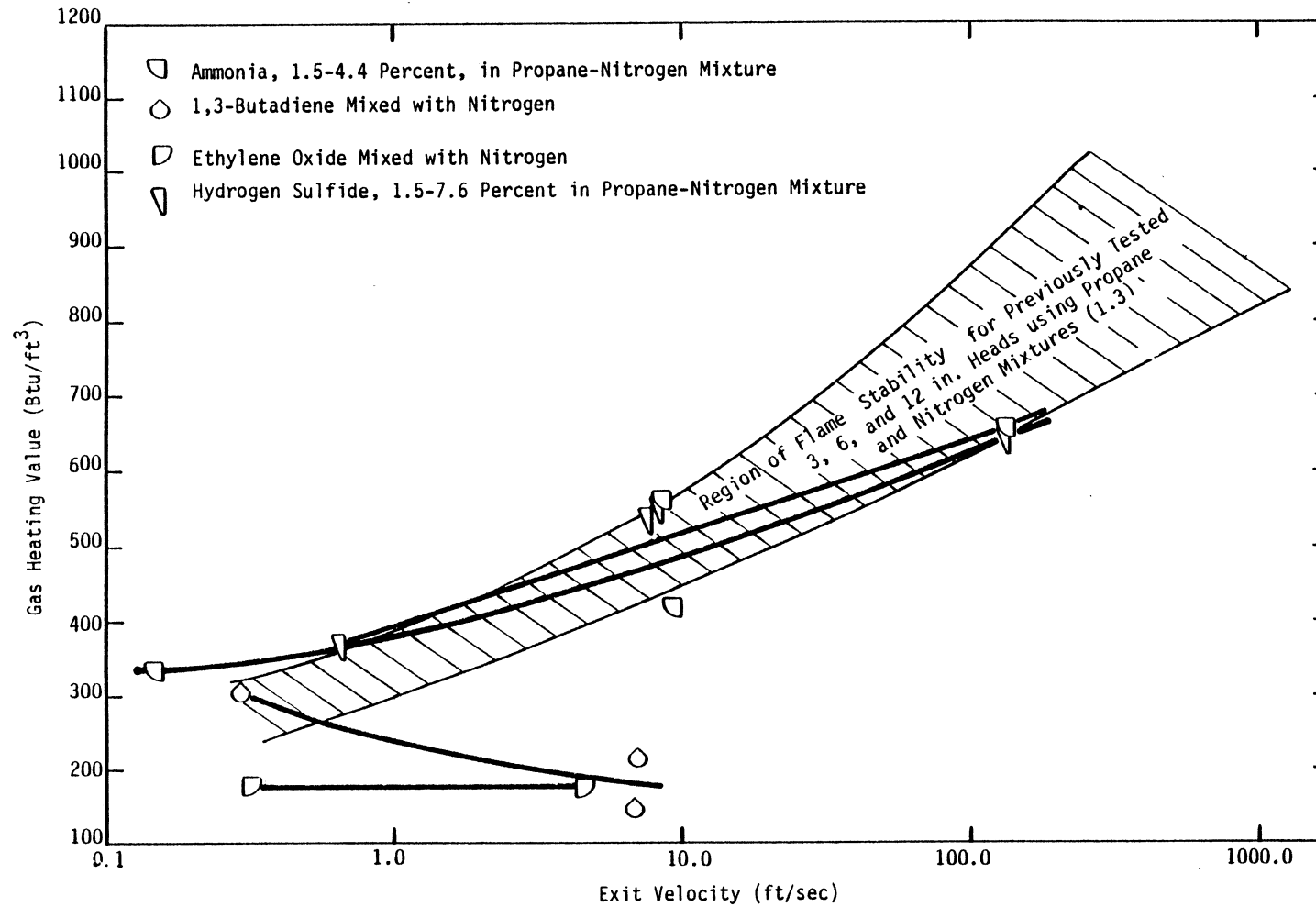


Figure 5-1. Region of flame stability for the 3 inch open pipe flare head burning selected relief gas mixtures.

Table 5-2  
 PHYSICAL PROPERTIES (1 ATM, 60°F) OF THE COMPOUNDS TESTED  
 USING THE FLARE TEST FACILITY

Name	Formula	M.W.	Spec. Vol. (ft <sup>3</sup> /lb)	Lower Htg Value (Btu/ft <sup>3</sup> )	Flammability Limits in Air (%)		Adiabatic Flame Temp. (°R) <sup>1</sup>	Ignition Temp (°F)
					Lower	Upper		
Propane	C <sub>3</sub> H <sub>8</sub>	44.097	8.606	2350	2.1	10.1	3838	871
Ammonia	NH <sub>3</sub>	17.031	22.28	359	15.50	27.00	3505	1204
Ethylene Oxide	(CH <sub>2</sub> ) <sub>2</sub> O	44.053	8.62	1349	3.0	10.0	4105	NA <sup>2</sup>
1,3-Butadiene	(C <sub>4</sub> H <sub>6</sub> )	54.092	7.016	2730	2.0	11.5	4038	484
Hydrogen Sulfide	H <sub>2</sub> S	34.076	11.14	588	4.3	45.5	3338	558

Data From: Balzhiser, R. E., M. R. Samuels, and J. D. Eliasson, Chemical Engineering Thermodynamics, 1972  
 CRC Handbook of Tables for Applied Engineering Science. 2nd Ed. 1976  
 CRC Handbook of Chemistry and Physics, 53rd Ed., 1972-73  
 Howard, H. F. and G. W. Jones, "Limits of Flammability of Gases and Vapors", USBM Bulletin 503, 1952  
 GPSA Engineering Data Book, 1972  
 Gas Engineers Handbook, 1st Ed., 1965  
 Chemical Engineers Handbook, 5th Ed. 1973

1. Calculated by integration of heat capacity data
2. Not Available


operations. Figure 5-2 shows the destruction efficiency of ammonia, 1,3-butadiene, ethylene oxide, and propane correlated to flame stability. The measured destruction efficiency varied with compounds. Destruction efficiency results for hydrogen sulfide are not reported because they were found to be in error, due to collection and analysis problems unique to H<sub>2</sub>S and SO<sub>2</sub> mixtures. The analytical and sampling techniques have been improved since this testing was completed and further hydrogen sulfide destruction efficiency measurements are planned for the next series of tests. The results shown for H<sub>2</sub>S in Figure 5-2 are the destruction efficiency of  in propane-H<sub>2</sub>S mixtures. why?

Figure 5-3 shows the hydrocarbon combustion efficiency for the gas mixture tests. Since the ammonia and hydrogen sulfide gas mixtures contained propane support gas, the hydrocarbon combustion efficiency is the combustion efficiency of propane to carbon dioxide and water. For the 1,3-butadiene and ethylene oxide test, no propane was added, and hydrocarbon combustion efficiency is the respective conversion efficiency of 1,3-butadiene and ethylene oxide to carbon dioxide and water.

Comparison of Figures 5-2 and 5-3 shows that as the flame stability limit is approached, both destruction and combustion efficiency decrease for all the species tested. This behavior is identical to previous test results for propane-nitrogen mixtures flared with a variety of flare heads. Ethylene oxide combustion efficiency was quite high, only slightly lower than ethylene oxide destruction efficiency. Small amounts of CO and soot were produced by flaring 1,3-butadiene, although both combustion and destruction efficiencies were high. Figures 5-2 and 5-3 also show that when the combustion efficiency of the support propane was high in combustion tests with ammonia-propane mixtures, ammonia destruction efficiency was correspondingly high.

Destruction efficiencies measured on the FSF are not directly comparable with those measured on the FTF. Figure 5-4 shows that for propane, ammonia, and 1,3-butadiene, the destruction efficiency measured on the FTF were lower than those measured on FSF. The values measured on the FTF are more closely related to industrial practice since the 3 inch flare head on the FTF is

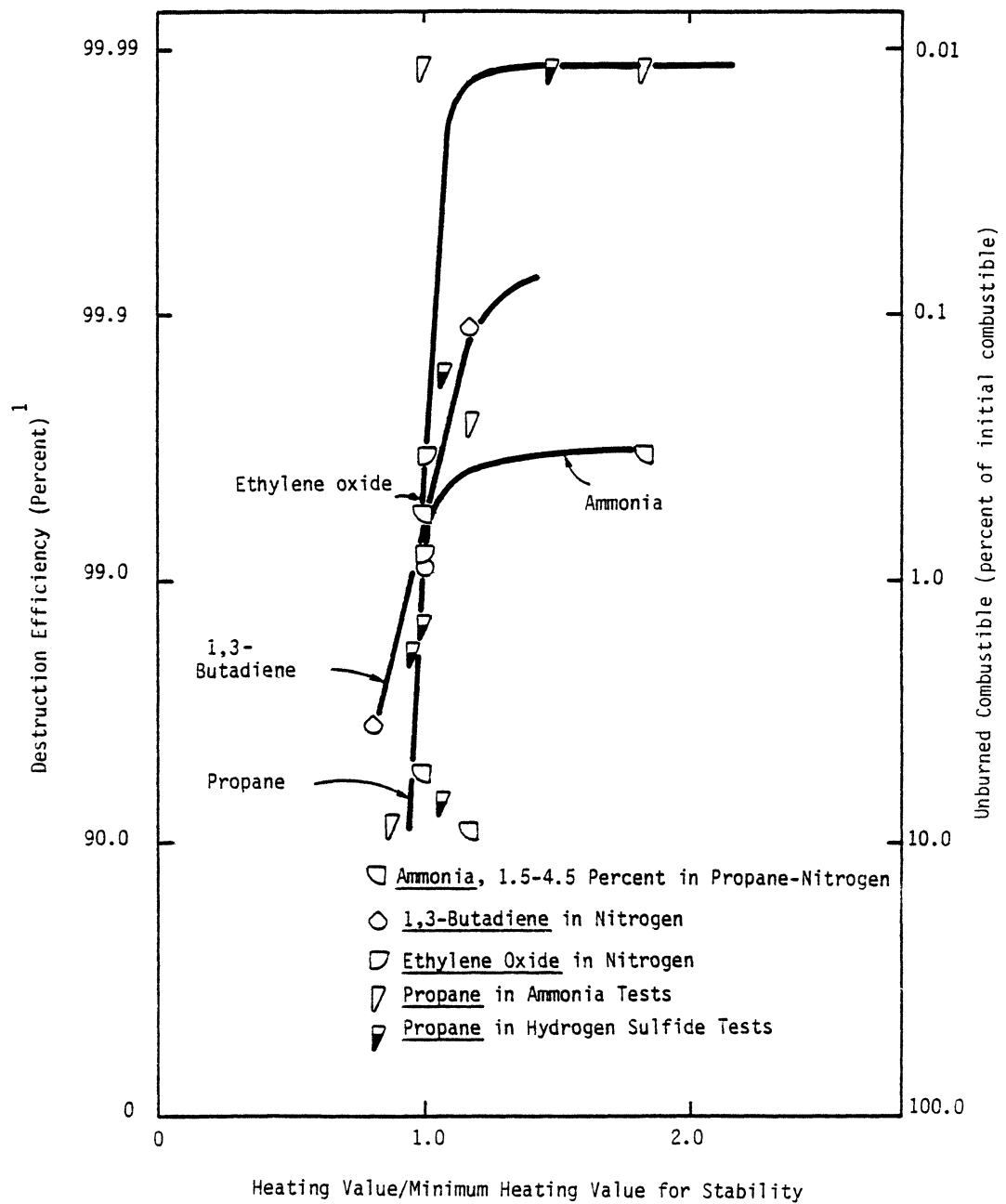


Figure 5-2. Destruction efficiency of different gases.

<sup>1</sup> Scale is  $\log(100-DE)$

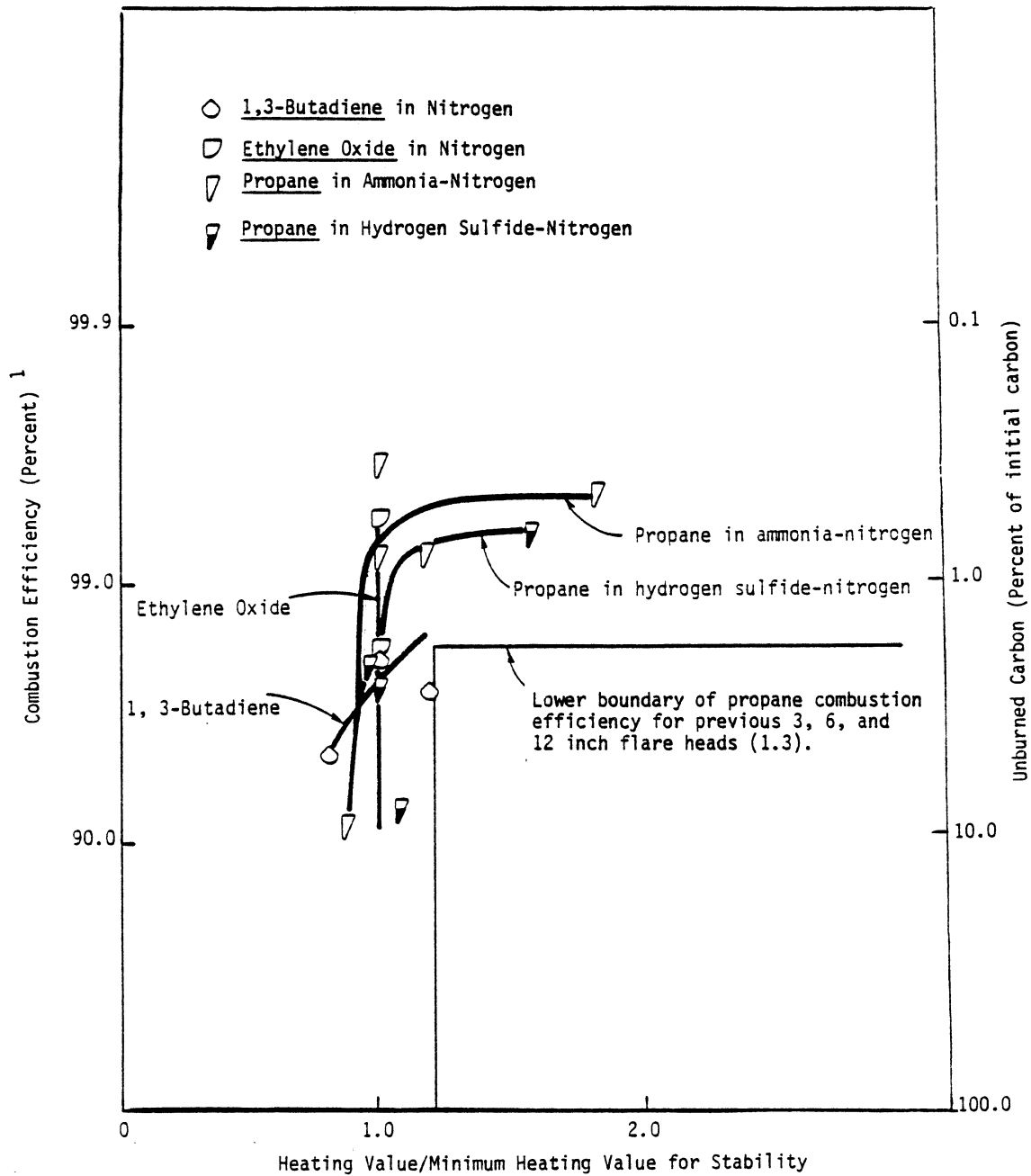


Figure 5-3. Hydrocarbon combustion efficiency of gas mixtures.

<sup>1</sup> Scale is  $\log(100-CE)$

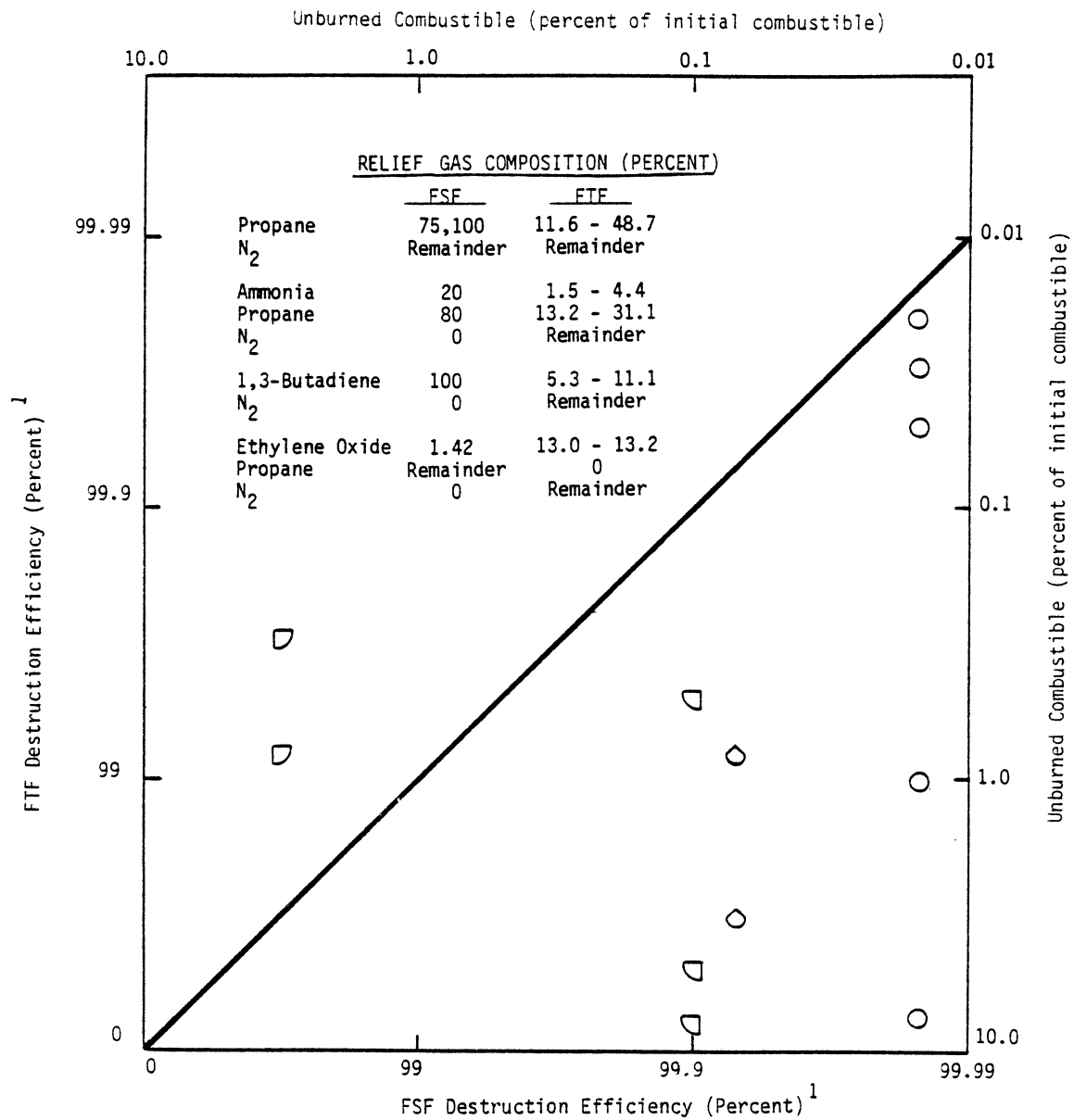


Figure 5-4. Pilot-scale FTF destruction efficiency results compared to lab-scale FSF destruction efficiency results. All results at operating conditions near the stability limit. FTF nozzle size = 3 inches. FSF nozzle size = 0.042 inches.

<sup>1</sup> Scale is  $\log(100-DE)$

aerodynamically similar to that of industrial flares, while the small 1/16 inch diameter nozzle used in the FSF is not. Destruction efficiencies measured on the FSF can be used to judge the relative destruction efficiency of different compounds. Values of absolute destruction efficiency measured on the FSF can not be extrapolated to estimate emissions from industrial flares. Also, although poor flaring performance for these gases has been shown on the lab-scale FSF, in industry these compounds are successfully flared by employing combustion enhancement techniques such as steam, air, or pressure-assist, support gas or pilots, or flame retention devices.

#### 5.4 Flame Stability Correlations

It has been shown in Section 5.3 that high combustion efficiency can be expected for the conditions and gas mixtures tested in this study if the flame is above the stability limit (Figure 5-3). Pohl, et al. (5.1, 5.2) Noble, et al. (5.3) reached the same conclusion. As shown in Figure 5-1, the gas heating value at the flame stability limit can be different for different gas mixtures. For example, the lower stability limit of propane-nitrogen mixtures flared at 10 ft/sec using a 3 inch open pipe flare is around 500 Btu/ft<sup>3</sup>. At the same conditions, the stability limit heat content of 1,3-butadiene is only 180 Btu/ft<sup>3</sup>. Clearly, gas heating value is not the only factor affecting flame stability.

The flame stability limit is approached when the flame velocity approaches the relief gas velocity. The determination of flame velocity is very complex, involving reaction kinetics and mixing (5.4). The inherent complexities discourage a direct evaluation of flare flame kinetic and mixing rates. However, empirical relations between gas parameters and flame stability may prove tractable. Besides the heating value of a given gas or gas mixture, there are (1) adiabatic flame temperature, (2) upper and lower flammability limits in air, (3) minimum ignition temperature, (4) maximum flame velocity, and (5) bond energies. Unfortunately, much of this data is unavailable for many gases and most gas mixtures flared.

A simplistic approach is to relate flame stability to flame temperature as a surrogate for reaction kinetics, diffusion, and flame velocity. Is it reasonable to assume that the flame velocity depends upon temperature, since reaction kinetic rates are strongly temperature dependent. A high calculated adiabatic flame temperature for a gas or gas mixture would theoretically indicate a fast flame velocity and a correspondingly low gas heating value at the stability limit.

The relationship between adiabatic flame temperature and limiting nozzle exit velocity for the relief gas is shown in Figure 5-5 for the gases tested in this study. The stability correlations are different for propane, 1,3-butadiene, and ethylene oxide mixtures. This shows that flame temperature correlates the limiting velocity at stability for a single gas but cannot correlate the stability limit of different gases. Both 1,3-butadiene-N<sub>2</sub> and ethylene oxide-N<sub>2</sub> mixtures can be stably flared at a lower heating value (Figure 5-1) and flame temperature than can propane-N<sub>2</sub> mixtures, with the same exit velocity. Evidently, 1,3-butadiene and ethylene oxide are more reactive with air than propane.

Another measure of reactivity of a compound with air is the range of flammability of that compound in air. Table 5-2 shows that the range of flammability for both ethylene oxide and 1,3-butadiene are greater than for propane. A flame stability correlation has been developed by Noble, et al. (5.3) that includes both a measure of flame temperature and the range of flammability limits in air for a gas or gas mixture:

$$N = \frac{LHV}{Q} \left( \frac{UFL}{LFL} \right) \quad 5-1$$

where N = "Experimental Index"

LHV = lower heating value of the relief gas (Btu/ft<sup>3</sup>)

Q = enthalpy at 2700 R of stoichiometric products of combustion of one cubic foot of the relief gas (Btu/ft<sup>3</sup>)



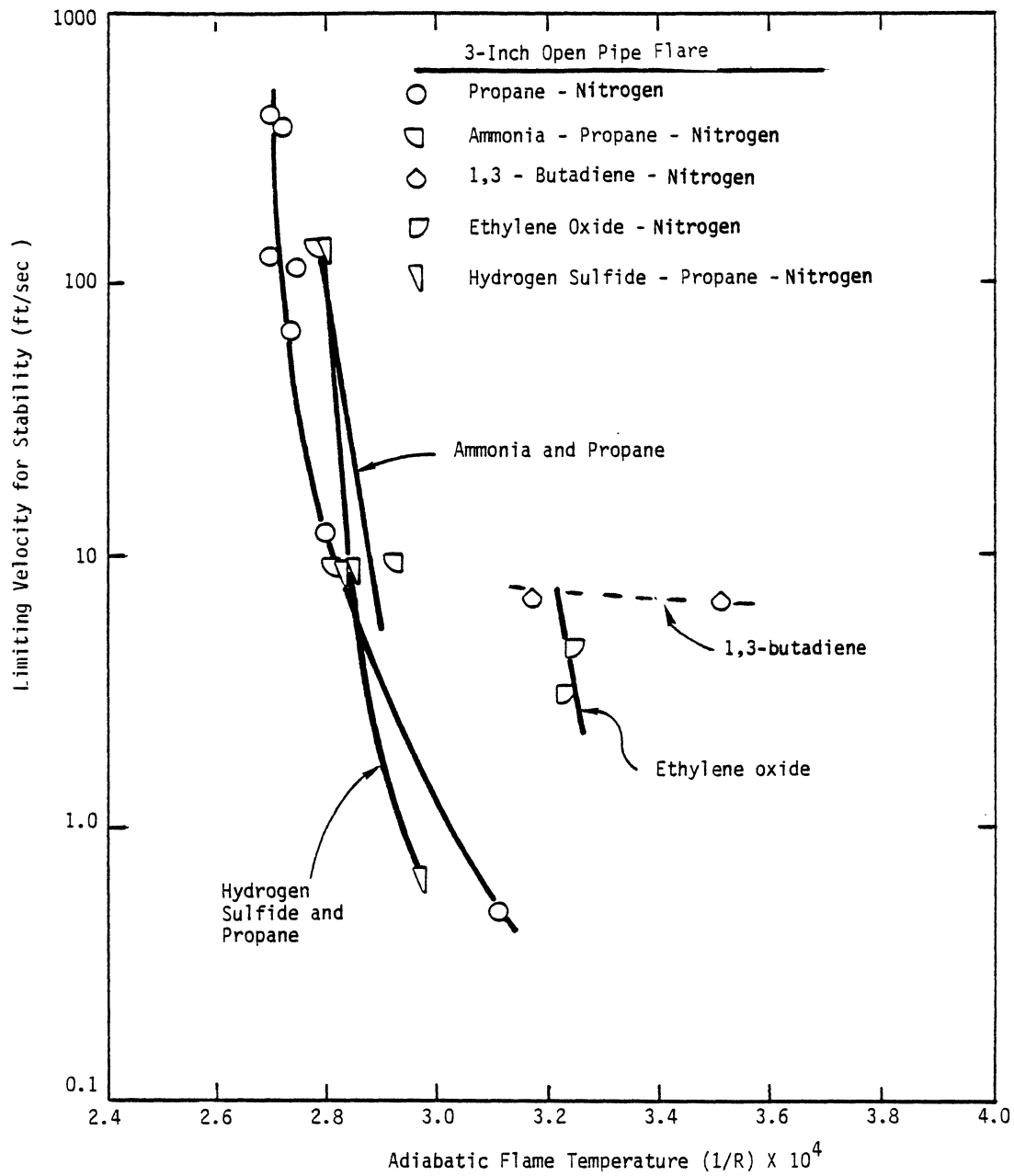


Figure 5-5. Calculated adiabatic flame temperature vs limiting stable gas exit velocity for different gas mixtures.

UFL,LFL = upper and lower flammability limits of the relief gas in air, estimated using calculation method in Gas Engineers Handbook (5.5) for gas mixtures and gas flammability limits from (5.6) and (5.7)

The term  $LHV/Q$  is a ratio of the flame temperature to a minimum temperature of 2700 R, the calculated temperature of lower limit hydrocarbon-air flames. The ratio UFL/LFL adjusts the flame temperature ratio to account for the reactivity of the relief gas.

The Experimental Index,  $N$ , is then correlated to the limiting nozzle mach number (the exit velocity/sonic velocity) of the relief gas. This correlation is shown in Figure 5-6(a) for the results of Noble, et al. (5.3). Darkened points in Figure 5-6(a) indicate flame blow-out, and open points indicate a flame is present. The stability limit is the line separating the majority of darkened points from open points. Figure 5-6(b) shows the results of this work compared to the correlation line of Noble's data. The closed points indicate combustion efficiency less than 98 percent, and the open points indicate combustion efficiency greater than 98 percent. Only the results of tests conducted near the stability limit were used in this comparison. Even so, a difference is seen between the results of this study and Noble's results. Although there is a good deal of scatter in both data sets, the location and slope of the stability limit lines are different. These differences may be due to the difference in head size (2 inch vs 3 inch), head design, and the difference in determination of stability limit (point of incipient flame-out vs point of 98 percent CE on the two studies. It should also be noted that the parameter used does not clearly separate the region of stability from instability and errors of a factor of two in velocity can be expected. The separation is even less distinct when the relationship is used to divide flares with high combustion efficiency (>98 percent) from those with low combustion efficiency (<98 percent).

The stability limit line for the EER data is nearly vertical, indicating that nozzle exit velocity depends very little upon  $N$ , but that there is a limit of  $N$  between 4 - 7, below which instability occurs regardless of exit velocity. This boundary is more restrictive than the boundary defined by

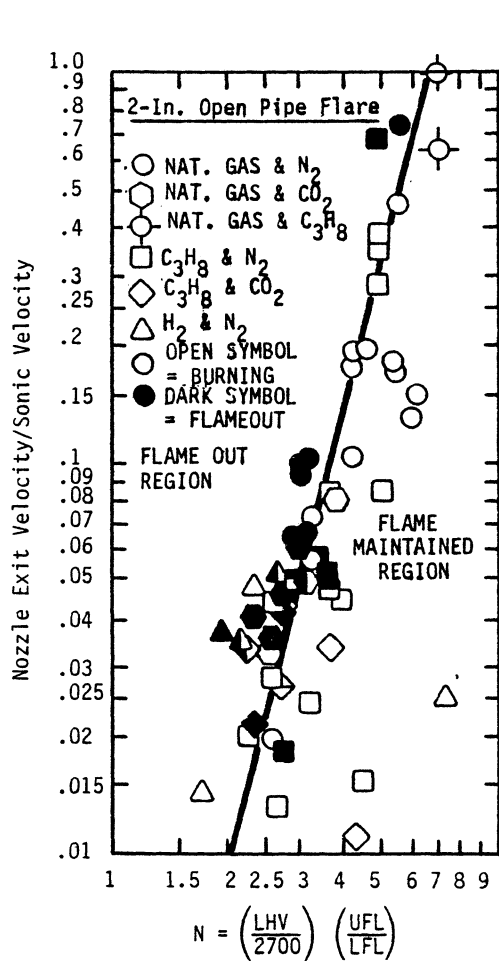


Figure 5-6(a). Nozzle velocity vs Experimental Index for data from Noble, et al. (5.1).

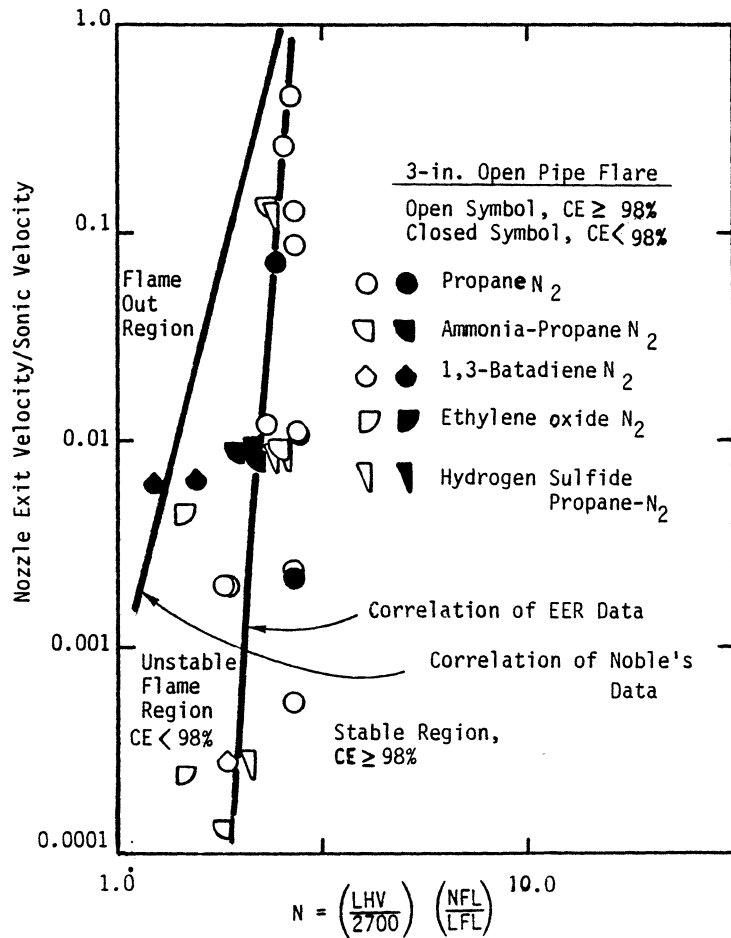


Figure 5-6(b). Nozzle exit velocity vs Experimental Index for gas mixture tests.

Noble's data, where  $N$  can be as low as 1.5 at low exit velocities. The region between the two correlation lines could represent an unstable flame region, where CE may be less than 98 percent even though the flame is still marginally maintained. Such a wide region of indicated flame instability and low CE is not surprising, considering the data scatter and that, when a flame is near instability, minor variations in operating or ambient conditions can greatly effect stability and combustion efficiency.

5.5        References

- 5.1 Pohl, J. H., R. Payne, and J. Lee, "Evaluation of the Efficiency of Industrial Flares: Test Results", EPA Report No. 600/2-84-095, May 1984.
- 5.2 Pohl, J. H., J. Lee, R. Payne and B. Tichenor, "The Combustion Efficiency of Flare Flames", 77th Annual Meeting and Exhibition of the Air Pollution Control Association, San Francisco, CA, June 1984.
- 5.3 Noble, R. K., M. R. Keller, and R. E. Schwartz, "An Experimental Analysis of Flame Stability of Open Air Diffusion Flames", AFRC International Symposium on Alternative Fuels and Hazardous Wastes, Tulsa, OK, 1984.
- 5.4 Burgess, D. and M. Hertzberg, "The Flammability Limits of Lean Fuel Air Mixtures: Thermochemical and Kinetic Criteria for Explosion Hazards", ISA Transactions 14(2), p. 129, 1974.
- 5.5 Gas Engineers Handbook, First Edition, Industrial Press, p. 2/75, 1965.
- 5.6 Zabatakis, M. G., "Flammability Characteristics of Combustible Gases and Vapors", U.S.B.M. Bulletin 627, 1965.
- 5.7 Coward, H. F. and G. W. Jones, "Limits of Flammability of Gases and Vapors", U.S.B.M. Bulletin 503, 1952.

## 6.0 FLARE $\text{NO}_x$ AND HYDROCARBON EMISSIONS.

Emissions of  $\text{NO}_x$  and hydrocarbons were measured in conjunction with measurements of combustion and destruction efficiency. Figure 6-1 shows  $\text{NO}_x$  concentration (on an air-free basis, 0 percent  $\text{O}_2$ ) at the plume centerline for the tests of this study. This figure show only a vague general relationship between  $\text{NO}_x$  formation and combustion efficiency;  $\text{NO}_x$  concentration increases with increasing combustion efficiency for most flare heads and gas mixtures. Results for the coanda steam-injected head are contrary to this trend, but  $\text{NO}_x$  emissions for this head were measured only over a narrow combustion efficiency range (99.6-99.9 percent). The poor correlation between  $\text{NO}_x$  concentrations in the plume and combustion efficiency results from some variables influencing  $\text{NO}_x$  formation and combustion efficiency differently. Figure 6-2 shows the correlation of total  $\text{NO}_x$  emissions with flare heat release rate. This figure shows a trend of increased  $\text{NO}_2$  emissions per  $10^6$  Btu with increasing heat release for all of the flare heads and gas mixtures. The values of NO and  $\text{NO}_2$  were determined by radial integration of local fluxes. Emissions of  $\text{NO}_x$  were almost entirely NO except for tests of the ammonia gas mixtures. The reported  $\text{NO}_2$  emission levels for the ammonia tests are generally between 2-100 times as high as  $\text{NO}_2$  emissions of the other tests. The highest  $\text{NO}_x$  emission level was for the ammonia mixture and was under 1 lb  $\text{NO}_2/10^6$  Btu.  $\text{NO}_x$  emissions from other tests were typically less than 0.1 lb  $\text{NO}_2/10^6$  Btu for hydrocarbon gas mixtures.

Limited qualitative and semi-quantitative hydrocarbon emissions were measured for the gas mixture tested. Hydrocarbon emissions were measured for 1,3-butadiene using the Flare Screening Facility. Table 6-1 shows that very low concentrations of hydrocarbons were detected in the plume samples. The concentration measurements are accurate to within one order of magnitude.

Hydrocarbon emission measurements were also made for the gas mixture tests on the Flare Test Facility. Results are shown in Table 6-2. These results have been corrected for background air hydrocarbon levels. Many of the species detected were present in very low concentrations. A few species

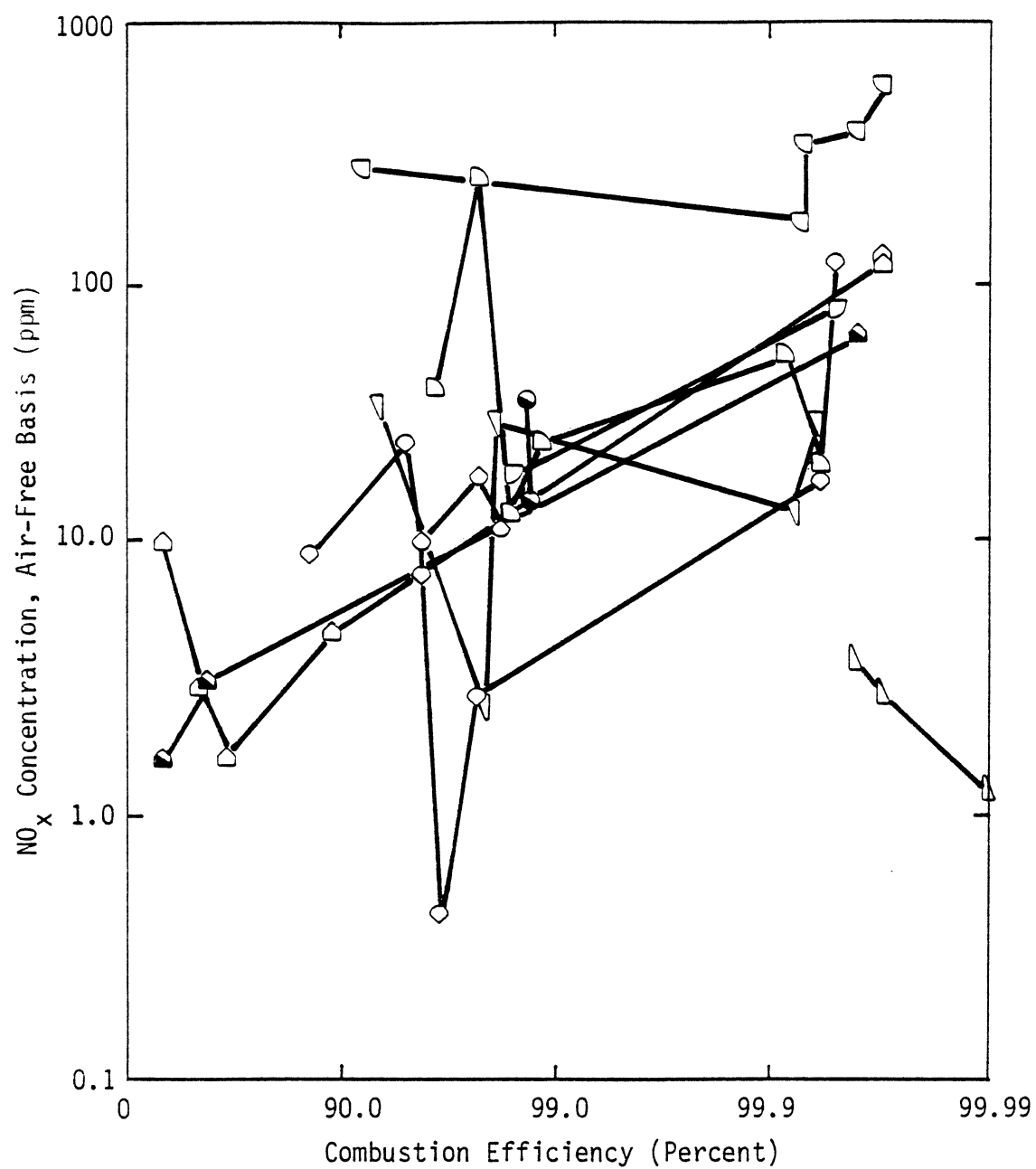


Figure 6-1. NO<sub>x</sub> concentration (air-free basis) at the plume centerline from pilot-scale flares.

## Legend for Figure 6-1

- △ Coanda 12 in. Steam Injected Head D
- ◐ 1.5 in. Pressure Assisted Head E
- ◑ 3.8 in. Pressured Assisted Head F
- ◒ 1.5 in. Air-Assisted Head G
- ◓ 1.5 in. Air-Assisted Head G with Pilot<sup>1</sup>
- 3 in. Open Pipe Head with Pilot<sup>1</sup>
- ◔ 3 in. Open Pipe Head, Ammonia-Propane-N<sub>2</sub> Mix
- ◕ 3 in. Open Pipe Head, 1,3 Butadiene-N<sub>2</sub> Mix
- ◖ 3 in. Open Pipe Head, Ethylene Oxide-N<sub>2</sub> Mix
- ◗ 3 in. Open Pipe Head, Hydrogen Sulfide-Propane N<sub>2</sub> Mix

<sup>1</sup>Heat release includes pilot when operating



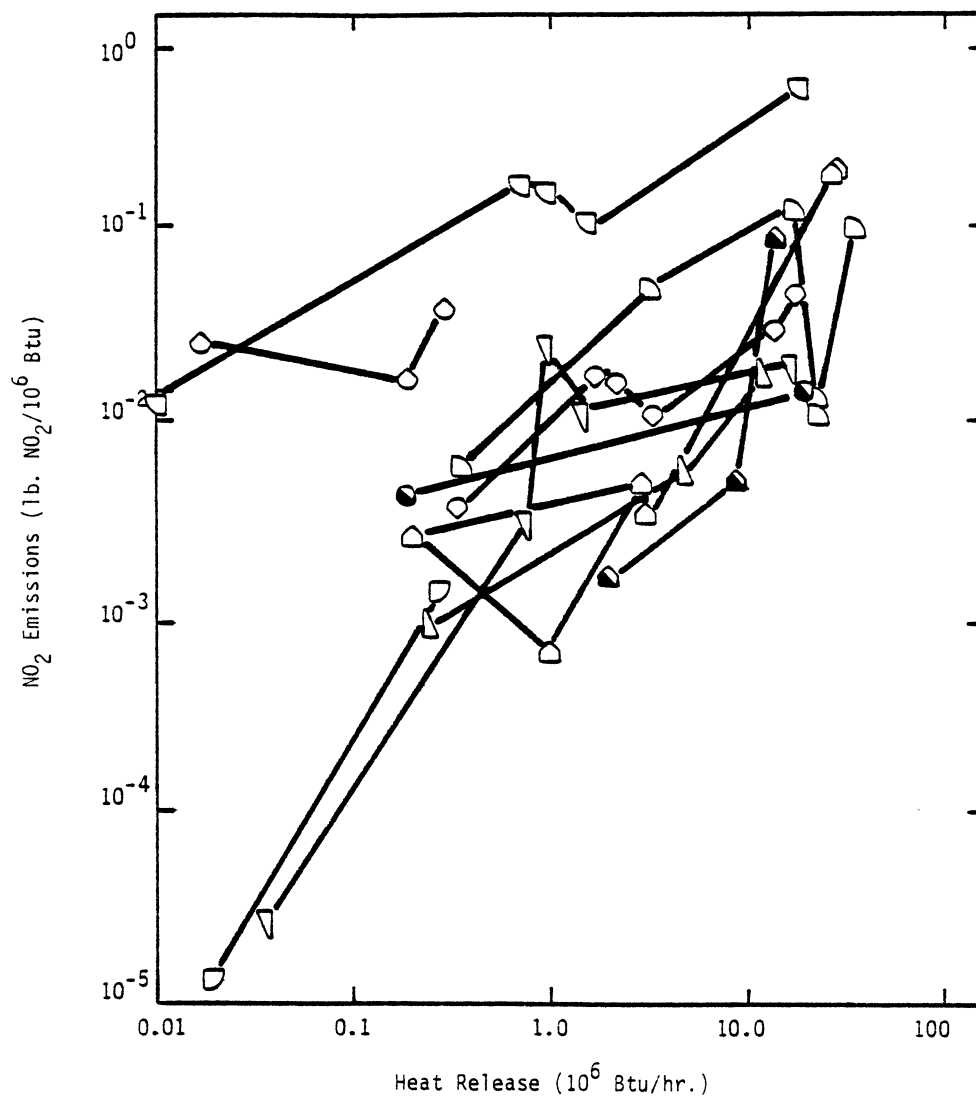


Figure 6-2. NO<sub>2</sub> emissions from pilot-scale flares.

## Legend for Figure 6-2

- ▷ Coanda 12 in. Steam Injected Head D
- ◻ 1.5 in. Pressure Assisted Head E
- ◊ 3.8 in. Pressured Assisted Head F
- ◻ 1.5 in. Air-Assisted Head G
- ◼ 1.5 in. Air-Assisted Head G with Pilot<sup>1</sup>
- 3 in. Open Pipe Head with Pilot<sup>1</sup>
- ◻ 3 in. Open Pipe Head, Ammonia-Propane-N<sub>2</sub> Mix
- ◊ 3 in. Open Pipe Head, 1,3 Butadiene-N<sub>2</sub> Mix
- ◻ 3 in. Open Pipe Head, Ethylene Oxide-N<sub>2</sub> Mix
- ▽ 3 in. Open Pipe Head, Hydrogen Sulfide-Propane-N<sub>2</sub> Mix

<sup>1</sup>Heat release includes pilot when operating

Table 6-1.

## GC-MS ANALYSIS OF PLUME SAMPLE FROM LABORATORY-SCALE TEST

Compound	Estimated Concentration (ppm)		Potentially Hazardous <sup>1</sup>
	224 Percent Excess Air	0 Percent Excess Air	
Acenaphthylene	0.0002	0.0006	
Benzaldehyde	0.005	0.02	
Benzofuran	0.001	0.001	
Biphenyl (or acenaphthene)	0.0004	0.001	
Dibromomethane <sup>2</sup>	0.0002	0.0006	X
Ethenylbenzene	0.005	0.02	
Ethynylbenzene	0.01	0.03	
Ethynyl-methylbenzene	0.01	0.03	
Methyl naphthalene	0.0006	0.002	
Naphthalene	0.01	0.03	X
Phenol	0.005	0.02	X
Tetrachloroethene <sup>2</sup>	0.0005	0.002	X
Toluene	0.01	0.03	X

<sup>1</sup>Listed as hazardous under Appendix 8 Regulation, EPA (Hazardous Waste and Consolidated Permit Regulations), Federal Register 45:98 (May 19, 1980) and Federal Register 45:138 (July 16, 1980).

<sup>2</sup>Result of contamination.

Table 6-2

GC-MS ANALYSIS OF PLUME CENTERLINE SAMPLES FROM  
GAS MIXTURE TESTS, USING A 3 IN. OPEN PIPE FLARE

Compound	Approximate Concentration (air-free, 0 percent O <sub>2</sub> ) ppm			
	Test No. 285	No. 289	No. 292	No. 295
Propane	6	200	40	0
Methyl Chloride <sup>1</sup>	0	0	100	400
Methyl Ethyl Ketone	300	200	300	50
1,1,1-Trichloroethane	0.3	4	0	0
1,2-Dichloropropane	0	8	6	1
Toluene	0.4	1	1	4
Butylcellosolve (2-butoxyethanol)	0	0	2	0.1
Xylene	0.4	0	1	0.4
Trichloroethylene	0	2	0	0.2
Thiophene	1.8	5.2	20	10
Hexane	0.1	0.2	1	0.4
Tetrachloroethene	TR<0.009	0.2	1	0.4
Methyl Cyclohexane	0	0.1	0.6	0.4
Methyl Bromide <sup>1</sup>	TR<0.009	0.02	0.06	0.07
Benzene	TR<0.02	0.07	0.3	0.1
1,3-Butadiene	0	0	2	0
4-Vinyl Cyclohexane	0	0	5	0
-----				
Combustion Efficiency (%)	92.1	99.2	99.8	99.5
Gas Htg Value (Btu/ft <sup>3</sup> )	416	539	145	175
Gas Comp. Propane (%)	19.2	28.7	0	0
Nitrogen (%)	78.8	63.7	94.68	87.0
(Other) (%)	2.0 (NH <sub>3</sub> )	7.6 (H <sub>2</sub> S)	5.32 (1,3-butadiene)	13.0 (ethylene oxide)
Exit Velocity (ft/sec)	9.56	8.04	6.87	4.63
Dilution Factor (DF)	45.4	69.5	60	36.4
SO <sub>2</sub> Tracer Used	Yes	No	Yes	No

NOTE: Approximate plume concentrations are found by dividing the air-free value by (DF + 1)

<sup>1</sup> Probable contaminant

<sup>2</sup> Trace detected, but below indicated minimum measurable concentration level.

were measured in significant amounts in one or more of the samples. Of these, the most common were propane, methyl chloride, and thiophene. The compounds, 1,3-butadiene, butyl cellosolve, and 4-vinyl cyclohexane were found only in the test of 1,3-butadiene. No nitrogen-bearing hydrocarbons were detected for any of the samples including tests of ammonia doped flames. Only one sulfur-bearing species (thiophene) was detected. It was detected in all the samples. All but one test included either H<sub>2</sub>S or SO<sub>2</sub> tracer in the relief gas, possible sources for thiophene. The source of thiophene in the other test (No. 255) is unknown, but the thiophene level in this test was very low and may be contamination. Many chloride-containing species were detected in varying amounts. These species are thought to result from contaminants in the relief gas or in the sampling and analytic procedure as no chlorine compounds were intentionally introduced to the flames or samples.

## APPENDIX A

### EPA FLARE TEST FACILITY AND TEST PROCEDURES

#### A.1 Flare Test Facility

The EPA Flare Test Facility (FTF), shown in Figure A-1, was designed and built by EER at their El Toro Test Site for the U.S. Environmental Protection Agency, under EPA Contract No. 68-02-3661. The facility was completed in 1982.

For wind protection, the FTF is located in a box canyon surrounded by 70-foot cliffs. The facility includes gas delivery systems, a flare head mount enclosed in a framework structure supporting (1) screens for additional wind protection, and (2) plume sample probes, and a building containing delivery system controls and analytical instruments. The facility is designed for relief gas flows ranging from 10 to over 40,000 SCFH. The maximum flow depends on gas composition. The facility is reviewed briefly below, and is described in more detail by Pohl, et al. (1.3) and Joseph, et al. (1.11).

Gases are delivered to the flare and auxiliary equipment through parallel manifolds shown in Figure A-2. Propane, natural gas, and nitrogen manifolds each have three orifice meters and one small rotameter, each with its own control valve. These manifolds were designed to accurately measure and control a wide range of flowrates. One additional manifold of two parallel orifice meters (not shown) is used to measure the flow of one additional flare gas. The propane, natural gas, and nitrogen manifolds and flow lines are constructed of carbon steel. The flow line and manifold system for the additional flare gas is constructed of stainless steel, to allow use of corrosive gases such as ammonia and hydrogen sulfide.

There are also similar supply systems for steam, sulfur dioxide (tracer) and air. Steam is used (1) for steam-assisted flare tests, (2) in steam heat

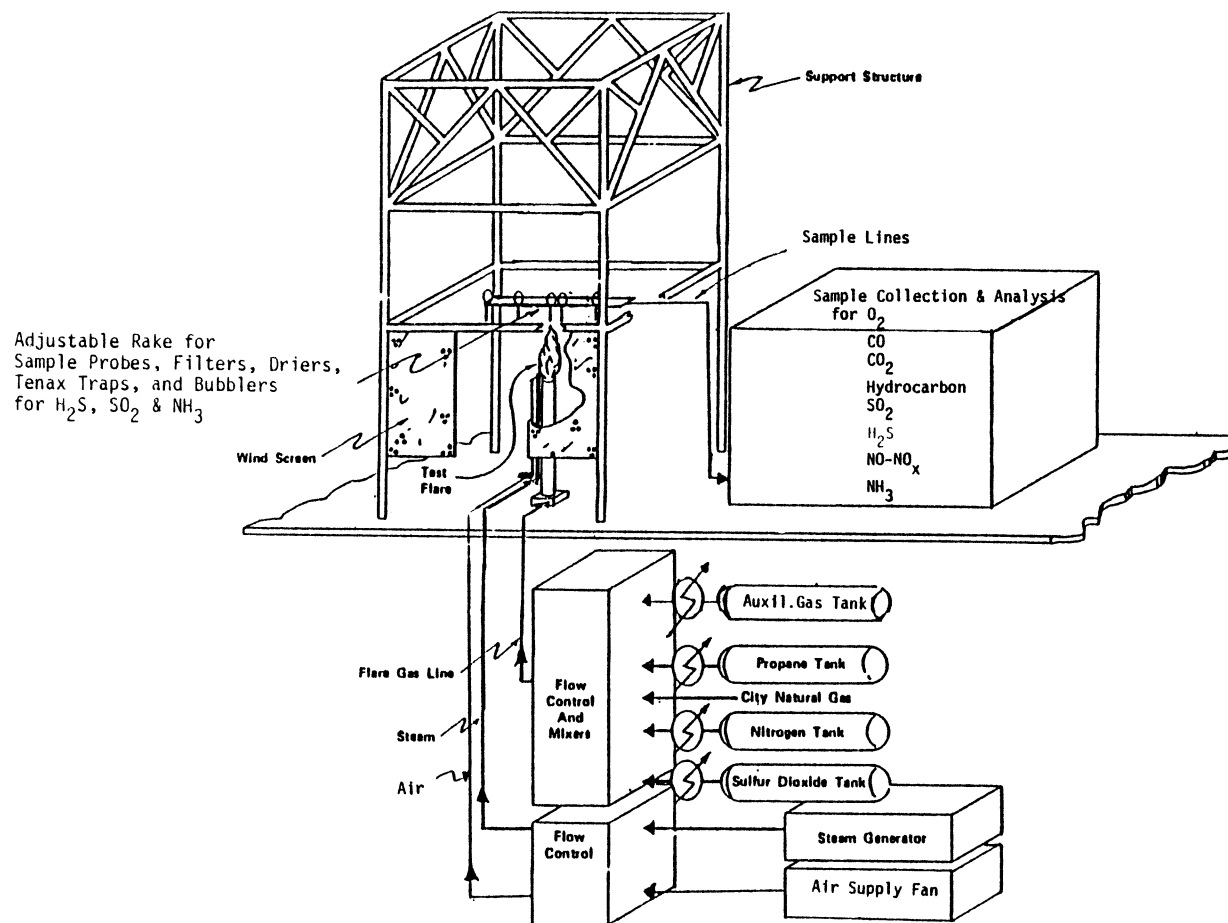


Figure A-1. EPA flare test facility (FTF) at EER.

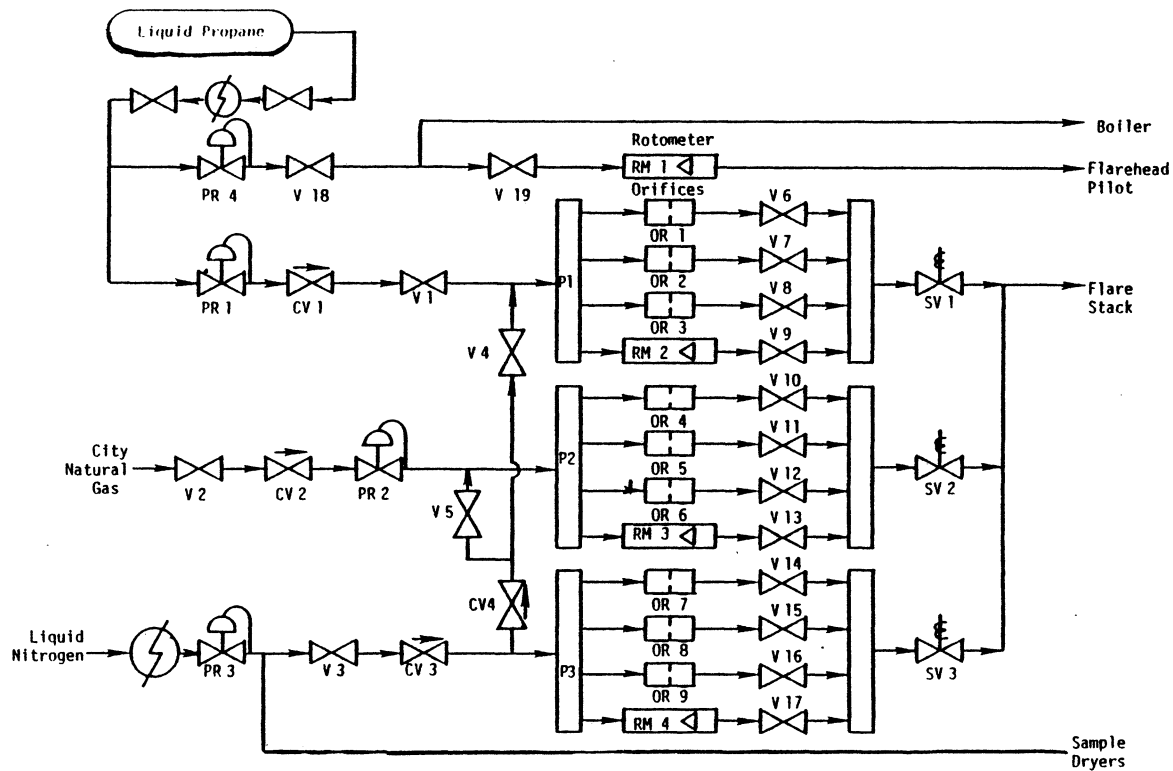


Figure A-2. Fuel flow control and metering system schematic.



exchangers for vaporizing sulfur dioxide and flare test gases, and (3) for sample probe heating. Sulfur dioxide is used as a tracer for flare test mass balances. Air is used during air-assisted flare tests.

These supply systems can provide and mix propane, natural gas, nitrogen, one additional flare gas (such as ammonia or hydrogen sulfide) and sulfur dioxide tracer. Propane is stored as a liquid in a 2,100 gallon tank. At low flowrates, natural vaporization is sufficient to supply propane gas for flaring; at higher flowrates, propane-fired vaporizers are used to increase the propane flowrate up to 15,000 SCFH. Natural gas is supplied by the local utility at a maximum flowrate of 7,000 SCFH. Nitrogen gas is used to vary the heating value of the flared gas. Nitrogen is delivered from liquid nitrogen cylinders to banks of finned-tube atmospheric vaporizers capable of providing a maximum nitrogen flowrate exceeding 24,000 SCFH.

The system to supply an additional gas is new to the FTF. Portable cylinders of a liquefied test gas such as ammonia or hydrogen sulfide can be connected to this system. A steam heat exchanger vaporizes the compound, and the flow rate is controlled and metered using pressure regulators, control valves, and orifice meters. This system is constructed of stainless steel to resist corrosion, and can deliver up to 4,000 SCFH of gas, depending upon the compound.

Steam is produced in a 15 hp gas-fired boiler. The boiler can supply up to 400 lbs/hr of 100 psig saturated steam. Sulfur dioxide, used as an inert tracer, is fed from liquid SO<sub>2</sub> cylinders and vaporized through a steam-heated vaporizer at 7 SCFH. Air is supplied by a forced-draft fan at a maximum flowrate of 60,000 SCFH, at a static pressure of 17.6 inches H<sub>2</sub>O.

The sample collection and analysis system is shown in Figure A-3. Plume samples are collected using five stainless-steel, steam-heated probes mounted on a movable rake. Samples are collected concurrently from five different radial locations in the plume. Pumps draw the soot- and moisture-laden samples into the probes, where filters collect the soot for subsequent weight measurement. Permapure dryers using membrane tube bundles selectively remove

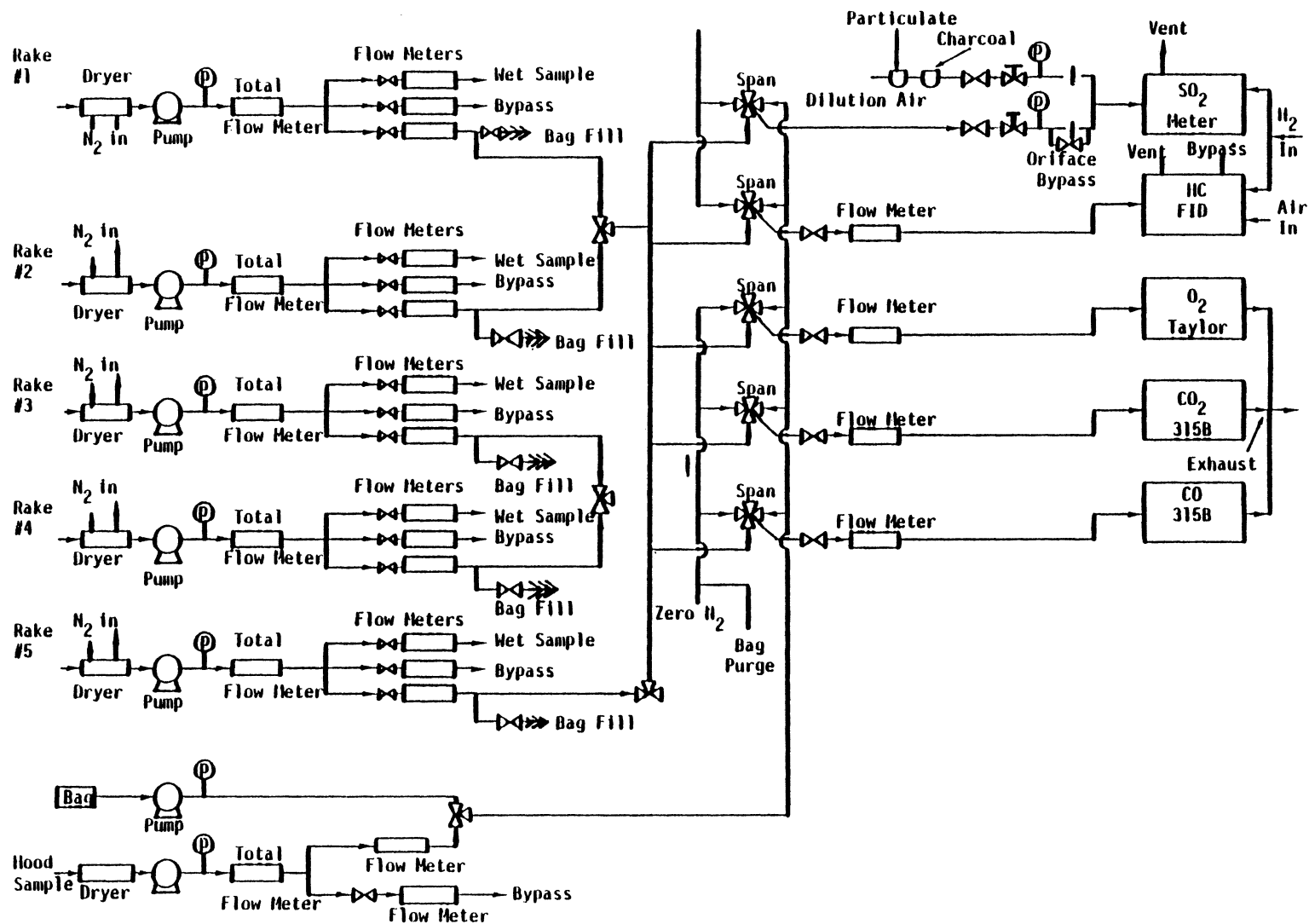


Figure A-3. Flare test facility sample system.

water vapor from the sample stream. The dried gas samples are collected in Tedlar bags for analysis of  $O_2$ , CO,  $CO_2$ , total hydrocarbons,  $SO_2$ , and  $NO/NO_x$  content.

Other species such as  $SO_2$ ,  $H_2S$  or  $NH_3$  are absorbed into liquid solutions in absorption bubblers. The concentrations of  $H_2S$  and  $SO_2$  are measured by titration and  $NH_3$  concentration is measured using an ion-specific electrode.

## A.2 FTF Test Procedure

The Flare Test Facility (FTF) test procedure includes measuring background conditions, igniting the flame, establishing test conditions, sampling, and analysis. Tests are not conducted in rainy weather or at wind speeds greater than 5 mph. Most testing is done in the morning, when the weather is calm. A typical test requires about 4 hours, although the actual sample period is only 20 minutes.

Before each test, the ambient air is sampled and analyzed for background levels of  $O_2$ , CO,  $CO_2$ , hydrocarbons,  $SO_2$ ,  $NO/NO_x$ , soot, and for  $H_2S$  or  $NH_3$ , if applicable. The flame is then ignited using a hand-held spark igniter or a Zink igniter, and the test conditions are set by adjusting the gas flowrates. Most of the tests were conducted near the stability limit of the flame. The flame stability limit is determined by adjusting the flowrates until the flame becomes unstable and is eventually extinguished.

After test conditions are set, plume samples are collected for 20 minutes in order to time-average perturbations and collect sufficient amounts of sample for analysis. Samples are collected from five different radial locations, at a height above the flame experimentally determined to be beyond the flame. If the probes are too high, air dilution of the samples reduces combustion product measurement accuracy. If the probes are located too low, inside the flame envelope, incompletely burned samples may be collected, which would result in artificially low combustion efficiency measurements.

While the plume is being sampled, the flame structure and other characteristics such as color are recorded visually and photographically. After sample collection and flame observations are complete, the flame is shut down. Sample analysis is then conducted to measure levels of  $O_2$ , CO,  $CO_2$ , HC, NO/ $NO_x$ , soot, and other species in the plume samples.

## APPENDIX B

### FLARE SCREENING FACILITY AND TEST PROCEDURES

#### 8.1 Flare Screening Facility

The laboratory-scale Flare Screening Facility (FSF) is used to inexpensively, quickly, and easily identify potential difficulties in flaring a wide variety of compounds. Advantages of the FSF over the Flare Test Facility are its small size, low operating cost for gases and materials, the ability to obtain complete, undiluted samples of flare combustion products, the ability to close mass balances, and the increased safety for flaring toxic gases.

Figure B-1 shows the FSF schematic. This facility is an adaptation of EER's Turbulent Flame Reactor, originally designed to measure emissions and combustion efficiency of hazardous waste compounds. The facility was adapted to burn either liquid or gaseous compounds supplied from pressure cylinders and metered through calibrated rotameters. Combustion air is injected to the reactor co-axially with the fuel stream, through a flow straightening screen. By maintaining a very low air velocity relative to the fuel velocity, effects of the co-current air stream on the fuel stream are minimized. Test results verify that the flame behaves similarly to a jet in a quiescent atmosphere.

The flame is completely enclosed in a water-cooled reactor shell, with sample probes located at the reactor outlet. The shell isolates the flame from the environment and prevents air dilution of the flare products. This allows complete mass balance closure over the system.

Instrumentation for plume sampling and analysis is shown in Figure B-2. There are two separate sample systems: one for continuous monitors and one for gas chromatograph samples. The sample for the continuous monitors is run through a heated filter and divided into two streams. One leads to a total

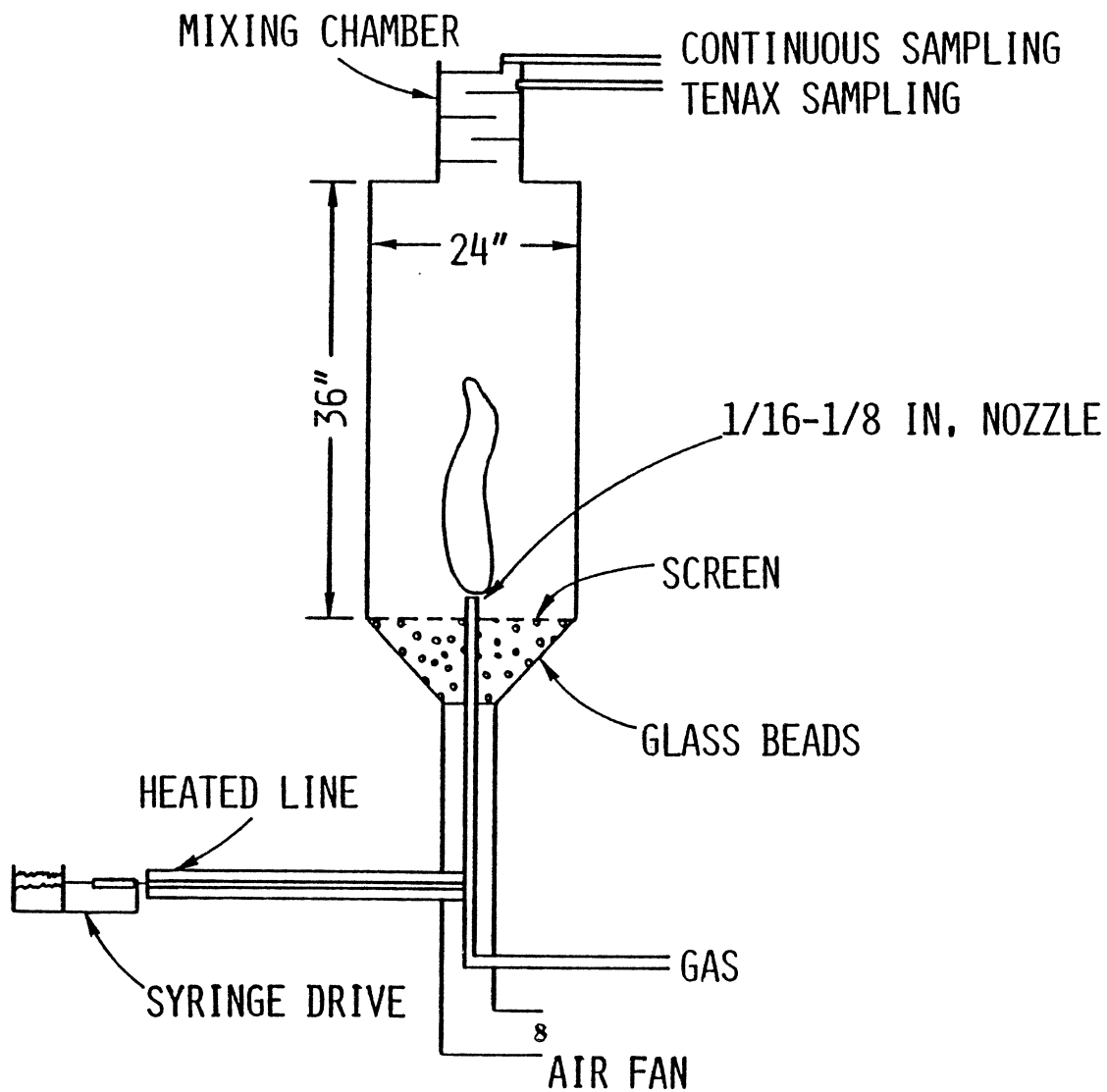


Figure B-1. Flare Screening Facility (FSF).

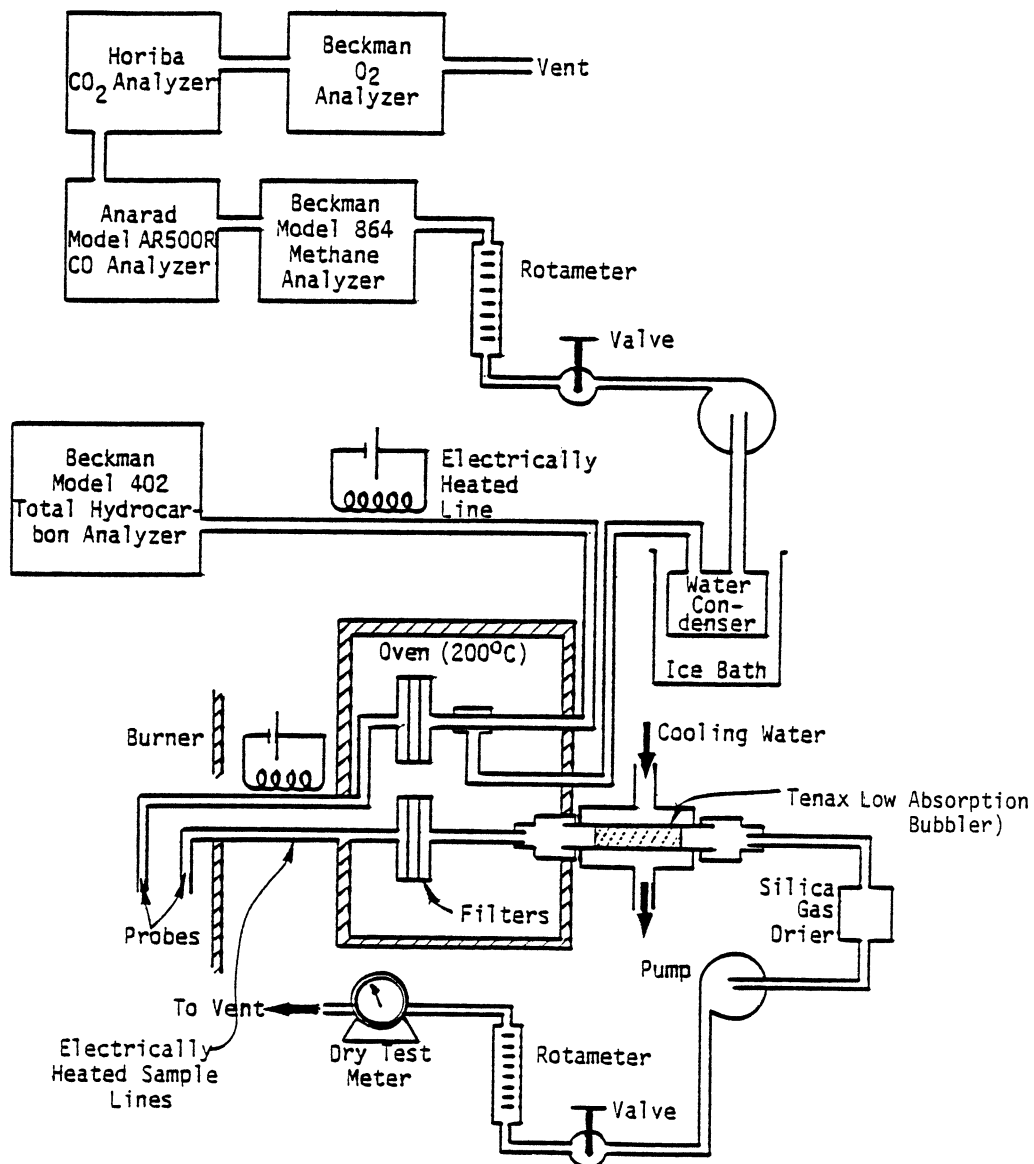


Figure B-2. Flare Screening Facility sample system.

hydrocarbon analyzer (flame ionization detector) and the other passes through a water-bath and then to CO, CO<sub>2</sub>, CH<sub>4</sub>, and O<sub>2</sub> analyzers.

A second sample stream passes through a filter into either a solid sorbent cartridge or an absorption bubbler. The solid sorbent, Tenax and activated charcoal, is used to collect and concentrate heavy and light hydrocarbons in the gas sample. Aqueous solutions in the absorption bubblers collect and concentrate other species in the sample, such as HCN and NH<sub>3</sub>. The hydrocarbon species adsorbed in the sorbent cartridges are subsequently desorbed by heating for gas chromatographic analysis and/or mass spectrometry analysis. Species collected in the absorption bubblers are subsequently measured by titration, ion-specific electrodes, or colometric techniques.

## B.2 FSF Test Procedures

The FSF test procedures are more simple than the FTF test procedures. Since the facility is enclosed, it is not subject to environmental conditions such as wind or rain. The system is smaller and hence, more easily monitored. Probe positioning is unnecessary, since the sample probes are located permanently at the reactor outlet.

For each test, all the instruments are zeroed and calibrated. After the flame is ignited and the air and fuel flowrates are adjusted, on-line sample collection and analysis is initiated. The effects of air and fuel flowrate changes on flare emissions can be monitored by varying the flowrates while operating the on-line sample system. Solid sorbent and bubbler collection of sampled species is time-averaged, however, and can only be conducted while air and fuel flowrates are kept constant. Final on-line emission measurements are made of plume species after the on-line instruments indicate that steady state has been reached for the system.

Solid sorbent samples of plume species can be sealed, cooled, and stored for short periods of time. Quantitative and qualitative analysis of these samples is conducted by heating the sample to desorb the concentrated hydrocarbons into a gas chromatograph (GC) and/or mass spectrometer (MS).



Species types and concentration are determined by comparing the results to standards.

Bubbler samples, depending upon the sampled species, can be titrated for HCL, H<sub>2</sub>S or SO<sub>2</sub>, or analyzed using ion-specific electrodes for NH<sub>3</sub> or HCN.

## APPENDIX C

### DATA ANALYSIS

#### C.1 FTF Data Analysis

Data analysis procedures for the pilot-scale FTF tests were developed in previous EER flare studies and reported by Pohl, et al. (1.3). Analysis of the pilot-scale tests is much more complicated than analysis of flare screening tests done on the laboratory-scale FSF. Results of FTF tests must be corrected for background levels of sampled species and air dilution of the plume. Also, numerical integration must be conducted using the local probe measurements and velocities calculated from jet theory. These steps are unnecessary in the FSF analysis procedures, because the flare is isolated from the environment, and well-mixed samples are collected at the outlet of the reactor. Since the development and details of the Flare Test Facility data analysis procedures are already reported (1.3), only a brief summary and new additions will be reported here. The terminology, however, has been changed to be more uniform and compatible with the additions.

Data reduction is conducted on the FTF plume sample results to determine local air dilution of the combustion products, local combustion and destruction efficiencies, and integrated overall average combustion and destruction efficiencies. The local dilution factor is:

$$DF = \frac{Y_m - Y_{af}}{Y_b - Y_m} \quad C-1$$

where DF = dilution factor = volume of air in the local sample divided by the volume of stoichiometric combustion products.

Y = local concentration of O<sub>2</sub>, CO<sub>2</sub>, or SO<sub>2</sub> (tracer)

m = measured in plume  
 af = air-free, stoichiometric basis  
 b = background

Combustion efficiency is defined as the degree to which all fuel materials have been completely oxidized. The local combustion efficiency is based upon local probe measurements of plume constituents, whereas the integrated average combustion efficiency is calculated by integrating the local plume fluxes to obtain average compositions of plume species. Since local plume measurements are diluted by ambient air, they must be corrected for the background levels of plume species in the ambient air. These corrections are made using equation C-2:

$$Y_{h,c} = Y_{h,m} - \left( \frac{DF}{DF+1} \right) Y_{h,b} \quad C-2$$

where h = plume species  
 c = corrected

Local combustion efficiency (CE) can then be calculated using equation C-3:

$$CE = 1 - \frac{\sum_i v_i Y_{i,c}}{\sum_j v_j Y_{j,c}} \quad C-3$$

where v = stoichiometric coefficient  
 i = incompletely burned species  
 j = completely and incompletely burned species

Local destruction efficiency is similar to local combustion efficiency, but is a measure of the degree of destruction of the particular fuel material.

It is equal to the combustion efficiency for that species only when there are no incompletely burned intermediates, such as CO or soot for hydrocarbon species. Local destruction efficiency (DE) for a fuel species is calculated using equation C-4:

$$DE = 1 - \frac{Y_{k,c}}{\sum_l Y_{l,c}} \quad C-4$$

where k = fuel species

l = completely and incompletely burned species from fuel species.

Integrated average combustion and destruction efficiencies are computed by first combining the local corrected plume composition with the local plume velocity to obtain a local corrected mass flux for each plume constituent. The local corrected plume species concentrations are found using equation C-2, and the local plume velocity is calculated from jet theory using equations C-5<sup>1</sup> and C-6:

$$V_{r,x} = V_{max} \exp \left[ -5 \frac{R_r}{x} \right]^2 \quad C-5$$

$$V_{max} = V_o \left[ 0.16 \left( \frac{x}{d} \right) - 1.5 \right] \quad C-6$$

---

<sup>1</sup>The coefficient preceeding  $R_r/x$  in equation C-5 was reported as -90 in a previous EER report (1.3), based upon jet theory. In order to better match radial profiles measured in the flare tests, the coefficient was changed to -5.

where V = velocity

R = radial distance from plume centerline

X = probe axial distance above flare head

r = radial position

max = maximum

o = flare head outlet

Numerical integration of the local fluxes is used to calculate average combustion and destruction efficiencies using equations C-7, C-8, and C-9:

$$CE = 1 - \frac{\sum_r \sum_i v_i Y_{i,c} V_r A_r}{\sum_r \sum_j v_j Y_{j,c} V_r A_r} \quad C-7$$

$$DE = 1 - \frac{\sum_r Y_{k,c} V_r A_r}{\sum_r \sum_l v_l Y_{l,c} V_r A_r} \quad C-8$$

$$A_r = \pi(R_{r+1}^2 - R_r^2) \quad C-9$$

where  $A_r$  = radial area sampled by probe r (Figure C-1).

## C.2 FSF Data Analysis

Data analysis for the Flare Screening Facility (FSF) test results is much simpler than for the Flare Test Facility (FTF) test results. The FSF flare flame is completely enclosed within a steel reactor shell. The inlet fuel and combustion air flowrates are metered, so the plume flowrates of excess air and air-free combustion products can be directly calculated based upon the combustion stoichiometry of the gas:

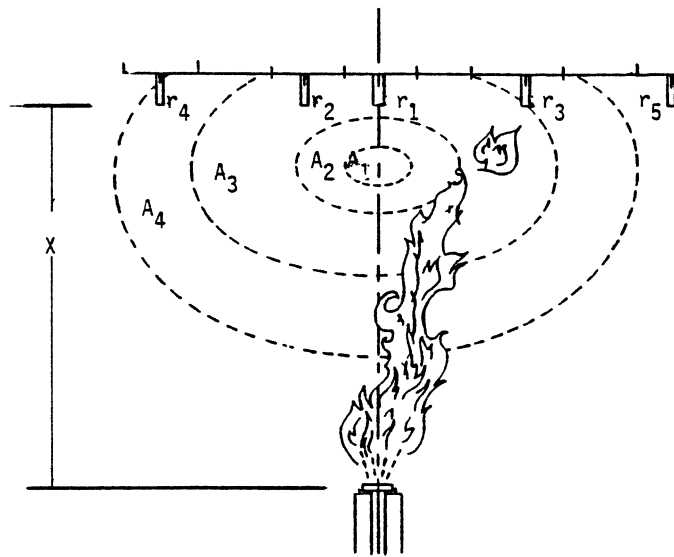


Figure C-1. Schematic of integration geometry.

$$\dot{V}_{e.a.} = (SR-1) \dot{V}_{r.a.} \quad C-10$$

where  $\dot{V}$  = volumetric flowrate, SCFH  
 e.a. = excess air  
 S.R. = stoichiometric ratio  
 r.a. = required air for 100% combustion

$$\dot{V}_p = \dot{V}_g \sum_i \nu_i P_i \quad C-11$$

where  $p$  = stoichiometric products of combustion with air (air-free basis, 0 percent  $O_2$ )  
 $g$  = inlet gas  
 $\nu$  = stoichiometric coefficient  
 $i$  = combustion species "i"

$$\dot{V}_t = \dot{V}_{e.a.} + \dot{V}_p \quad C-12$$

where  $t$  = total plume

This approach assumes 100 percent combustion, in order to determine the excess air, combustion product, and total plume flowrates. The same assumption was used in data reduction of the pilot-scale tests. Where combustion is only slightly less than 100 percent, flowrate errors due to this assumption are small. Even where combustion is significantly less than 100 percent, the error in total plume flowrate is small, because a majority of the plume gas is nitrogen, unaffected by combustion efficiency (discounting  $N_2 \rightarrow NO_x$  reactions and combustion of nitrogen-containing fuel species).

The plume is sampled at the reactor exit, where the plume is well mixed. This eliminates the need for collection of multiple local plume samples across the plume radius, assumptions of local velocities at radial locations in the plume, and the integration of local species fluxes to calculate total plume species flowrates. Species concentrations in the plume sample are representative of average plume concentrations. Species flowrates in the plume are calculated using the measured concentrations and the plume flowrate found from equation C-13:

$$\dot{V}_i = \dot{V}_t Y_i \quad \text{C-13}$$

where  $Y$  = mole fraction

In cases of high combustion efficiency, the plume concentration levels of incompletely combusted species such as CO and hydrocarbons are near background levels. The plume species flowrates must then be corrected by subtracting the background contribution:

$$\dot{V}_{i,c} = \dot{V}_i - \dot{V}_a Y_{i,b} \quad \text{C-14}$$

where  $c$  = corrected  
 $b$  = background

Combustion and destruction efficiencies are calculated using equations C-15 and C-16.

$$CE = 1 - \frac{\sum_i v_i \dot{V}_{i,c}}{\sum_j v_j \dot{V}_{j,c}} \quad \text{C-15}$$



where  $i$  = incompletely burned species .  
 $j$  = incompletely and completely burned species

$$DE = 1 - \frac{\dot{V}_{k,c}}{\sum_l \nu_l \dot{V}_{l,c}} \quad C-16$$

where  $k$  = fuel species  
 $l$  = incompletely and completely burned species that came from  
the fuel species

## C.2 References

- C.1 Beer, J.M. and Chigier, Combustion Aerodynamics, Halsted Press Division, John Wiley and Sons, Inc., New York, 1982.

## APPENDIX D

### QUALITY ASSURANCE

#### D.1 Flowrate Measurement

Accurate measurement of the gas flowrates is very important in determining the relief gas composition and velocity. Also, since the level of air-assist has such a strong impact upon the stability and combustion efficiency of the air-assisted head, accurate air-assist flowrate measurements are also important.

Square-edged orifice plates were used to measure the flare gas flowrates. Each orifice was calibrated using air and a laminar flowmeter, dry gas meter, or wet test meter to obtain an orifice coefficient, to be used in equation D-1 for flowrate measurement:

$$\dot{V} = K F_g \left( \frac{P \Delta P}{MW T} \right)^{\frac{1}{2}} \quad D-1$$

where  $\dot{V}$  = flowrate, SCFM  
K = orifice coefficient  
 $F_g$  = gas correction factor  
P = static orifice pressure, psia  
 $\Delta P$  = orifice differential pressure, feet H<sub>2</sub>O column  
MW = gas molecular weight  
 $T$  = orifice temperature, R.

The standard deviation of K for 21 different orifices was less than 7.9%, and less than 3.0% for the majority. For air and nitrogen,  $F_g = 1.00$ . For the other gases,  $F_g$  was determined by calibration.

The air-assist flowrate was measured using a venturi meter, which was calibrated by using a laminar flowmeter to determine a flow coefficient for use in equation D-1.

## D.2 Sample Analysis

Accurate sample analysis is critical for determining reliable combustion and destruction efficiency results. Table D-1 shows the analytical methods, instruments, and accuracies used in this test program. The listed accuracies are for the concentration ranges most typically encountered at the Flare Test Facility. Accuracy for a specific method may change if concentration levels for the sampled species are outside the ranges listed in Table D-1.

Many of the analytical methods of Table D-1 were developed in previous EER flare studies (1.3), but several additional methods were developed during this study. New techniques were needed for the analysis of previously untested non-hydrocarbon gas species,  $\text{H}_2\text{S}$  and  $\text{NH}_3$ . Also, in order to qualitatively measure hydrocarbon emissions, a method was required which could analyze very low concentrations of hydrocarbon species in plume samples.

For measuring  $\text{H}_2\text{S}$  emissions, an adaptation of EPA Method 11 (D.1) was used. This method involved (1) absorption  $\text{H}_2\text{S}$  from plume samples in gas bubblers of and (2) iodometric titration of the bubbled solution. The method can be very accurate, depending upon bubbler collection efficiency, the aqueous  $\text{H}_2\text{S}$  concentration, and bubbled gas flowrate measurement accuracy. For this study, the combined accuracy for measuring gaseous  $\text{H}_2\text{S}$  concentrations of 1-100 ppm is  $\pm 15$  percent. This accuracy was not achieved due to  $\text{SO}_2$  presence in the bubbled solutions, which caused great errors when the aqueous  $\text{SO}_2$  concentration was high relative to the  $\text{H}_2\text{S}$  concentration. Accurate techniques for determining  $\text{H}_2\text{S}$  and  $\text{SO}_2$  concentrations in mixtures have been developed for future  $\text{H}_2\text{S}$ - $\text{SO}_2$  analysis.

Emission of  $\text{NH}_3$  in the flare plume was measured by absorption of  $\text{NH}_3$  in gas bubblers, followed by aqueous analysis using ion-specific electrodes.

TABLE D-1

## FLARE FACILITY ANALYTICAL METHODS

SPECIES	INSTRUMENT	PRINCIPLE	RANGE	ACCURACY	MEASURED CONCENTRATIONS
O <sub>2</sub>	Taylor 570A	Paramagnetic	0-100%	±0.2%	18-21%
CO	Beckman 315A	NDIR	0-2%	±0.1 ppm	3-200 ppm
CO <sub>2</sub>	Beckman 315B	NDIR	0-20%	±0.02%	0.05-2%
Total Hydrocarbons	Beckman 400	FID	0-5000 ppm	±0.5 ppm	3-300 ppm
Individual Hydrocarbons	Tenax Cartridge GC-MS	FID, Spectroscopy	0.0002-1 ppm	One order of magnitude	0.0002-1 ppm
H <sub>2</sub> S	Titration	Iodometric Method	1-100 ppm	±15% of Measured	5-100 ppm
SO <sub>2</sub>	Titration	Perchlorate RXN	1-200 ppm	±15% of Measured	10-200 ppm
	Melloy SA 260	FPD	0.5-10 ppm	±1% of Measured	
NH <sub>3</sub>		Ion-Specific Electrode	0.1-10 ppm	±15% of Measured	0.1-0.6 ppm
NO/NO <sub>x</sub>	Teco 14B-E	Chemiluminescence	0.05-10 ppm	±5% of Measured	0.02-10 ppm
Particulate	Filter	Timed Collection	0-10 <sup>-6</sup> lb/ft <sup>3</sup>	±10% of Measured	10 <sup>-8</sup> -10 <sup>-6</sup> lb/ft <sup>3</sup>

The accuracy of this method,  $\pm 15$  percent, depends on the bubbler collection efficiency, the aqueous  $\text{NH}_3$  level, and the accuracy of the bubbled gas volume measurement.

Qualitative analysis of flare hydrocarbon emissions is usually very difficult, because of the typically low concentrations of specific hydrocarbon species in the flare plume. These species were collected from plume samples by adsorption using solid sorbent cartridges. High molecular weight molecules were adsorbed onto Tenax, and low molecular weight hydrocarbons were adsorbed onto charcoal. The samples were subsequently analyzed qualitatively and semi-quantitatively by gas chromatography and mass spectrometry. Quantitative accuracy was low (one order of magnitude) because expense prohibited using calibration standards. Since measured levels of these species were very low compared to the predominant species  $\text{CO}$ ,  $\text{CO}_2$ , total hydrocarbons, and soot, this error had negligible impact on combustion and destruction efficiency results.

### D.3 Quality Control Problems and Solutions

Few quality assurance problems were encountered during this program. A key problem, mentioned in Section D-2, was that for a few tests, the sampled concentration levels of various species were outside the range of accurate measurement indicated in Table D-1. In these cases, the data for those species was considered invalid. Usually the remainder of the test data was still reliable. For example, an inaccurate soot measurement for a particular test invalidated the soot values, but negligibly affected the carbon mass balance and efficiency calculations, when the flare was operated under smokeless conditions.

Related to this problem was the problem of reliable mass balances using  $\text{SO}_2$  as a tracer. Accurate plume  $\text{SO}_2$  concentration measurements required  $\text{SO}_2$  plume levels of 10 ppm or greater. Under many of the flare conditions of this test program, this required a higher  $\text{SO}_2$  tracer flowrate than available. To remedy this, an additional  $\text{SO}_2$  vaporizer was designed and constructed, but

was not installed until after completion of the test program. It is, however, available for future test programs.

There was a distinct problem with the H<sub>2</sub>S measurement technique, which invalidated all of the H<sub>2</sub>S destruction efficiency results. In sampling the plume for H<sub>2</sub>S and SO<sub>2</sub> levels, absorption bubblers were used in series, one for H<sub>2</sub>S collection, and the second for SO<sub>2</sub> collection. After the completion of the H<sub>2</sub>S test series, it was discovered by follow-up testing that the H<sub>2</sub>S bubbler also collected SO<sub>2</sub>, and vice versa. The SO<sub>2</sub> titration method is relatively insensitive to H<sub>2</sub>S presence, but SO<sub>2</sub> presence in the H<sub>2</sub>S bubbler greatly affected the H<sub>2</sub>S results. The accuracy of several methods for measuring H<sub>2</sub>S levels in H<sub>2</sub>S-SO<sub>2</sub> mixtures has recently been verified at EER for use in future flare test programs. These methods include (1) colorimetry, (2) Draeger tubes, and (3) gas chromatography using a flame photometric detector.

#### D.4 Reference

- D.1 "Revision of Reference Method 11", Federal Register, 43(6), p.1494, 1978.

## APPENDIX E

### CONVERSION FACTORS

<u>To Convert From</u> <u>English</u>	<u>To</u> <u>Metric</u>	<u>Multiply</u> <u>By</u>
Btu	KJ	1.055
CFM	m <sup>3</sup> /h	1.700
in.	m	0.0254
in. H <sub>2</sub> O	Pa	249
psi	Pa	6893
ft	m	0.3048
ft <sup>3</sup>	m <sup>3</sup>	0.02832
lb	kg	0.4536
mph	km/h	1.609

°R (Rankine) is converted to °C (Celsius) via the following formula:

$$^{\circ}\text{C} = 5/9 (\text{R} - 492)$$

°F (Fahrenheit) is converted to °C (Celsius) via:

$$^{\circ}\text{C} = 5/9 (^{\circ}\text{F} - 32)$$

<b>TECHNICAL REPORT DATA</b> <i>(Please read Instructions on the reverse before completing)</i>			
1. REPORT NO. <b>EPA-600/2-85-106</b>	2.	3. RECIPIENT'S ACCESSION NO.	
4. TITLE AND SUBTITLE <b>Evaluation of the Efficiency of Industrial Flares: Flare Head Design and Gas Composition</b>		5. REPORT DATE <b>September 1985</b>	
7. AUTHOR(S) <b>J. H. Pohl and N. R. Soelberg</b>		6. PERFORMING ORGANIZATION CODE	
9. PERFORMING ORGANIZATION NAME AND ADDRESS <b>Energy and Environmental Research Corporation 18 Mason Irvine, California 92718</b>		8. PERFORMING ORGANIZATION REPORT NO.	
12. SPONSORING AGENCY NAME AND ADDRESS <b>EPA, Office of Research and Development Air and Energy Engineering Research Laboratory Research Triangle Park, NC 27711</b>		10. PROGRAM ELEMENT NO.	
		11. CONTRACT/GRANT NO. <b>68-02-3661</b>	
		13. TYPE OF REPORT AND PERIOD COVERED <b>Final; 10/83 - 12/84</b>	
		14. SPONSORING AGENCY CODE <b>EPA/600/13</b>	
15. SUPPLEMENTARY NOTES <b>AEERL project officer is Bruce A. Tichenor, Mail Drop 54; 919/541-2991. EPA-600/2-83-070 and -84-095 are earlier related (Phases 1 through 4) reports.</b>			
16. ABSTRACT <b>The report gives continued Phase 4 results of a research program to quantify emissions from, and efficiencies of, industrial flares. Initial results were limited to tests conducted burning propane/nitrogen mixtures in pipe flares without pilot light stabilization. The work reported here extends the previous results to other flare head designs and other gases and includes a limited investigation of the influence of pilot flames on flare performance. Results included: (1) flare head design influences the flame stability curve, (2) combustion efficiency can be correlated with flame stability for pressure heads and coanda steam injection heads; (3) for the limited conditions tested, flame stability and combustion efficiency of air-assisted heads correlated with the momentum ratio of air to fuel (the heating value of the gas had only minor influence), (4) limited data on an air-assisted flare show that a pilot light improves flame stability, (5) the destruction efficiency of compounds depends on the structure of the compounds, and (6) for compounds tested in this program, the destruction efficiency of different compounds could be correlated with the flame stability curve for each.</b>			
17. KEY WORDS AND DOCUMENT ANALYSIS			
a. DESCRIPTORS		b. IDENTIFIERS/OPEN ENDED TERMS	c. COSATI Field/Group
Pollution                      Analyzing Exhaust Gases                Design Efficiency                      Chemical Analysis Flames Measurement Surveys		Pollution Control Stationary Sources Industrial Flares Flare Head Design	13B 21B 14G                      07D  14B
18. DISTRIBUTION STATEMENT  <b>Release to Public</b>		19. SECURITY CLASS (This Report) <b>Unclassified</b> 20. SECURITY CLASS (This page) <b>Unclassified</b>	21. NO. OF PAGES <b>138</b> 22. PRICE